European Journal of Taxonomy 1013: 1–76
https://doi.org/10.5852/ejt.2025.1013.3057

europeanjournaloftaxonomy.eu
ISSN 2118-9773
2025 · Xavier C. *et al.*

Received: 13 January 2025 • *Accepted: 28 May 2025* • *Published: 15 September 2025*

Topic editor: Magalie Castelin • *Section editor: Arnaud Henrard* • *Desk editor: Pepe Fernández*

Monograph

urn:lsid:zoobank.org:pub:B7178210-C13F-4C78-9768-252971340F22

Revising the revision: on 12 new species of *Stethorrhagus* Simon, 1896 from Colombia and Ecuador (Araneae: Corinnidae: Corinninae), with reassessments of all previously described species

Cláudia XAVIER [1,*], Antonio D. BRESCOVIT [2] & Alexandre B. BONALDO [3]

[1,3] Museu Paraense Emílio Goeldi, Departamento de Zoologia, Laboratório de Aracnologia, Avenida Perimetral, nº 1901, CEP 6607077-830, Belém, Pará, Brazil.
[1,3] Programa de Pós-Graduação em Zoologia, Universidade Federal do Pará / Museu Paraense Emílio Goeldi, Instituto de Ciências Biológicas, Campus Básico, Rua Augusto Corrêa, 01, CEP: 66075-110, Guamá, Belém, PA, Brazil.
[2] Instituto Butantan, Laboratório de Coleções Zoológicas, Av. Vital Brasil, 1500, Butantã, 05503-900 São Paulo, SP, Brazil.

[*] Corresponding author: claudiaxavier.bio@gmail.com
[2] Email: antonio.brescovit@butantan.gov.br
[3] Email: bonaldo@museu-goeldi.br

Abstract. Twelve new species of the genus *Stethorrhagus* Simon, 1896 are described: *S. bradypus* sp. nov. (♂♀), *S. callithrix* sp. nov. (♂♀), *S. loxodonta* sp. nov. (♂♀), *S. naja* sp. nov. (♂♀), *S. papilio* sp. nov. (♀) and *S. sylvilagus* sp. nov. (♂♀) from Colombia; *S. canis* sp. nov. (♀), *S. felis* sp. nov. (♂♀), *S. mandrillus* sp. nov. (♂♀), *S. ovis* sp. nov. (♂♀), *S. sciurus* sp. nov. (♀) and *S. tremarctos* sp. nov. (♂♀) from Ecuador, increasing the number of known species in the genus from 15 to 27. Detailed morphological descriptions, photos of the body and copulatory organs, illustrations of copulatory organs, and comparisons with closely related species are given for all new species, along with emended diagnoses, distribution maps and an updated key to all currently accepted species in the genus. The geographical distribution of *S. lupulus* and *S. oxossi* are updated with new records from Brazil and Peru, and Brazil, respectively. Additionally, photographs of the type material of *S. limbatus* Simon, 1896, *S. nigrinus* (Berland, 1913), *S. maculatus* (L. Koch, 1866), *S. hyula* Bonaldo & Brescovit, 1994, *S. planada* Bonaldo & Brescovit, 1994, *S. duidae* Gertsch, 1942, *S. roraimae* Gertsch, 1942, *S. peckorum* Bonaldo & Brescovit, 1994, and *S. archangelus* Bonaldo & Brescovit, 1994 are supplied.

Keywords. Dionycha, soldier spiders, taxonomy, morphology, Neotropical Region.

Xavier C., Brescovit A.D. & Bonaldo A.B. 2025. Revising the revision: on 12 new species of *Stethorrhagus* Simon, 1896 from Colombia and Ecuador (Araneae: Corinnidae: Corinninae), with reassessments of all previously described species. *European Journal of Taxonomy* 1013: 1–76. https://doi.org/10.5852/ejt.2025.1013.3057

Introduction

The genus *Stethorrhagus* was proposed by Simon (1896) to include two Amazonian species: *S. limbatus* Simon, 1896 (type species) and *S. lupulus* Simon, 1896, both known from males and females at that time. Bonaldo & Brescovit (1994) revised the genus, recognizing 14 species. They defined as diagnostic for the genus the presence of a bifid embolic apex with the ejaculatory duct opening at the bifurcation in males and, in females, a single median copulatory opening and a sclerotized dorsal plate covering the posterior half of the epigynum. Bonaldo (2000) transferred an additional species from *Corinna* C.L. Koch, 1841 to *Stethorrhagus*, *S. maculatus* (L. Koch, 1866) (known only from the female, from Colombia). So far, 15 species of *Stethorrhagus* have been recognized, all of them from the Neotropical Region (World Spider Catalog 2025). When studying *Stethorrhagus*, Bonaldo & Brescovit (1994) transferred *Parachemmis* Chickering, 1937 from Liocranidae Simon, 1897 to Corinnidae Karsch, 1880, Corinninae, stating that these two genera share the presence of a pair of excavations on the anterior margin of the sternum and a ventral, apical articulated apophysis on the male palpal tibia. Subsequently, Bonaldo (2000) proposed the genus *Tupirinna*, including it in this putatively monophyletic group of genera.

Here, we describe and document twelve additional new species of *Stethorrhagus* from Colombia and Ecuador. Nine of these species are known from both sexes, while three are known only from females. The geographical distribution of two previously known species is updated: *S. lupulus*, previously known from Venezuela, Colombia (Meta Department), Peru (Loreto Department) and Brazil (states of Amazonas, Roraima) is newly recorded from the states of Acre, and Mato Grosso (Brazil) and Madre de Dios Department (Peru); *S. oxossi* Bonaldo & Brescovit, 1994, previously known only from the state of Bahia (northeastern Brazil), is here recorded in southeastern Brazil (states of Espírito Santo, Rio de Janeiro and São Paulo). Additionally, we provide photographs of the type specimens of *S. limbatus*, *S. nigrinus* (Berland, 1913), *S. maculatus*, *S. hyula* Bonaldo & Brescovit, 1994, *S. planada* Bonaldo & Brescovit, 1994, *S. duidae* Gertsch, 1942, *S. roraimae* Gertsch, 1942, *S. peckorum* Bonaldo & Brescovit, 1994 and *S. archangelus* Bonaldo & Brescovit, 1994, along with emended diagnoses, distribution maps and an updated key to all accepted species in the genus.

Material and methods

All specimens of the new species proposed here are preserved in 80% ethanol and were examined and illustrated using stereo microscopes Leica MZ16 (epigynes and male palp in retrolateral view) and Zeiss DV8 (male palps in ventral view) and photographed and measured using a Leica M205A stereo microscope with LAS software ver. 4.9, in MPEG. The dorsal view of the female genitalia of *S. lupulus*, *S. oxossi*, *S. mandrillus* sp. nov., *S. ovis* sp. nov., *S. callithrix* sp. nov., *S. bradypus* sp. nov., *S. naja* sp. nov. and *S. canis* sp. nov. was photographed using a Camera AmScope MU 1403 and the AmScope software ver. 4.12 attached to a Zeiss AxioStar Plus Trinocular Microscope; resulting images were stacked using Helicon Focus ver. 8.2.16, also in MPEG. The types of *S. limbatus* and *S. nigrinus* were examined at MNHN, using a Leica Wild M3C stereo microscope, photographed using a Nachet NS 50 trinocular stereo microscope for low magnification photos and Nachet 300 trinocular microscope for higher magnification photos, with the software of the camera for acquisition of photo stacks, and Helicon Focus software for treatments of stacks. The female holotype of *S. maculatus* was examined in a stereo microscope Zeiss ZV6 and photographed using a Zeiss Axio Zoom.V16 with AxioCam HRc with Zeiss ZEN 2 (blue edition) software and Helicon Focus ver. 5.3.14 in BMNH.

Male palps and epigynes were examined and illustrated after being dissected. Female genitalia was immersed in a solution with Ultrazyme to clean the soft tissues and then in clove oil for better visualization. Descriptions and morphogical terminologies follow Bonaldo & Brescovit (1994) and Bonaldo (2000), with novel contributions, mainly related to male tibial morphology. Eye sizes were

measured at the maximum diameter as seen in dorsal view. Leg measurements are shown as total length (femur, patella, tibia, metatarsus, and tarsus). All measurements are in millimeters.

The specimens examined here are deposited in the following institutions, curators in parentheses:

AMNH = American Museum of Natural History, New York, USA (L. Prendini)
BMNH = Natural History Museum, London, England (J. Beccaloni)
CAS = California Academy of Sciences, San Francisco, USA (L. Esposito),
IBSP = Instituto Butantan, São Paulo, Brazil (A.D. Brescovit)
ICN-Ar = Instituto de Ciencias Naturales, Bogotá, Colombia (J. Cabra-García)
MBUCV = Museo de Biología de la Universidad Central de Venezuela, Caracas, Venezuela (E. Guerrero)
MCN = Museu de Ciências Naturais, Porto Alegre, Brazil (R. Ott)
MCTP = Museu de Ciências e Tecnologia – Pontifícia Universidade Católica do Rio Grande do Sul, Porto Alegre, Brazil (R.A. Teixeira)
MCZ = Museum of Comparative Zoology, Harvard, MA, USA (G. Giribet)
MNHN = Muséum national d'Histoire naturelle, Paris, France (K. Privet)
MNRJ = Museu Nacional, Universidade Federal do Rio de Janeiro, Rio de Janeiro, Brazil (A.B. Kury)
MPEG = Museu Paraense Emílio Goeldi, Belém, Brazil (A.B. Bonaldo)
MUSM = Museo de Historia Natural de la Universidad Nacional Mayor de San Marcos, Lima, Peru (D. Silva)
QCAZI = Pontificia Universidad Católica del Ecuador, Quito, Ecuador (D. Vela)
SMF = Senckenberg Research Institute and Natural History Museum, Frankfurt, Germany (P. Jäger)
UFMG = Universidade Federal de Minas Gerais, Belo Horizonte, Brazil (A.J. Santos);
USNM = National Museum of Natural History, Smithsonian Institution, Washington D.C., USA (H. Wood)

Distribution maps were produced with QGIS, ver. 3.10 (QGIS Development Team 2019). Figures and plates were edited and prepared in Adobe Photoshop® 2024 ver. 25.12.1. The sequence of species presented in the paper strictly follows the order in which they appear in the key provided (except for *S. roraimae*). All new species are named after classical generic names across the animal kingdom, referring to pareidolic perceptions of animal shapes on photos of the female epigynum in ventral view.

Abbreviations

ALE = anterior lateral eyes
AME = anterior median eyes
AS = apical spur
C = conductor
CD = copulatory duct
CO = copulatory opening
DL = RTA dorsal lobe
dVL = dorsal process of ventral lobe of RTA
E = embolus
FD = fertilization ducts
mVL = median process of ventral lobe of RTA
PLE = posterior lateral eyes
PME = posterior median eyes
PVP = posterior vulvar plate

RTA = retrolateral tibial apophysis
SePP = sub-embolic prolateral process
SeRP = sub-embolic retrolateral process
SI = primary spermathecae
SII = secondary spermathecae
ST = subtegulum
TP1 = tegular process 1
TP2 = tegular process 2
VEP = ventral epigynal plate
VL = RTA ventral lobe
VTA = ventral tibial apophysis
vVL = ventral process of ventral lobe of RTA

Results

Taxonomy

Class Arachnida Cuvier, 1812
Order Araneae Clerck, 1757
Corinnidae Karsch, 1880

Genus ***Stethorrhagus*** Simon, 1896

Stethorrhagus Simon, 1896: 421.

Stethorrhagus – Simon 1898: 200, figs 198–199, 202 (type species by subsequent designation, *S. limbatus* Simon, 1896). — Bonaldo & Brescovit 1994: 34. — Bonaldo 2000: 125.

Diagnosis

Stethorrhagus shares with *Parachemmis* and *Tupirinna* a pair of anterolateral sternal excavations in both sexes and a ventral tibial apophysis (VTA) in the male palp (Figs 1C–F, 5C, 8D–E, 13B, 14A, 16C; Bonaldo & Brescovit 1994: figs 1c, 6c, 9b, 15a; Bonaldo 2000: figs 25–26, 116–118, 335, 344; Xavier & Bonaldo 2021: figs 8a, 21a, 22g). They differ from both *Parachemmis* and *Tupirinna* by the male palpal embolus with a bifid tip, with the ejaculatory duct opening on the bifurcation (Figs 14A, 17A, 20A; Bonaldo & Brescovit 1994: figs 5c–d, 6a) (embolus tip entire in *Parachemmis* and *Tupirinna*; Bonaldo 2000: figs 325–326, 328; Xavier & Bonaldo 2021: figs 8a–c, 20b–c). Females of *Stethorrhagus* further differ from *Parachemmis* by the single copulatory opening leading to a single copulatory duct that branches posteriorly (Figs 2C–D, 4C–D, 6C–D, 19C–D, 25C–D; Bonaldo & Brescovit 1994: figs 10f–g, 11c–d, 18a–b, 19c–d) (two separated epigynal copulatory openings that lead to long, wide copulatory ducts in *Parachemmis* – Bonaldo 2000: figs 333–334, 337–338) and from *Tupirinna* by the faint carapace color pattern, without the contrasting longitudinal median stripe (Figs 1A, 2A, 5A, 6A, 9A, 12A).

Description

See Bonaldo & Brescovit (1994: 34).

Composition

Stethorrhagus archangelus Bonaldo & Brescovit, 1994, *S. bradypus* sp. nov., *S. callithrix* sp. nov., *S. canis* sp. nov., *S. chalybeius* (L. Koch, 1866), *S. duidae* Gertsch, 1942, *S. felis* sp. nov., *S. hyula* Bonaldo & Brescovit, 1994, *S. latoma* Bonaldo & Brescovit, 1994, *S. limbatus* Simon, 1896, *S. loxodonta* sp. nov., *S. lupulus* Simon, 1896, *S. maculatus* (L. Koch, 1866), *S. mandrillus* sp. nov., *S. naja* sp. nov., *S. nigrinus* (Berland, 1913), *S. ovis* sp. nov., *S. oxossi* Bonaldo & Brescovit, 1994, *S. papilio* sp. nov.,

S. peckorum Bonaldo & Brescovit, 1994, *S. penai* Bonaldo & Brescovit, 1994, *S. planada* Bonaldo & Brescovit, 1994, *S. roraimae* Gertsch, 1942, *S. sciurus* sp. nov., *S. sylvilagus* sp. nov., *S. tremarctos* sp. nov., *S. tridentatus* Caporiacco, 1955.

Distribution

Neotropical region (Fig. 48).

Key to species of *Stethorrhagus* Bonaldo & Brescovit, 1994 (adapted from Bonaldo & Brescovit, 1994)

1. Males (those of *S. roraimae*, *S. maculatus*, *S. nigrinus*, *S. canis* sp. nov., *S. papilio* sp. nov. and *S. sciurus* sp. nov. unknown) 2
– Females (those of *S. duidae*, *S. latoma*, *S. peckorum* and *S. penai* Bonaldo & Brescovit, 1994, unknown) 22

2. Sternal excavations shallow, without delimited internal margin (Figs 1B, 2B, 3B, 4B, 7D, 8B) 3
– Sternal excavations deep, with delimited internal margin (Figs 9B, 12C–D, 15C–D, 22B, 24C–D) 8

3. Tibial dorsal apophysis (DTA) present; embolus insertion prolateral (Figs 1E–F, 3E–F; Bonaldo & Brescovit 1994: figs 10b, 13b) 4
– DTA absent; embolus insertion medial (Fig. 8D; Bonaldo & Brescovit 1994: figs 14b, 22b) 7

4. Sub-embolic prolateral process (SePP) shoulder-like, blunt, developed prolaterally (Figs 1C–D, 3C–D) 5
– SePP reduced to a small projection (Bonaldo & Brescovit 1994: figs 12a, 13a) 6

5. DTA large and rounded; ventral lobe of RTA with an intermediate process between ventral process of ventral lobe of RTA (vVL) and dorsal process of ventral lobe of RTA (dVL) (Fig. 1E–F; Bonaldo & Brescovit 1994: fig. 10b) ..... ***S. lupulus*** Simon, 1896
– DTA small, represented by a shallow excavation; intermediate process between vVL and dVL absent (Fig. 3E–F; Bonaldo & Brescovit 1994: fig. 11b) ..... ***S. oxossi*** Bonaldo & Brescovit, 1994

6. TP1 relatively small in relation to embolus, directed prolaterally, not covering embolar base (Fig. 5D–E; Bonaldo & Brescovit 1994: fig. 12b) ..... ***S. archangelus*** Bonaldo & Brescovit, 1994
– TP1 large in relation to embolus, directed apically, covering embolar base (Bonaldo & Brescovit 1994: fig. 13a) ..... ***S. latoma*** Bonaldo & Brescovit, 1994

7. Tibia with apical spur (AS) long, with wide base, inserted ventrally on tibial surface; embolus widened, flat and triangular, with reduced apical prongs (Fig. 7E–F; Bonaldo & Brescovit 1994: fig. 22a–b) ..... ***S. peckorum*** Bonaldo & Brescovit, 1994
– Tibia with AS short, inserted apically on vVL; embolus filiform, with long apical prongs (Fig. 8C–F; Bonaldo & Brescovit 1994: fig. 14a–b) ..... ***S. tridentatus*** Caporiacco, 1955

8. Ventral lobe of RTA composed only of vVL (Fig. 10C–D; Bonaldo & Brescovit 1994: fig. 9a–c) ..... ***S. limbatus*** Simon, 1896
– Ventral lobe of RTA bifid, composed of vVL and dVL (Figs 13B, 14B, 29A–B, 30A–B, 32A–B, 33A–B; Bonaldo & Brescovit 1994: fig. 15c) 9

9. Dorsal lobe of RTA wide, triangular; SePP and TP1 absent (Bonaldo & Brescovit 1994: fig. 15c) ..... ***S. penai*** Bonaldo & Brescovit, 1994
– Dorsal lobe of RTA finger-shaped or absent; SePP and/or TP1 present (Figs 14A–B, 30A–B, 33B) 10

10. dVL not protruding, represented by a slight elevation continuous to vVL (Figs 13B, 14B) 11
– dVL protruding (Figs 29B, 33B, 35C) 16

11. dVL glabrous; AS large, laminar, shifted dorsally (Figs 14A–B, 17A–B) 12
– dVL covered by long, thick modified hairs; AS indistinguishable from vVL (Figs 19B, 20B, 22E; Bonaldo & Brescovit 1994: figs 17b, 19b) 13

12. AS triangular in retrolateral view; embolus inserted between SePP and a Sub-embolic retrolateral process (SeRP) (Figs 13A–B, 14A–B) ..... ***S. tremarctos*** sp. nov.
– AS diamond-shaped in retrolateral view; SeRP absent (Figs 16A–C, 17A–B) .... ***S. mandrillus*** sp. nov.

13. SePP and embolus geminated at base; embolus short (Figs 19A, 20A) ..... ***S. loxodonta*** sp. nov.
– SePP and embolus separated at base (Figs 21C, 22C, 25A, 26A, 22C; Bonaldo & Brescovit 1994: fig. 19a) 14

14. TP1 represented by a wide, serrated keel (Figs 21C–D; Bonaldo & Brescovit 1994: Fig. 17b) .... ***S. planada*** Bonaldo & Brescovit, 1994
– TP1 tooth-like (Figs 22C, 25A; Bonaldo & Brescovit 1994: figs 17a, 19a) 15

15. TP1 curved, pointing prolaterally (Fig. 22C–E; Bonaldo & Brescovit 1994: fig. 19a) .... ***S. hyula*** Bonaldo & Brescovit, 1994
– TP1 straight, pointing apically (Figs 25A–B, 26A) ..... ***S. sylvilagus*** sp. nov.

16. vVL and dVL glabrous, without thick modified hairs (Figs 27C–D, 29A–B, 30A–B; Bonaldo & Brescovit 1994: Fig. 20b) 17
– vVL with thick modified hairs (Figs 32B, 35C) 18

17. vVL longer than dVL, bifid in the distal third; embolus wide-based, with reduced apical prongs (Fig. 27C–D; Bonaldo & Brescovit 1994: fig. 20a–b) ..... ***S. duidae*** Gertsch, 1942
– vVL slightly shorter than dVL, entire; embolus narrow-based, with well-developed apical prongs (Figs 29A–B, 30A–B) ..... ***S. ovis*** sp. nov.

18. Thick modified hairs present in both vVL and dVL (Figs 32B, 35B–C, 36B, 39C) 19
– Thick modified hairs present only in vVL; dVL glabrous (Figs 41B, 42C) 21

19. SePP with pointed tip directed retrolaterally (Figs 32A, 33A) ..... ***S. callithrix*** sp. nov.
– SePP with blunt tip directed apically (Figs 35B, 38A–C) 20

20. RTA with dorsal lobe (DL); tegulum with TP1 (Figs 35B, 36A–B) ..... ***S. felis*** sp. nov.
– Both DL and TP1 absent (Figs 38A–C, 39A–C) ..... ***S. bradypus*** sp. nov.

21. SePP finger-shaped as long as the embolus, tip blunt (Figs 41A–C, 42A–C) ..... ***S. naja*** sp. nov.
– SePP comma-shaped smaller than embolus, tip pointed (Bonaldo & Brescovit 1994: fig. 16a) .... ***S. chalybeius*** (L. Koch, 1866)

22. Sternal excavations shallow, without delimited internal margin 23
– Sternal excavations deep, with delimited internal margin 26

23. Ventral epigynal median plate (VEP) absent; dorsal plate with an accentuated V-shaped notch (Bonaldo & Brescovit 1994: fig. 14d–e) ..... ***S. tridentatus*** Caporiacco, 1955
– VEP present; dorsal plate without V-shaped notch 24

24. Copulatory opening (CO) circular; median plate not invaginated medially (Fig. 6C; Bonaldo & Brescovit 1994: fig. 12d) .....***S. archangelus*** Bonaldo & Brescovit, 1994
– CO otherwise; median plate invaginated medially (Bonaldo & Brescovit 1994: figs 10f, 11c) 25

25. CO V-shaped, with a clearly delimited anterior margin (Fig. 2C; Bonaldo & Brescovit 1994: fig. 10f) .....***S. lupulus*** Bonaldo & Brescovit, 1994
– CO U-shaped, without a clearly delimited anterior margin (Fig. 4C; Bonaldo & Brescovit 1994: fig. 11c) .....***S. oxossi*** Bonaldo & Brescovit, 1994

26. CO a large transverse excavation (nearly four times wider than long) (Fig. 11C, E; Bonaldo & Brescovit 1994: fig. 9d) .....***S. limbatus*** Simon, 1896
– Copulatory opening circular or a small transverse excavation (nearly as long as wide) (Figs 25C, 41D) 27

27. CO disposed anteriorly in relation to spermathecae (Figs 25C, 38D, 41D; Bonaldo & Brescovit 1994: figs 18a, 19a, 21b, 23a) 28
– CO disposed posteriorly in relation to spermathecae (Figs 16D, 19D, 29C; Bonaldo & Brescovit 1994: fig. 16d) 37

28. VEP present (Figs 38D, 41D) 29
– VEP absent (Figs 23C, 44C) 34

29. CO with straight posterior margin (Figs 38D, 41D) 30
– CO with U-shaped posterior margin (Figs 25C, 32C) 31

30. VEP placed medially on epigynal plate; primary spermathecae (SI) extended anteriorly, with long fertilization ducts inserted on the SI's extension, beyond CO level (Figs 38D–E, 39D–E) ....***S. bradypus*** sp. nov.
– VEP placed posteriorly on epigynal plate; primary spermathecae (SI) not extended anteriorly, below CO level (Figs 41D–E, 42D–E) .....***S. naja*** sp. nov.

31. VEP sub-rectangular, placed medially on epigynal plate (Bonaldo & Brescovit 1994: fig. 18a) ....***S. planada*** Bonaldo & Brescovit, 1994
– VEP gently procurved, placed posteriorly on epigynal plate (Figs 25C, 32C, 43C, E) 32

32. Copulatory duct (CD) long (from CO to posterior margin of VEP, more than six times as long as CO width) (Figs 32C–D, 33C–D) .....***S. callithrix*** sp. nov.
– CD short (from CO to posterior margin of VEP, less than four times as long as CO width) (Figs 25C, 43C, E) 33

33. Area between the posterior margin of VEP and the posterior margin of epigynal ventral plate bulging (Figs 25C, 26C) .....***S. sylvilagus*** sp. nov.
– Area between the posterior margin of VEP and the posterior margin of epigynal ventral plate depressed (Fig. 43C, E) .....***S. sciurus*** sp. nov.

34. Epigynal plate with a posterior median half-moon-shaped sclerotization (Fig. 23C; Bonaldo & Brescovit 1994: fig. 19c) .....***S. hyula*** Bonaldo & Brescovit, 1994
– Epigynal plate without such a sclerotization (Figs 45C–F; 44C–F, 11C; Bonaldo & Brescovit 1994: figs 21b, 23a) 35

35. CO small (width nearly 12 times smaller than the distance between CO and posterior margin of epigynal plate) (Fig 7C; Bonaldo & Brescovit 1994: fig. 23a) .....***S. roraimae*** Gertsch, 1942
– CO large (width four times smaller than the distance between CO and posterior margin of epigynal plate) (Figs 44C, 45C–F; Bonaldo & Brescovit 1994: fig. 21b) 36

36. CO with posterior border sinuous; CD's dorsal reinforcement rods not surpassing CO anteriorly (Fig. 44C–D; Bonaldo & Brescovit 1994: fig. 21b) .....***S. nigrinus*** (Berland, 1913)
– CO with posterior border straight; CD's dorsal reinforcement rods surpassing CO anteriorly (Fig. 45C–F) .....***S. papilio*** sp. nov.

37. CO circular or sub-circular (Figs 17D, 20C) 38
– CO slit-shaped (Figs 29C, 47C, E) 42

38. CO with anterior margin delimited by a protruding lip (Figs 16D, 17C; Bonaldo & Brescovit 1994: fig. 16d) 39
– CO with anterior margin not delimited, depressed (Figs 13D, 19D, 46C) 40

39. Lip divided into two humps (Bonaldo & Brescovit 1994: fig. 16d) ...***S. chalybeius*** (L. Koch, 1866)
– Lip entire (Figs 16D, 17C) .....***S. mandrillus*** sp. nov.

40. Depression anterior to CO deep, quadrangular (Figs 13D, 14C) ..... ***S. tremarctos*** sp. nov.
– Depression anterior to CO shallow, sub-triangular 41

41. VEP lateral margins straight, diverging anteriorly (Fig. 46C) ..... ***S. maculatus*** (L. Koch, 1866)
– VEP lateral margins curved, converging anteriorly (Figs 19D, 20C) ..... ***S. loxodonta*** sp. nov.

42. CO large (as wide as the distance between CO and posterior margin of epigynal plate), placed on the posterior half of the epigynal plate (Fig. 47C, E) .....***S. canis*** sp. nov.
– CO small (width five times smaller than the distance between CO and posterior margin of epigynal plate), placed on the anterior half of the epigynal plate (Figs 29C, 36C) 43

43. VEP posterior margin nearly straight (Figs 29C, 30C) ..... ***S. ovis*** sp. nov.
– VEP posterior margin procurved (Figs 35D, 36C) .....***S. felis*** sp. nov.

Stethorrhagus lupulus Simon, 1896
Figs 1–2, 49

Stethorrhagus lupulus Simon, 1896: 422, ♀.

Stethorrhagus lupulus – Bonaldo & Brescovit 1994: 44, fig. 10a–g, ♂♀.

Diagnosis

Males of *S. lupulus* resemble those of *S. oxossi*, *S. latoma* and *S. archangelus* by the presence of a DTA and by the prolaterally inserted embolus (Fig. 3B–F; Bonaldo & Brescovit 1994: figs 11a–b, 12a–c, 13a–c). They differ from those of *S. latoma* and *S. archangelus* by the SePP shoulder-like, blunt, developed prolaterally (Fig. 1B–F; Bonaldo & Brescovit 1994: fig. 10a) (SePP reduced to a small projection in *S. latoma* and *S. archangelus* – Fig. 5C–E; Bonaldo & Brescovit 1994: figs 12a, 13a) and from those of *S. oxossi* by the DTA large and rounded; VL with an intermediate process between vVL and dVL (Bonaldo & Brescovit 1994: fig. 10b) (DTA poorly developed, represented by a shallow excavation; intermedial process between vVL and dVL absent in *S. oxossi* – Fig. 3C–F, Bonaldo & Brescovit 1994: fig. 11b). Females are similar to those of *S. archangelus* and *S. oxossi* by the presence of a VEP (Bonaldo & Brescovit 1994: figs 11c, 12d). They differ from those of *S. archangelus* by the slit-shaped

CO and by the invaginated VEP (Fig. 2C; Bonaldo & Brescovit 1994: fig. 10f) (CO circular; VEP not invaginated in *S. archangelus* – Fig. 6C; Bonaldo & Brescovit 1994: fig. 12d) and from those of *S. oxossi* by the V-shaped CO, with a clearly delimited anterior margin (Fig. 2C; Bonaldo & Brescovit 1994: fig. 10f) (CO U-shaped, without a clearly delimited anterior margin in *S. oxossi* – Fig. 4C; Bonaldo & Brescovit 1994: fig. 11c).

Type material

Holotype

BRAZIL • ♀; Amazonas, São Paulo de Olivença; Mathan leg.; MNHN 8131 (examined).

Material examined (new records)

BRAZIL – **Acre** • 1 ♂, 1 juv.; Rio Branco, Reserva Extrativista de Humaitá; [9°40′24″ S, 67°38′31″ W]; 12 Apr. 1996; Equipe IBSP/SMNK leg; IBSP 8724 • 1 ♂; Campus Embrapa Acre; 10°1′30.8″ S,

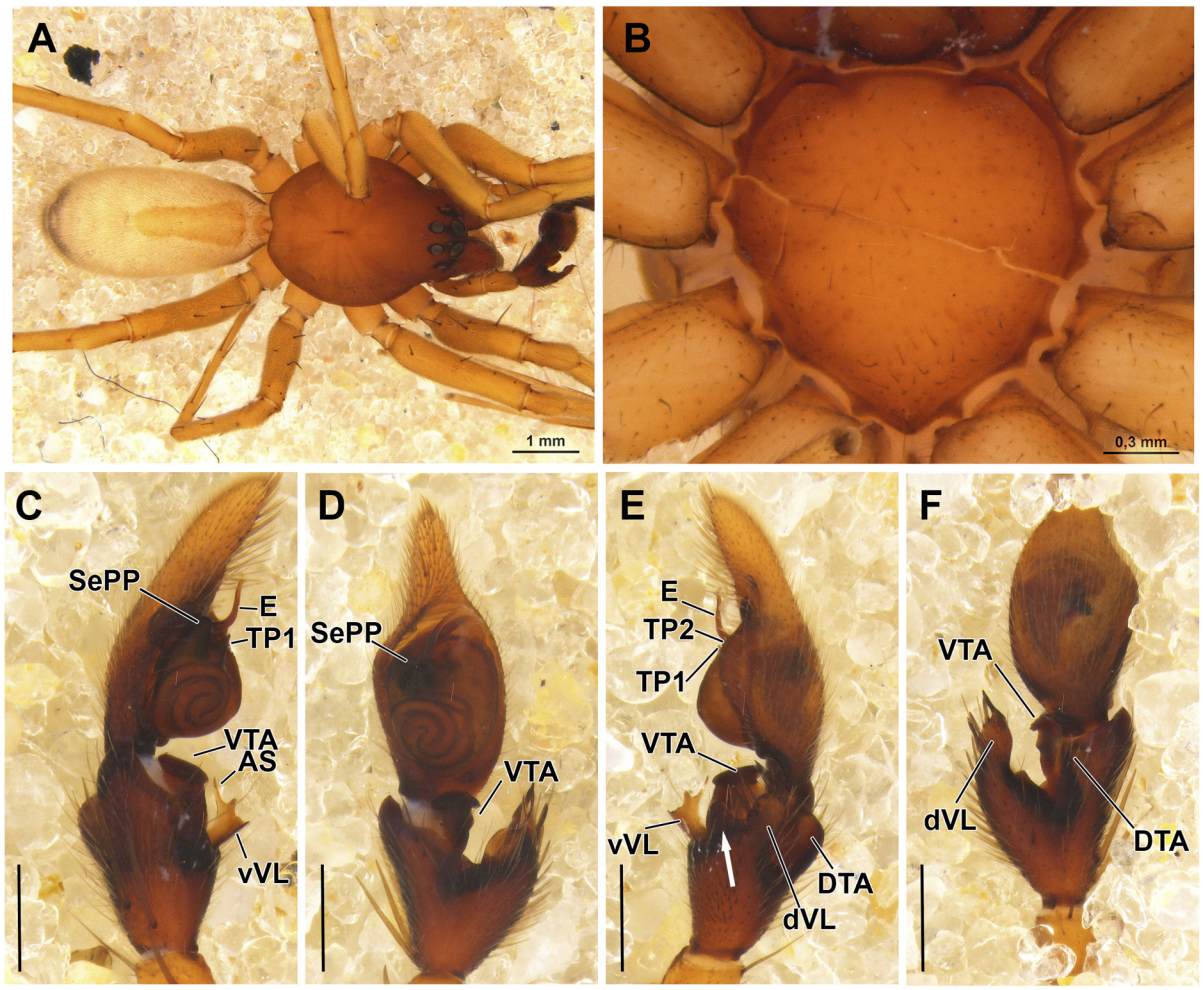

Fig. 1. *Stethorrhagus lupulus* Simon, 1896, ♂ (INPA). **A**. Habitus, dorsal view. **B**. Sternum. **C–F**. Male palp. **C**. Prolateral view. **D**. Ventral view. **E**. Retrolateral view, arrow pointing to the intermediate process between vVL and dVL. **F**. Dorsal view. Abbreviations: AS = apical spur; DTA = dorsal tibial apophysis; dVL = dorsal process of ventral lobe of RTA; E = embolus; SePP = sub-embolic prolateral process; TP1 = tegular process 1; TP2 = tegular process 2: vVL = ventral process of ventral lobe of RTA; VTA = ventral tibial apophysis. Scale bars: C–F = 0.2 mm.

67°41′35.9″ W; Sep. 2012; L.M.S. Costa leg.; UFMG 12409 • 1 ♂; Senador Guiomard, Reserva Extrativista de Catuaba; [10°4′20″ S, 67°37′39″ W]; 2002; E.F. Morato leg.; IBSP 135237. – **Amazonas** • 1 ♂; Coari, Porto Urucu, Urucu River, artificial forest gap, border; 4°52′36.8″ S, 65°9′05″ W; 14 Jul. 2003; A.B. Bonaldo leg.; collected with beating tray; MPEG 39917 • 1 ♀; same data as for preceding; 4°49′33.9″ S, 65°1′50.6″ W; 18 Jul. 2003; MPEG 39918 • 1 ♀; same data as for preceding, medium regenerated forest gap; 4°50′01″ S, 65°1′53″ W; 3 Jul. 2006; D.F. Candiani leg.; MPEG 39921 • 1 ♀; same data as for preceding, highly regenerated clearing; 4°45′48″ S, 65°2′41″ W; 26 Sep. 2006; D.F. Candiani leg.; MPEG 39919 • 1 ♀; Coari, Urucu River basin, highly regenerated forest gap; 4°48′56″ S, 65°1′53″ W; 20 Jul. 2006; L.T. Miglio leg.; manual collection at night; MPEG 39920. – **Mato Grosso** • 1 ♀; Cotriguaçu, Fazenda São Nicolau; 9°50′24″ S, 58°14′54″ W; 2–14 Oct. 2010; A.J. Santos leg.; UFMG 7773 • 1 ♀; same data as for preceding; UFMG 7792. – **Pará** • 1 ♀; Bagre, Igarapé Sequitã, Comunidade São Sebastião; 2°5′7.5″ S, 50°29′36.9″ W; 28 Jun. 2015; Josimar leg.; collected with beating tray; MPEG 39912.

PERU – **Loreto** • 3 ♀♀; Cocha Shuinguito, Río Samiria; 5°8′ S, 74°45′ W; ca 100 m; May–Jun. 1990; T. Erwin *et al.* leg.; fogging; MUSM 0504401 • 1 ♂, 1 ♀; same data as for preceding; MUSM 0504404. – **Madre de Dios** • 1 ♀; Cuenca, Río Los Amigos, Centro de Investigación y Capacitación Río Los Amigos, CICRA; [12°34′27″ S, 70°4′3″ W]; 2 Mar. 2006; M. Deza leg.; UA 564 • 1 ♀; Tambopata, Trocha La Torre; 12°50′ S, 69°17′ W; 30 Jul. 1987; D. Silva leg.; MUSM 0504340.

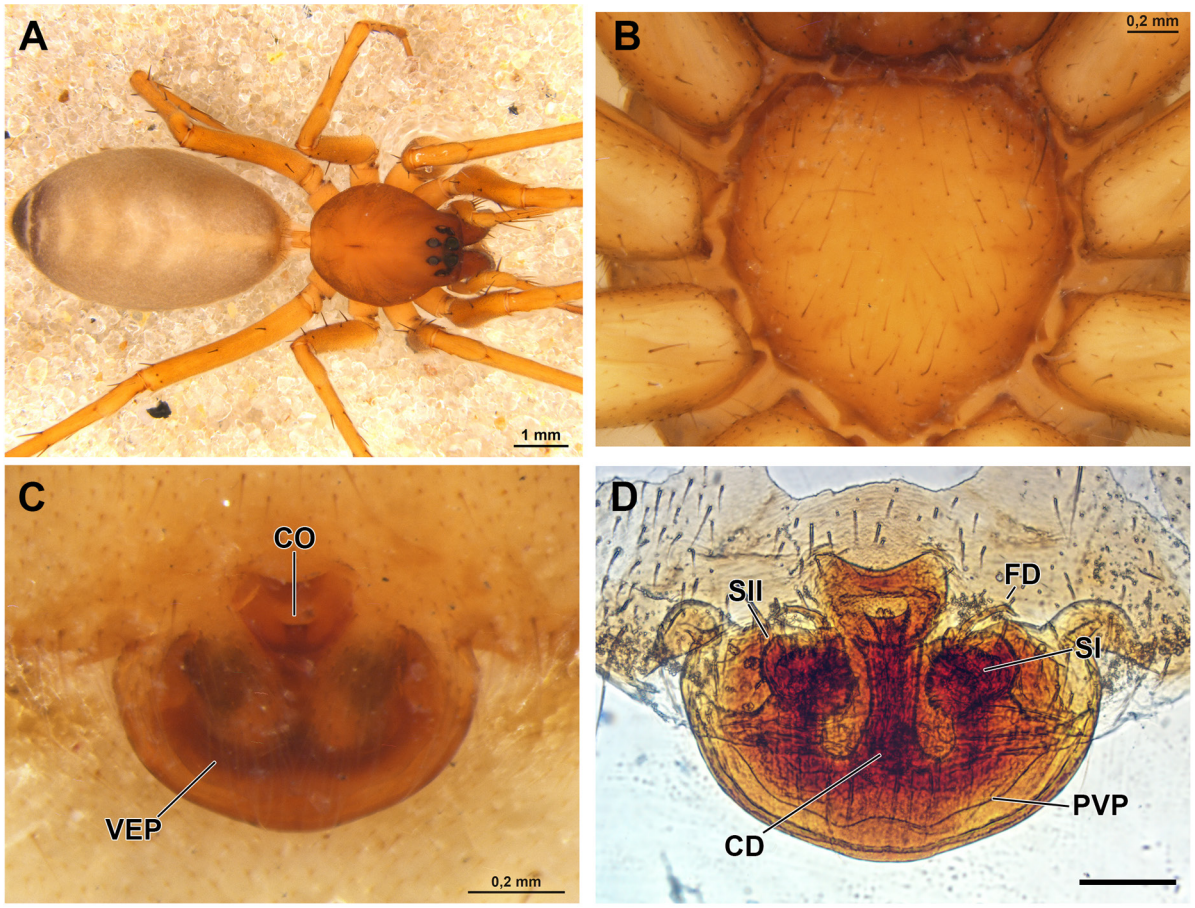

Fig. 2. *Stethorrhagus lupulus* Simon, 1896, ♀ (MPEG 39688). **A**. Habitus, dorsal view. **B**. Sternum. **C–D**. Epigynum. **C**. Ventral view. **D**. Dorsal view. Abbreviations: CD = copulatory duct; CO = copulatory opening; FD = fertilization duct; PVP = posterior vulvar plate; SI = primary spermathecae; SII = secondary spermathecae; VEP = ventral epigynal plate. Scale bar: D = 0.5 mm.

Description

Male and female, see Bonaldo & Brescovit (1994: 44). Additional documentation in Figs 1–2.

Distribution

Venezuela, Colombia, Peru and Northern Brazil (Fig. 49).

Remarks

Bonaldo & Brescovit (1994) refer to the locality Ariquemes, Ji-Paraná River, as belonging to the state of Roraima (north of the state of Amazonas). In fact, it belongs to the state of Rondônia in Brazil (south of the state of Amazonas). This mistake is corrected on the map of Fig. 49.

Stethorrhagus oxossi Bonaldo & Brescovit, 1994
Figs 3–4, 49

Stethorrhagus oxossi Bonaldo & Brescovit, 1994: 46, figs 2f, 6a–e, 7d–f, 11a–d, ♂♀.

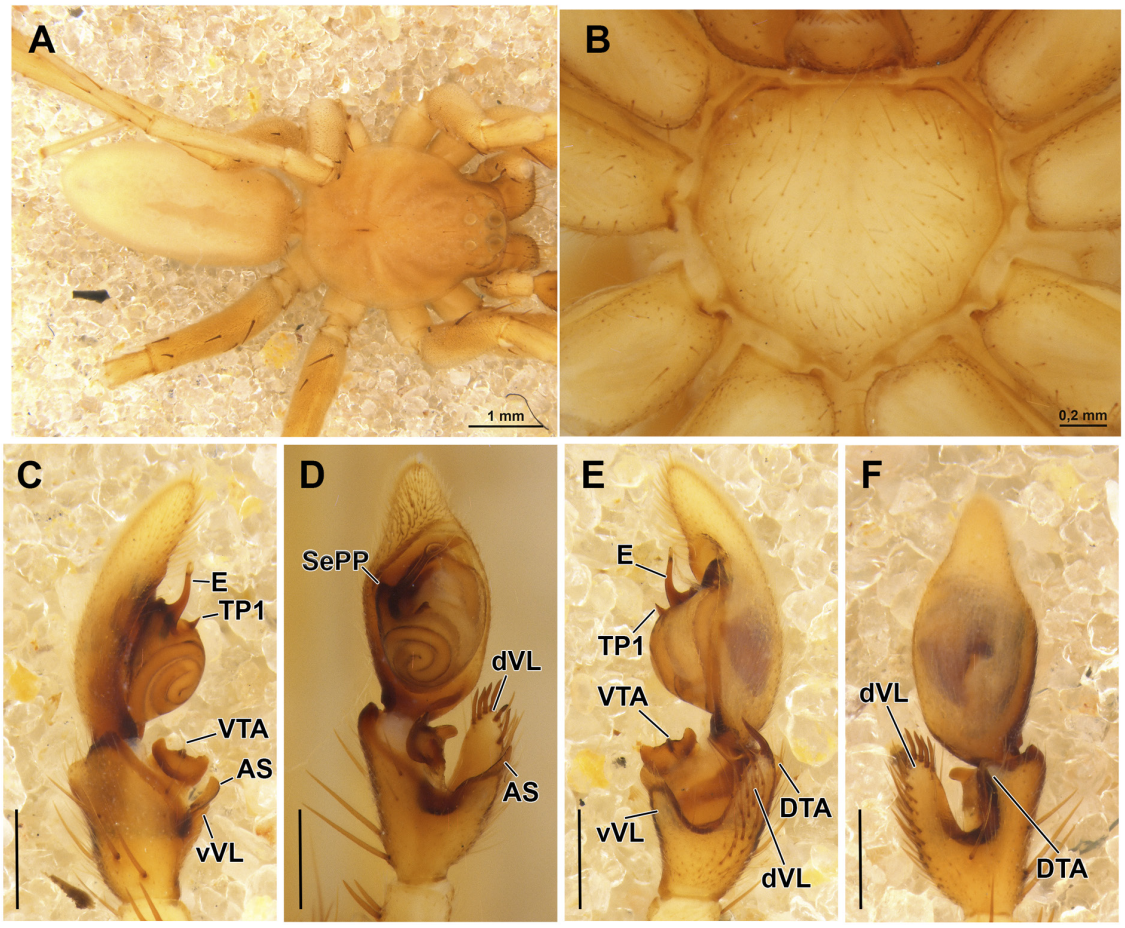

Fig. 3. *Stethorrhagus oxossi* Bonaldo & Brescovit, 1994, ♂ (MNRJ 13149). **A**. Habitus, dorsal view. **B**. Sternum. **C–F**. Male palp. **C**. Prolateral view. **D**. Ventral view. **E**. Retrolateral view. **F**. Dorsal view. Abbreviations: AS = apical spur; DTA = dorsal tibial apophysis; dVL = dorsal process of ventral lobe of RTA; E = embolus; SePP = sub-embolic prolateral process; TP1 = tegular process 1; vVL = ventral process of ventral lobe of RTA; VTA = ventral tibial apophysis. Scale bars: C–F = 0.2 mm.

Diagnosis

Males of *S. oxossi* resemble those of *S. lupulus*, *S. latoma* and *S. archangelus* by the presence of a DTA and by the prolaterally inserted embolus (Bonaldo & Brescovit 1994: figs 11a–b, 12a–c, 13a–c). They differ from those of *S. latoma* and *S. archangelus* by the SePP shoulder-like, blunt, developed prolaterally (Fig. 3D; Bonaldo & Brescovit 1994: fig. 11a) (SePP reduced to a small projection in *S. latoma* and *S. archangelus* – Fig. 5C–D; Bonaldo & Brescovit 1994: figs 12a, 13a) and from those of *S. lupulus* by the DTA poorly developed, represented by a shallow excavation; VL without intermediate process between vVL and dVL – Bonaldo & Brescovit 1994: fig. 11b (DTA large and rounded; intermedial process between vVL and dVL in *S. lupulus* - Bonaldo & Brescovit 1994: fig. 10b). Females are similar to those of *S. archangelus* and *S. lupulus* by the presence of a VEP (Bonaldo & Brescovit 1994: figs 11c, 12d). They differ from those of *S. archangelus* by the slit-shaped CO and by the invaginated VEP (Fig. 4C; Bonaldo & Brescovit 1994: fig. 11c) (CO circular; VEP not invaginated in *S. archangelus* – Fig. 6C; Bonaldo & Brescovit 1994: fig. 12d) and from those of *S. lupulus* by the U-shaped CO, without a clearly delimited anterior margin (Fig. 4C; Bonaldo & Brescovit 1994: fig. 11d) (CO V-shaped, with a clearly delimited anterior margin in *S. lupulus* – Fig. 2C; Bonaldo & Brescovit 1994: fig. 10c).

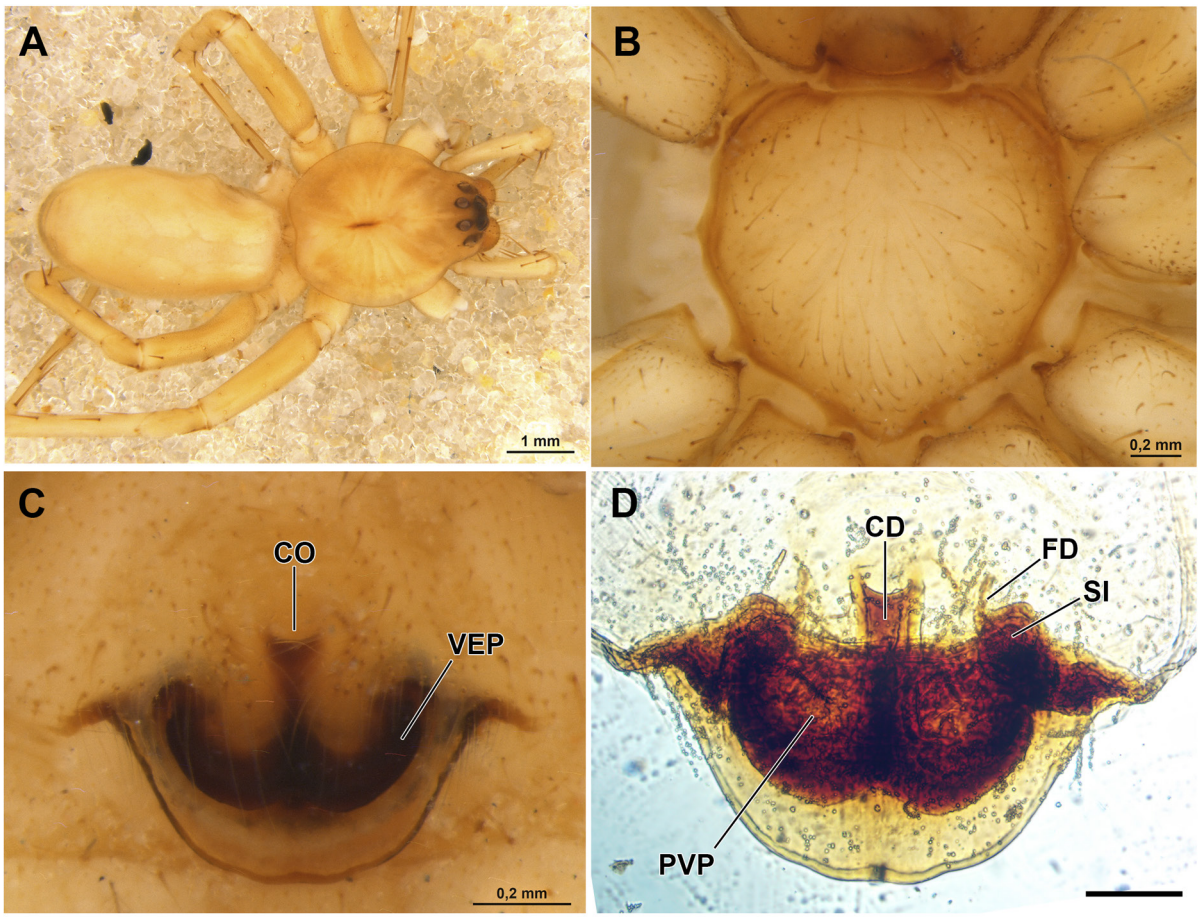

Fig. 4. *Stethorrhagus oxossi* Bonaldo & Brescovit, 1994, ♀ (MNRJ 13149). **A**. Habitus, dorsal view. **B**. Sternum. **C–D**. Epigynum. **C**. Ventral view. **D**. Dorsal view. Abbreviations: CD = copulatory duct; CO = copulatory opening; FD = fertilization duct; PVP = posterior vulvar plate; SI = primary spermathecae; VEP = ventral epigynal plate. Scale bar: D = 0.5 mm.

Type material

Holotype

BRAZIL • ♂; Bahia, Itamaraju; [17°01′51″ S, 39°31′56″ W]; MCN 24053 (not re-examined).

Paratype

BRAZIL • 1 ♀; same data as for holotype; MCN 24053 (not re-examined).

Material examined (new records)

BRAZIL – **Rio de Janeiro** • 1 ♀; Volta Redonda, Floresta da Cicuta; [22°32′56″ S, 44°05′29″ W]; Aug. 2002; M.O. Gonzaga leg.; IBSP 48940 • 1 ♂; Paraty, Prainha, entre Mambucaba e Tarituba; [23°02′30″ S, 44°34′18″ W]; 13 Dec. 1974; MNRJ. – **São Paulo** • 1 ♂; Peruíbe, Estação Ecológica de Juréia-Itatins (Núcleo Arpoador); 24°23′13.6″ S, 47°0.1′3.3″ W; 21–26 Apr. 2012; G.H.F. Azevedo and J.P.P. Pena-Barbosa leg.; UFMG 13009.

Description

Male and female, see Bonaldo & Brescovit (1994: 46). Additional documentation in Figs 3–4.

Distribution

Brazilian states of Bahia, Rio de Janeiro, and São Paulo (Fig. 49).

Stethorrhagus archangelus Bonaldo & Brescovit, 1994
Figs 5–6, 49

Stethorrhagus archangelus Bonaldo & Brescovit, 1994: 46, fig. 12a–e, ♂♀.

Diagnosis

Males of *S. archangelus* resemble those of *S. lupulus*, *S. latoma* and *S. oxossi* by the presence of a DTA and by the prolaterally inserted embolus (Bonaldo & Brescovit 1994: figs 11a–b, 12a–c, 13a–c). They differ from those of *S. lupulus* and *S. oxossi* by the SePP reduced to a small projection (Bonaldo & Brescovit 1994: fig. 12b) (SePP shouder-like in *S. lupulus* and *S. oxossi* – Bonaldo & Brescovit 1994: figs 10a, 11a) and from those of *S. latoma* by the TP1 relatively small, directed prolaterally, not covering the embolar base (Bonaldo & Brescovit 1994: fig. 12b) (TP1 directed apically, covering the embolar base in *S. latoma* – Bonaldo & Brescovit 1994: fig. 13a). Females are similar to those of *S. lupulus* and *S. oxossi* by the presence of a VEP (Bonaldo & Brescovit 1994: figs 10f, 11c, 12d). They differ from those of both these species by the CO circular and VEP round, not invaginated (Fig. 43C; Bonaldo & Brescovit 1994: fig. 12d–e) (CO slit-shaped; VEP invaginated in *S. lupulus* and *S. oxossi* – Bonaldo & Brescovit 1994: figs 10f, 11c).

Type material

Holotype

BRAZIL • ♂; Amazonas, São Gabriel da Cachoeira, Pico da Neblina; [0°24′40″ N, 65°54′28″ W]; 8 Nov. 1990; A.A. Lise leg; MCTP 1210.

Paratype

BRAZIL • 1 ♀; same data as for holotype; MCN 25461 (not re-examined).

Material examined (new record)

BRAZIL – **Amazonas** • 1 ♂; same data as for holotype; elev. 1550 m; 1 Oct. 2007; D. Candiani leg.; MPEG 39922.

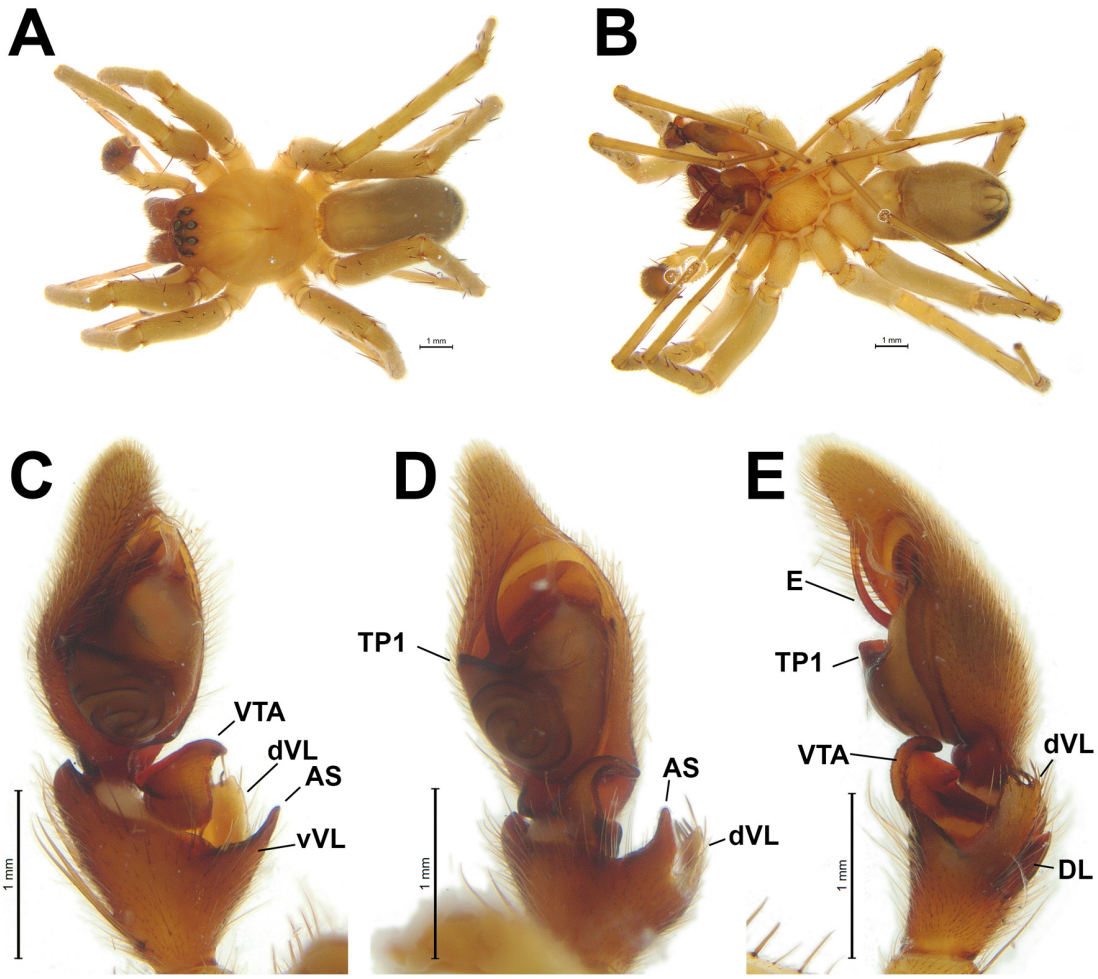

Fig. 5. *Stethorrhagus archangelus* Bonaldo & Brescovit, 1994, holotype, ♂ (MCP 1210). **A**. Habitus, dorsal view. **B**. Habitus, ventral view. **C–E**. Male palp. **C**. Pro-ventral view. **D**. Ventral-retrolateral view. **E**. Retrolateral view. Photos by Alessandra Mielke. Abbreviations: AS = apical spur; DL = RTA dorsal lobe; dVL = dorsal process of ventral lobe of RTA; E = embolus; TP1 = tegular process 1; vVL = ventral process of ventral lobe of RTA; VTA = ventral tibial apophysis.

Description

Male and female, see Bonaldo & Brescovit (1994: 46). Additional documentation in Fig. 5.

Distribution

Known only from the type locality (Fig. 49).

Stethorrhagus latoma Bonaldo & Brescovit, 1994
Fig. 50

Stethorrhagus latoma Bonaldo & Brescovit, 1994: 49, fig. 13a–c, ♂.

Diagnosis

Males of *S. latoma* resemble those of *S. archangelus* by the presence of a DTA in the male palp and SePP reduced to a small projection (Bonaldo & Brescovit 1994: figs 12a–b, 13a, c). They differ by the DTA

small and pointed; TP1 large, covering the embolar insertion in ventral view (Bonaldo & Brescovit 1994: fig. 13a–b) (DTA represented by a shallow excavation; TP1 smaller, embolar insertion visible in ventral view in *S. archangelus* – Bonaldo & Brescovit 1994: fig. 12b–c).

Type material

Holotype

VENEZUELA • ♂; Mérida, La Montana Cable Car Station; [8°34′59.57″ N, 71°7′44.45″ W]; 23–25 Feb. 1968; P. and B. Wigodzinski and M. Cormons leg.; USNM (not re-examined).

Description

Male, see Bonaldo & Brescovit (1994: 49). Female unknown.

Distribution

Merida, Venezuela (Fig. 50).

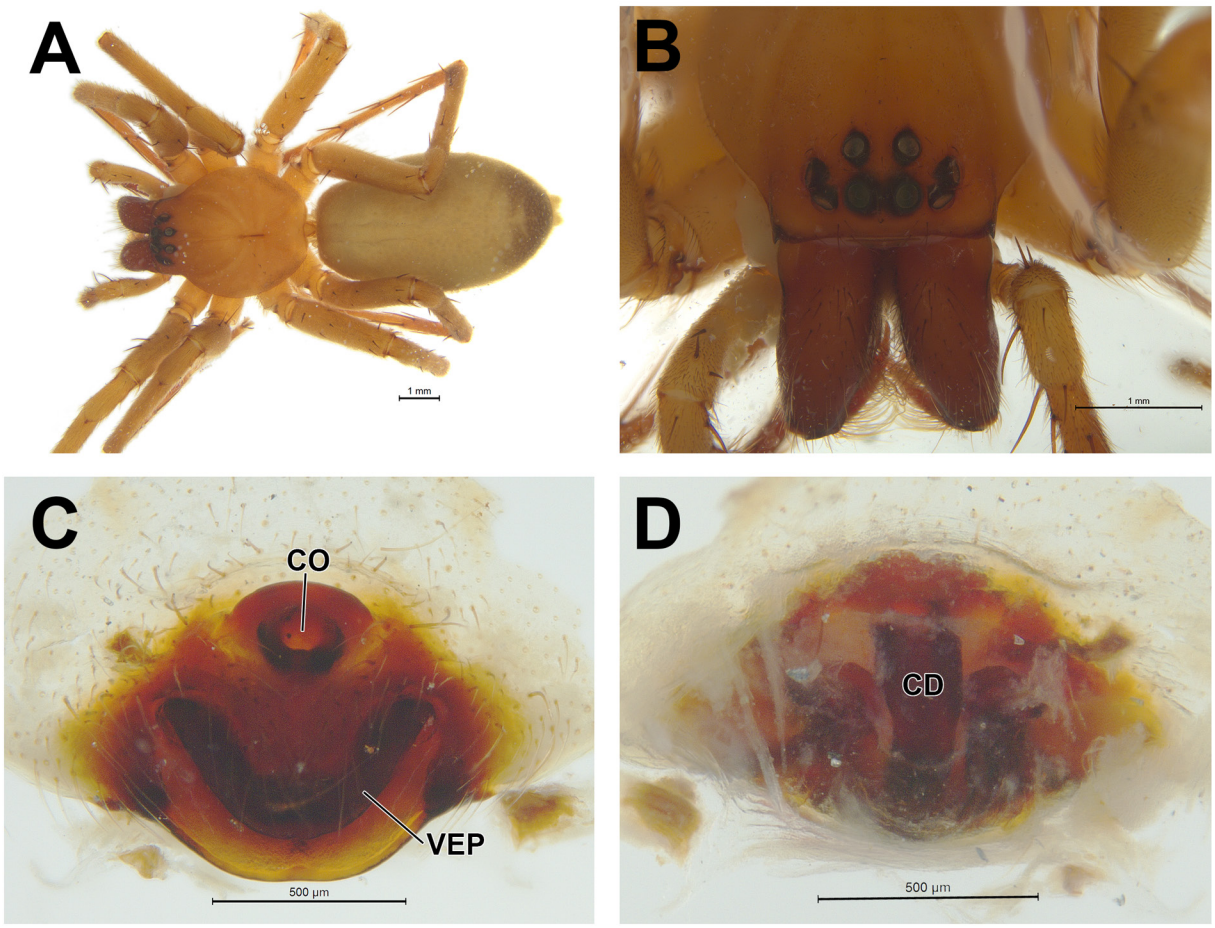

Fig. 6. *Stethorrhagus archangelus* Bonaldo & Brescovit, 1994, paratype, ♀ (MCP 1210). **A**. Habitus, dorsal view. **B**. Prosoma, frontal view. **C**. Epigynum ventral view. **D**. Epigynum dorsal view. Photos by Alessandra Mielke. Abbreviations: CD = copulatory duct; CO = copulatory opening; VEP = ventral epigynal plate.

Stethorrhagus peckorum Bonaldo & Brescovit, 1994
Figs 7D–F, 50

Stethorrhagus peckorum Bonaldo & Brescovit, 1994: 61, fig. 22a–b, ♂.

Diagnosis

Males of *S. peckorum* resemble those of *S. tridentatus* by the DTA absent and by the medially inserted embolus (Fig. 7E–F, 8C–F; Bonaldo & Brescovit 1994: figs 14a–b, 22a–b). They differ by the tibia with the AS long, with a wide base, inserted on the tibial surface; embolus widened, flat and triangular, with reduced apical prongs (Fig. 7E–F; Bonaldo & Brescovit 1994: fig. 22a–b) (AS short, inserted apically on vVL; embolus filiform, with long apical prongs in *S. tridentatus* – Fig. 8C–F; Bonaldo & Brescovit 1994: fig. 14a–b).

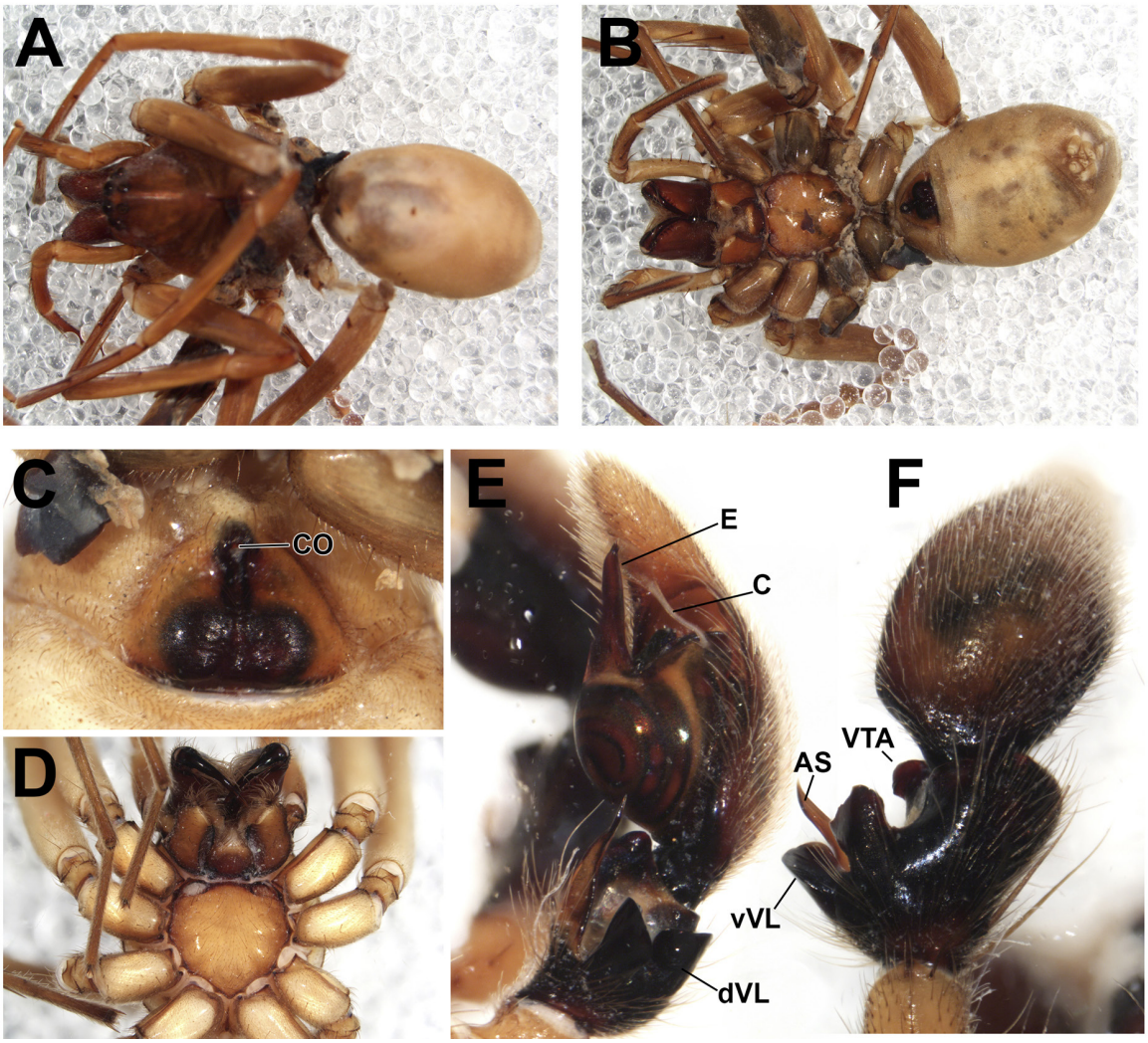

Fig. 7. A–C. *Stethorrhagus roraimae* Gertsch, 1942, holotype, ♀ (AMNH). **A**. Habitus, dorsal view. **B**. Habitus, ventral view. **C**. Epigynum ventral view. **D–F**. *Stethorrhagus peckorum* Bonaldo & Brescovit, 1994, holotype, ♂ (AMNH). **D**. Sternum. **E**. Palp, retrolateral view. **F**. Palp, dorsal view. Photos by Paulo Pantoja. Abbreviations: AS = apical spur; C = conductor; CO = copulatory opening; dVL = dorsal process of ventral lobe of RTA; E = embolus; vVL = ventral process of ventral lobe of RTA; VTA = ventral tibial apophysis.

Type material

Holotype

VENEZUELA • ♂; Bolívar, Gran Sabana, 10 km N of Luepa; [5°20′49.85″ N, 61°42′02.03″ W]; 26 Jun.–11 Jul. 1987; S. and J. Peck leg.; AMNH (examined).

Paratype

VENEZUELA • 1 ♂; same data as for holotype; AMNH (examined).

Description

Male, see Bonaldo & Brescovit (1994: 49). Female unknown. Additional documentation of the male holotype in Fig. 7D–F.

Distribution

Bolívar, Venezuela (Fig. 50).

Stethorrhagus tridentatus Caporiacco, 1955
Figs 8, 50

Stethorrhagus tridentatus Caporiacco, 1955: 379, fig. 47a–b, ♂.

Stethorrhagus tridentatus – Bonaldo & Brescovit 1994: 49, fig. 14a–e, ♂♀.

Diagnosis

Males of *S. tridentatus* resemble those of *S. peckorum* by the DTA absent and by the medially inserted embolus (Fig. 8C–F; Bonaldo & Brescovit 1994: figs 14a–b, 22a–b). They differ by the tibia with AS short, inserted apically on vVL; embolus filiform, with long apical prongs (Bonaldo & Brescovit 1994: fig. 14a–b) (AS long, with wide base, inserted on tibial surface; embolus widened, flat and triangular, with reduced apical prongs in *S. peckorum* – Bonaldo & Brescovit 1994: fig. 22a–b). Females differ from those of other species with shallow sternal excavations (*S. lupulus*, *S. oxossi* and *S. archangelus*) by the absence of a VEP and by the dorsal plate with an accentuated V-shaped notch (Bonaldo & Brescovit 1994: fig. 14d–e) (VEP present; dorsal epigynal plate not notched in *S. lupulus*, *S. oxossi* and *S. archangelus* – Bonaldo & Brescovit 1994: figs 10f–g, 11c–d, 12d–e).

Type material

Holotype

VENEZUELA • ♂; Distrito Federal, El Junquito; [10°27′43.83″ N, 67°4′59.43″ W]; 1948; Marcuzzi leg.; MUCV 703 (examined).

Material examined

VENEZUELA – **Caracas** • 1 ♂; [10°28′00″ N, 67°17′00″ W]; 1990; G. Sponga leg.; sample 860(1); MPEG 40146.

Description

Male and female, see Bonaldo & Brescovit (1994: 49, fig. 14a–e). Additional documentation of the male in Fig. 8.

Distribution

Venezuela (Fig. 47).

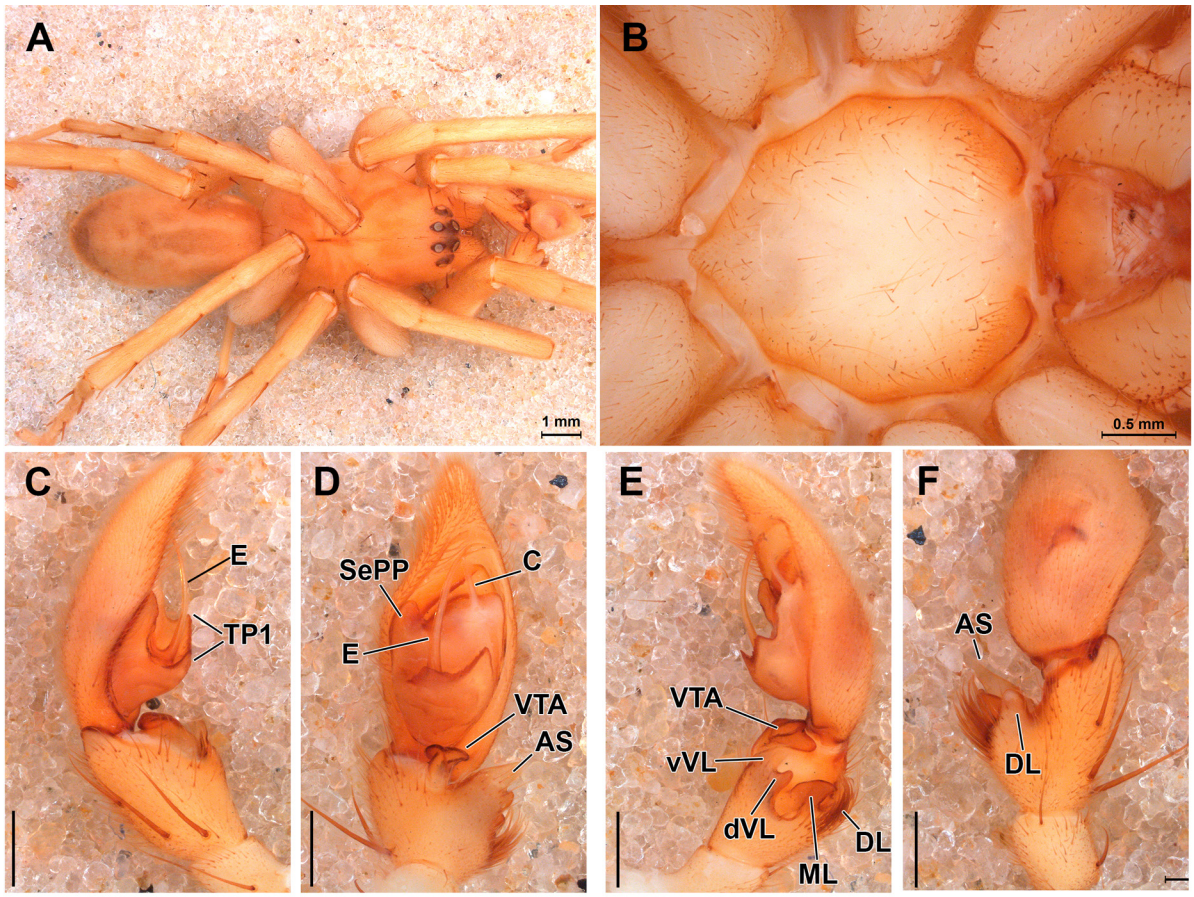

Fig. 8. *Stethorrhagus tridentatus* Caporiacco, 1955, ♂ (ex-MNHN 10914). **A**. Habitus, dorsal view. **B**. Sternum. **C–F**. Male palp. **C**. Ventral view. **D**. Retrolateral view. **E**. Dorsal view. **F**. Prolateral view. Abbreviations: AS = apical spur; C = conductor; DL = RTA dorsal lobe; dVL = dorsal process of ventral lobe of RTA; E = embolus; ML = RTA median lobe; SePP = sub-embolic prolateral process; TP1 = tegular process 1; vVL = ventral process of ventral lobe of RTA; VTA = ventral tibial apophysis. Scale bars: C–F = 0.2 mm.

Stethorrhagus limbatus Simon, 1896
Figs 9–11, 49

Stethorrhagus limbatus Simon, 1896: 421, ♂♀.
Stethorrhagus abrahami Mello-Leitão, 1948: 183, fig. 24, ♂ (synonymized with *Stethorrhagus limbatus* by Bonaldo & Brescovit 1994: 39, figs 8a–b, 9a–e).

Diagnosis

Males of *Stethorrhagus limbatus* differ from those of all other species with deep sternal excavations by the VL entire and the dVL absent (Fig. 10A–D; Bonaldo & Brescovit 1994: fig. 9a–c) (VL bifid, composed of vVL and dVL in all other species – Figs 3E, 7E–F, 13A–B); they are similar to those of *S. penai* by the SePP indistinguishable from the embolar base; absence of TP1 and presence of TP2 (Bonaldo & Brescovit 1994: fig. 15a–b) but may be recognized by the absence of the dVL and by the median sector of the spermophore coiling on the prolatero-basal region of the tegulum (Figs 10A–D; Bonaldo & Brescovit 1994: figs 9b–c) (dVL present, median sector of the spermatophore coiling on the

ventral region of tegulum in *S. penai* – Bonaldo & Brescovit 1994: fig. 15b). Females differ from those of other species with the CO disposed anteriorly in relation to the SI and without VEP (*S. nigrinus*, *S. hyula* and *S. roraimae*) by the CO composed of a large transversal excavation (nearly four times as wide as long) (Fig. 11C–E; Bonaldo & Brescovit 1994: fig. 9v) and by the wide longitudinal rods on the CD wall (Fig. 11D; Bonaldo & Brescovit 1994: fig. 9e) (CO narrower and rods inconspicuous in *S. nigrinus* and *S. hyula*; not observed in *S. roraimae* – Bonaldo & Brescovit 1994: figs 19c–d, 21b–c, 23a–b).

Type material

Lectotype of *Stethorrhagus limbatus* Simon, 1896 (designated by Bonaldo & Brescovit 1994) BRAZIL • ♂; Amazonas, Tefé; [3°23′57″ S, 64°42′58″ W]; De Mathan leg.; MNHN 3616–AR14829 (examined).

Paralectotypes of *Stethorrhagus limbatus* Simon, 1896
BRAZIL • 1 ♀; São Paulo de Olivença; 3°25′42″ S, 68°48′16″ W; De Mathan leg.; MNHN 3616–AR14830 (examined). • 1 ♀; Le Para [Belém]; [1°27′30″ S, 48°5′31″ W]; De Mathan leg.; MNHN 3616–AR14830 (examined).

Fig. 9. *Stethorrhagus limbatus* Simon, 1896, lectotype, ♂ (MNHN 3616– AR14829). **A**. Habitus, dorsal view. **B**. Habitus, ventral view. **C**. Prosoma, dorsal view. **D**. Prosoma, ventral view. Photos by Yvan Montardi.

Holotype of *Stethorrhagus abrahami* Mello-Leitão, 1948

GUIANA • ♂; Guest, Moraballi, Essequibo River; [6°23′53″ N, 58°37′44″ W]; 20 Aug. 1929; R.W.G. Hingston leg.; BMNH 1930.4.15.1A (examined).

Description

Male and female, see Bonaldo & Brescovit (1994: 39, figs 8a–b, 9a–e). Additional documentation of the habitus and copulatory organs is provided in Figs 9–11.

Distribution

States of Amazonas and Pará, Brazil; Guiana (Fig. 49).

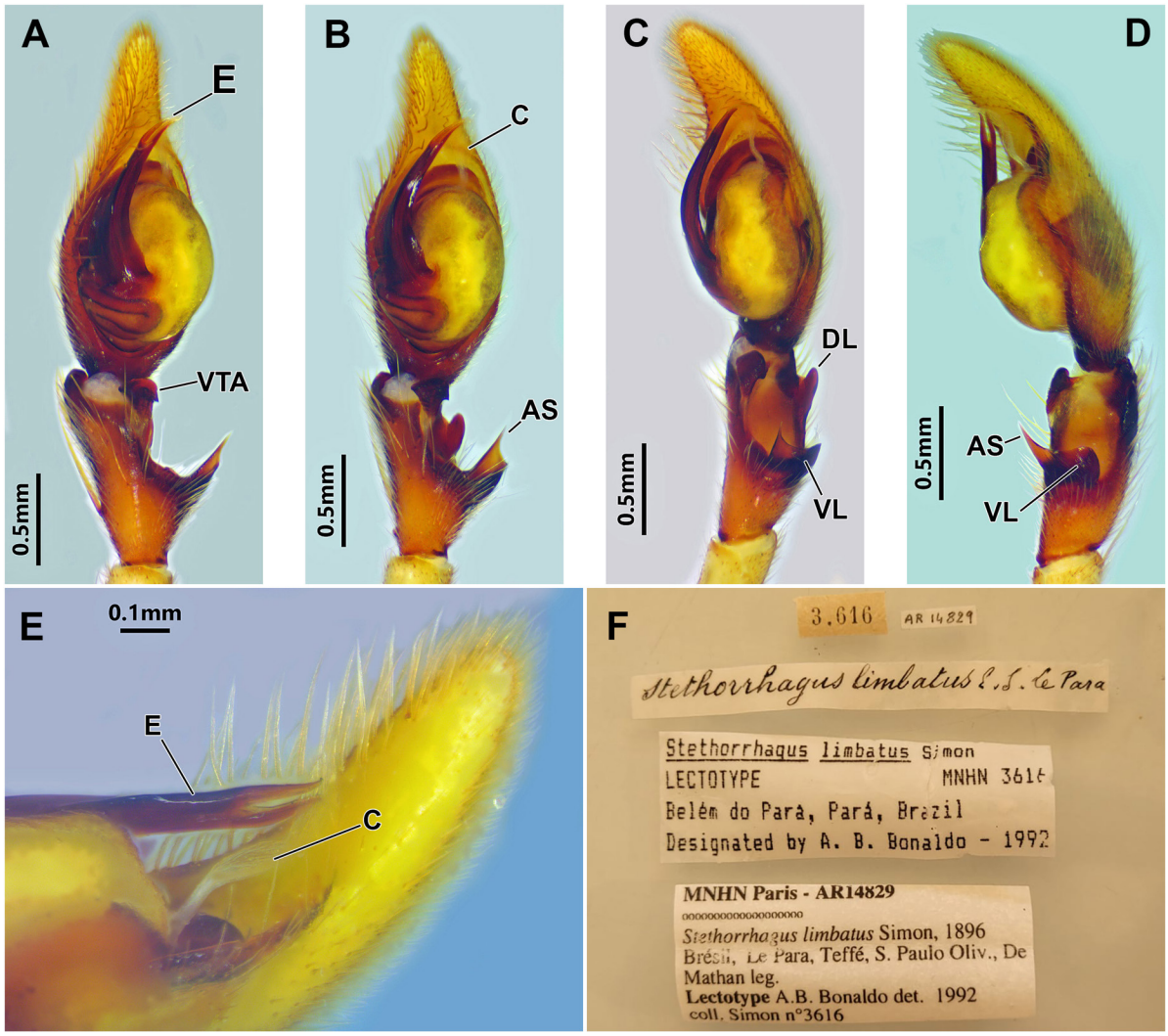

Fig. 10. *Stethorrhagus limbatus* Simon, 1896, lectotype, ♂ (MNHN 3616–AR14829), palp. **A**. Proventral view. **B**. Ventral view. **C**. Ventro-retrolateral view. **D**. Retrolateral view. **E**. Retrolateral view, detail. **F**. Labels. Photos A–E by Yvan Montardi. Abbreviations: AS = apical spur; C = conductor; DL = RTA dorsal lobe; E = embolus; VL = RTA ventral lobe; VTA = ventral tibial apophysis.

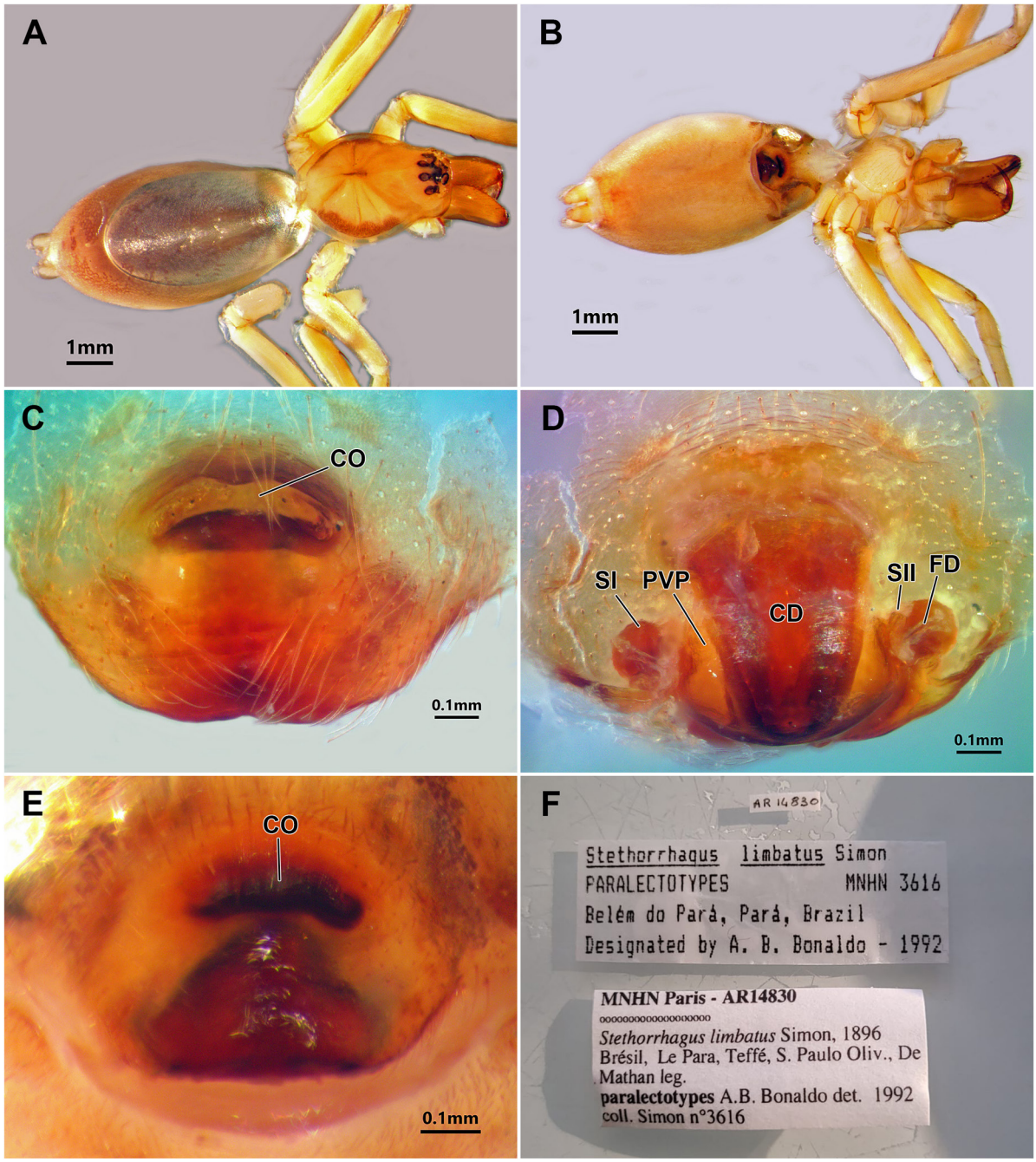

Fig. 11. *Stethorrhagus limbatus* Simon, 1896, paralectotypes ♀♀ (MNHN 3616–AR14830). **A**. Habitus, dorsal view. **B**. Habitus, ventral view. **C**, **E**. Epyginum, ventral view. **D**. Epyginum, dorsal view. **F**. Labels. Photos A–E by Yvan Montardi. Abbreviations: CD = copulatory duct; CO = copulatory opening; FD = fertilization duct; PVP = posterior vulvar plate; SI = primary spermathecae; SII = secondary spermathecae.

Stethorrhagus penai Bonaldo & Brescovit, 1994
Fig, 51

Stethorrhagus penai Bonaldo & Brescovit, 1994: 52: fig. 15a–c, ♂.

Diagnosis

Males of *Stethorrhagus penai* resemble those of *S. limbatus* by the SePP indistinguishable from the embolar base, the absence of TP1 and the presence of TP2 (Bonaldo & Brescovit 1994: figs 9b, 15b), but it may be recognized by the presence of dVL and by the median sector of the spermophor coiling on the ventral region of the tegulum (Bonaldo & Brescovit 1994: fig. 15b–c) (dVL absent; median sector of the spermophor coiling on the prolatero-basal region of the tegulum in *S. limbatus* – Bonaldo & Brescovit 1994: fig. 9a–b).

Type material

Holotype

ECUADOR • ♂; northern Ecuador, without specific locality; Sep. 1977; E.L. Peña leg.; AMNH (not re-examined).

Description

Male, see Bonaldo & Brescovit (1994: 49). Female unknown.

Distribution

Ecuador (Fig. 51).

Stethorrhagus tremarctos sp. nov.
urn:lsid:zoobank.org:act:A17E4137-B0AC-4474-B51E-561A44DFFB6C
Figs 12–14, 51

Diagnosis

Males of *S. tremarctos* sp. nov. resemble those of *S. mandrillus* sp. nov. by the glabrous dVL and AS large, laminar and shifted dorsally (Figs 13A–C, 14A–B, 16A–C, 17A–B). They can be readily distinguished by the AS triangular in retrolateral view, by the embolus inserted between SePP and SeRP, and by the VTA not bulging (Figs 13A–C, 14A–B) (AS diamond-shaped in retrolateral view, SeRP absent, and VTA bulging in *S. mandrillus* – Figs 16A–C, 17A–B). Females resemble those of *S. mandrillus*, *S. chalybeius*, *S. maculatus* and *S. loxodonta* sp. nov. by the presence of a circular CO disposed posteriorly in relation to SI (Figs 13D–E, 16D–E, 46C), differing from *S. mandrillus* and *S. chalybeius* by the anterior margin of CO not delimited by a protruding lip (lip present in *S. mandrillus*, Fig. 9D, and *S. chalybeius* – Bonaldo & Brescovit 1994: fig. 16d) and from those of *S. maculatus* and *S. loxodonta* by the deep, large quadrangular depression anterior to CO (Figs 13D, 14C) (shallow, sub-triangular depression in *S. maculatus* and *S. loxodonta* – Figs 19D, 46C).

Etymology

The specific name is a noun in apposition in reference to the monotypic genus *Tremarctos* Gervais, 1855, represented by the spectacled bear from South America, since the general conformation of the epigynum (as in Fig. 8D) resembles a bear head in frontal view.

Material examined

Holotype

ECUADOR • ♂; Napo**,** Yanayacu, Cantón Quijos; 00°35′57.8″ S, 77°53′25.3″ W; elev. 2132 m; 23–30 Nov. 2009; A.B. Bonaldo leg.; QCAZI 280513.

Paratypes

ECUADOR • 1 ♀; same data as for holotype; QCAZI 280514 • 1 ♀; same data as for holotype; MPEG 40000.

Description

Male (holotype – QCAZI 280513)

Coloration. Cephalothorax red-brown. Legs orange. Abdomen dorsally gray with orange muscular impressions, light gray ventrally (Fig. 12A). Sternum with deep sternal excavations (Fig. 12C).

Measurements. Total length 6.76. Carapace 3.42 long, 2.66 wide. Clypeus 0.23. Leg measurements: I: femur 3.00/ patella 1.24/ tibia 2.70/ metatarsus 2.45/ tarsus 1.49/ total 10.88; II: 2.95/ 1.12/ 2.38/ 2.10/ 1.47/ 10.02; III: 2.00/ 1.05/ 1.88/ 2.13/ 1.08/ 8.14; IV: 2.81/ 1.15/ 2.58/ 3.07/ 1.32/ 10.93. Eye diameters: AME 0.23, ALE 0.21, PME 0.18, PLE 0.21. Chelicerae 1.67 long, with three promarginal teeth and five retromarginal denticles.

Leg spination. I – femur d1-1-0, p0-0-1, r0; tibia d0, p0, r0, v2-2-2; metatarsus d0, p0, r0, v2-2-0. II – femur d1-1-0, p0-0-1, r0; tibia d0, p0, r0, v1r-1r-0; metatarsus d0, p0, r0, v2-2-0. III – femur d1-1-1, p0-1-1, r0-0-1; tibia d0, p1-1-0, r1-1-0, v2-2-2; metatarsus d0, p0-1-0, r0-1-0, v2-2-1. IV – femur d1-1-0, p0-0-1, r0; tibia d0, p1-1-0, r1-1-0, v1p-2-2; metatarsus d0, p1-1-1, r1-1-1, v2-2-12.

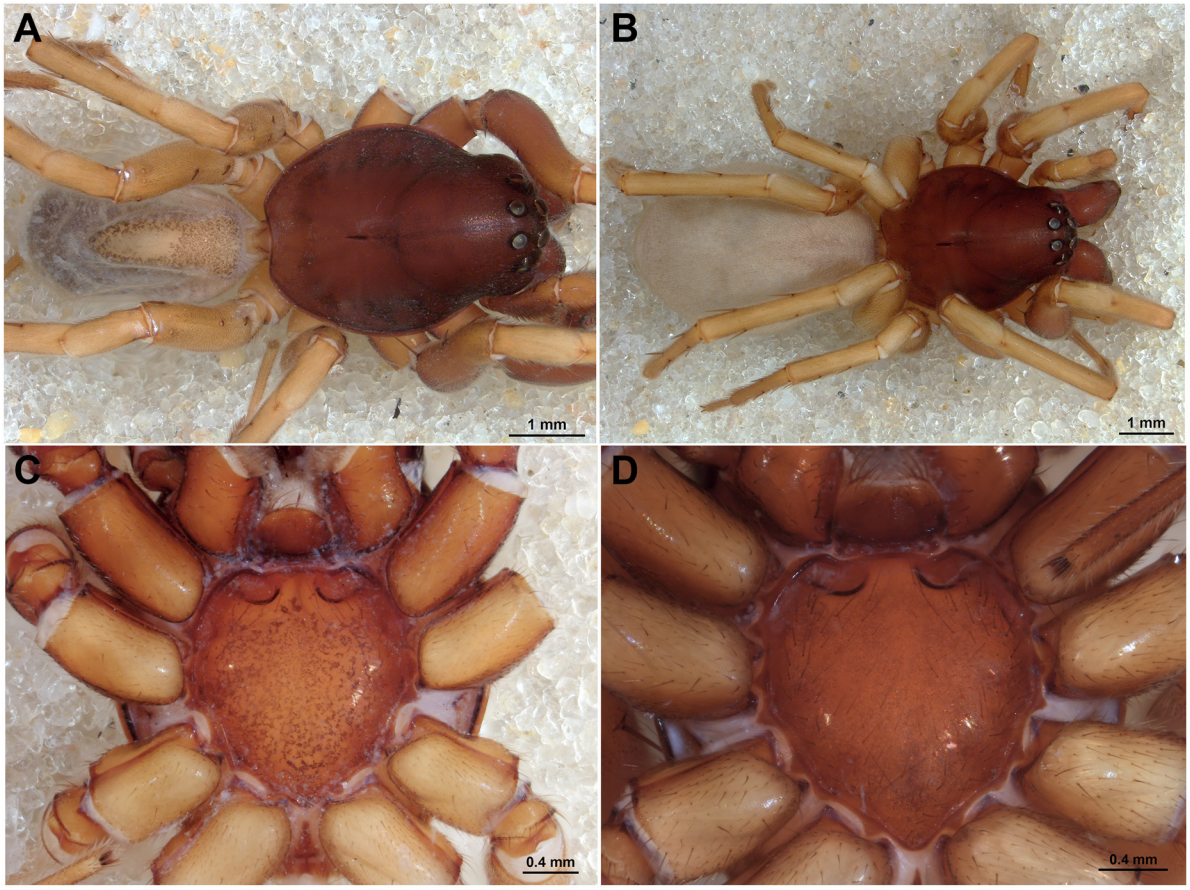

Fig. 12. *Stethorrhagus tremarctos* sp. nov. **A, C**. Holotype, ♂ (QCAZI 280513). **B, D**. Paratype, ♀ (MPEG 40000). **A–B**. Habitus, dorsal view. **C–D**. Sternum.

Palp. Retrolateral surface of femur and patella with a cluster of modified hairs, vVL with three modified hairs on the apex, dVL glabrous and not protuding, AS triangular in retrolateral view and shifted dorsally, DL reduced, spermophor situated prolaterally, TP1 short and pointed, situated medially on tegulum, embolus short and slightly curved in retrolateral view, VTA longer than broad in ventral view (Figs 13A–C, 14A–B).

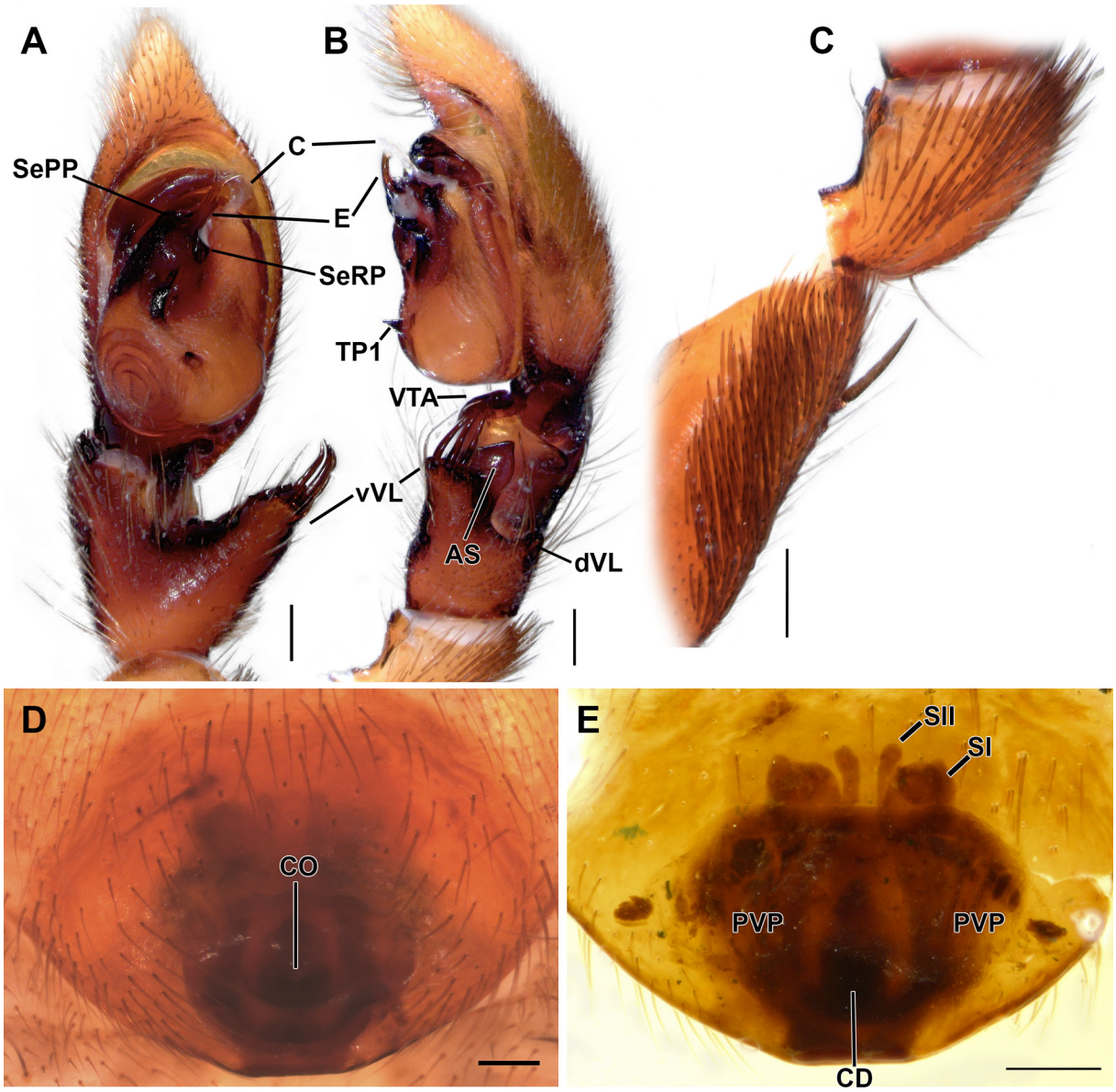

Fig. 13. *Stethorrhagus tremarctos* sp. nov., genitalia. **A–C**. Holotype, ♂ palp (QCAZI 280513). **A**. Ventral view. **B**. Retrolateral view. **C**. Femur and patella, retrolateral view. **D–E**. Paratype, ♀ (MPEG 40000), epigynum. **D**. Ventral view. **E**. Dorsal view. Abbreviations: AS = Apical spur; C = conductor; CD = copulatory duct; CO = copulatory opening; dVL = dorsal process of ventral lobe of RTA; E = embolus; PVP = posterior vulvar plate; SePP = sub-embolic prolateral process; SI = primary spermathecae; SII = secondary spermathecae; SePP = sub-embolic prolateral process; TP1 = tegular process 1; vVL = ventral process of ventral lobe of RTA; VTA = ventral tibial apophysis. Scale bars = 0.2 mm.

Female (paratype – MPEG 40000)

Coloration. As in male, except pedipalps orange-brown (Fig. 12B). Sternum with excavations as in male (Fig. 12D).

Measurements. Total length 7.90. Carapace 3.18 long, 2.65 wide. Clypeus 0.28. Eye diameters: AME 0.22, ALE 0.19, PME 0.21, PLE 0.19. Chelicerae 1.56 long, with three promarginal teeth and five retromarginal denticles. Leg measurements: I: femur 2.94/ patella 1.26/ tibia 2.49/ metatarsus 2.30/ tarsus 1.39/ total 10.38; II: 2.83/ 1.27/ 2.28/ 2.12/ 1.34/ 9.84; III: 2.39/ 1.13/ 1.88/ 2/ 1.15/ 8.55; IV: 3.06/ 1.19/ 2.53/ 3.02/ 1.22/ 11.02.

Leg spination. I – femur d1-1-0, p0-0-1, r0; tibia d0, p0, r0, v2-2-2; metatarsus d0, p0, r0, v2-2-0. II – femur d1-1-0, p0-0-1, r0; tibia d0, p0, r, v1r-1r-2; metatarsus d0, p0, r0, v2-2-0. III – femur d1-1-1, p0-1-1, r0; tibia d0, p1-1-0, r1-1-0, v2-2-2; metatarsus d0, p0-1-1, r0-1-1, v2-2-1. IV – femur d1-1-1, p0-0-1, r0-0-1; tibia d0, p1-1-0, r1-1-0, v1p-2-2; metatarsus d0, p1-1-1, r1-1-1, v2-2-1.

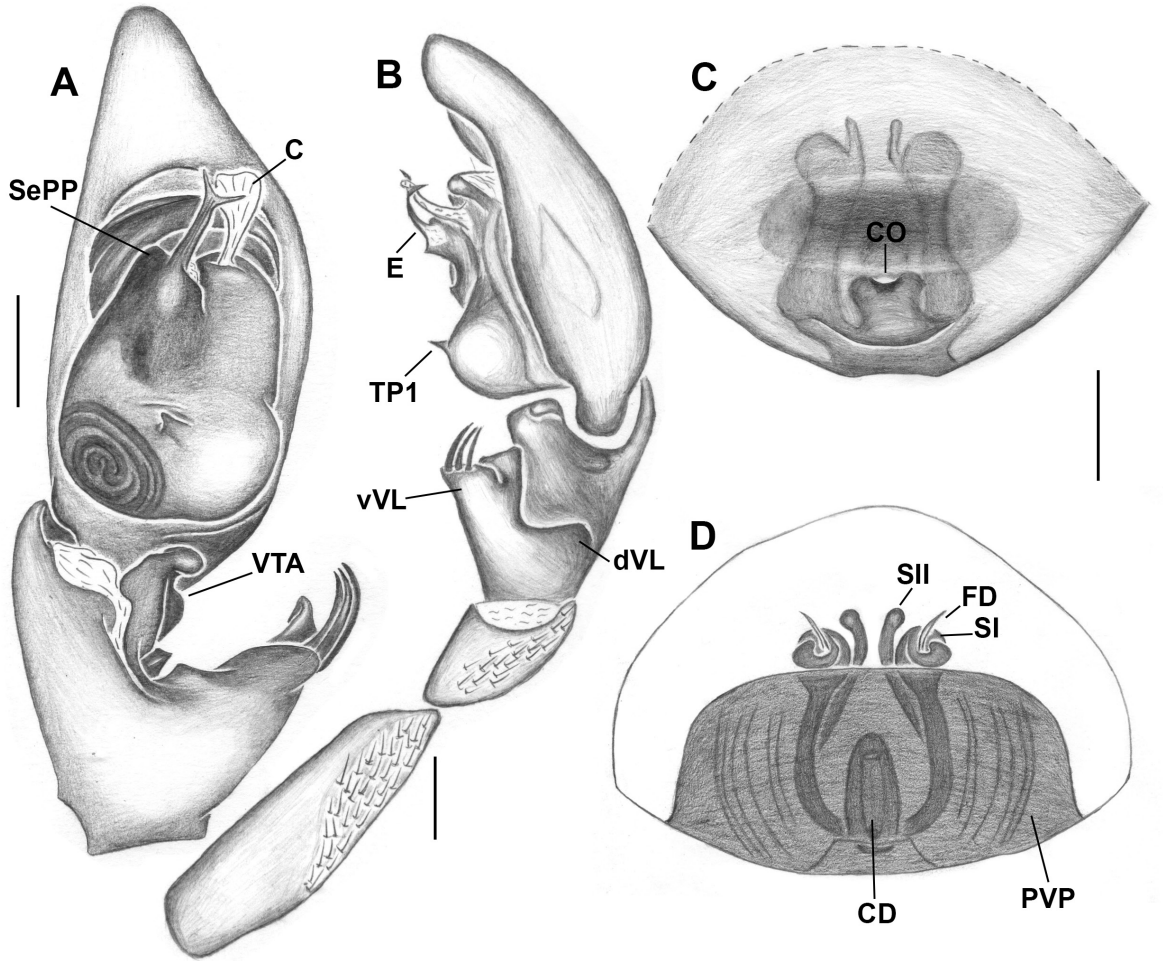

Fig. 14. A–D. *Stethorrhagus tremarctos* sp. nov. **A–B**. Holotype, ♂ (QCAZI 280513), palp. **A**. Ventral view. **B**. Retrolateral view. **C–D**. Paratype, ♀ (MPEG 40000), epigynum. **C**. Ventral view. **D**. Dorsal view. Abbreviations: C = conductor; CD = copulatory duct; CO = copulatory opening; dVL = dorsal process of ventral lobe of RTA; E = embolus; FD = fertilization ducts; PVP = posterior vulvar plate; SePP = sub-embolic prolateral process; SI = primary spermathecae; SII = secondary spermathecae; TP1 = tegular process 1; vVL = ventral process of ventral lobe of RTA; VTA = ventral tibial apophysis. Scale bars = 0.25 mm.

Epigynum. Copulatory opening circular, posteriorly situated in relation to spermathecae, anterior margin not delimited and depressed, depression anterior to CO deep, triangular, VEP present, PVP covering up to the first half of SI, secondary spermathecae elongated (Figs 13D–E, 14C–D).

Distribution

Known only from the type locality (Fig. 51).

Stethorrhagus mandrillus sp. nov.
urn:lsid:zoobank.org:act:7761DFE2-F531-4457-8D98-5158A480DFF6
Figs 15–17, 49

Diagnosis

Males of *S. mandrillus* sp. nov. resembles those of *S. tremarctos* sp. nov. by the glabrous dVL and AS large, laminar, shifted dorsally (Figs 13A–C, 14A–B, 16A–C, 17A–B). They can be readily distinguished by the AS diamond-shaped in retrolateral view, by the absence of a SeRP and by the VTA bulging (Figs 16A–C, 24A–B) (AS triangular in retrolateral view, embolus inserted between SePP and SeRP and VTA not bulging in *S. tremarctos* – Figs 13A–C, 14A–B). Females resemble those of *S. chalybeius* by the anterior margin of the CO delimited by a protruding lip, differing by the lip being entire (Fig. 16D), whereas the lip is divided into two humps in *S. chalybeius* (Bonaldo & Brescovit 1994: fig. 16d).

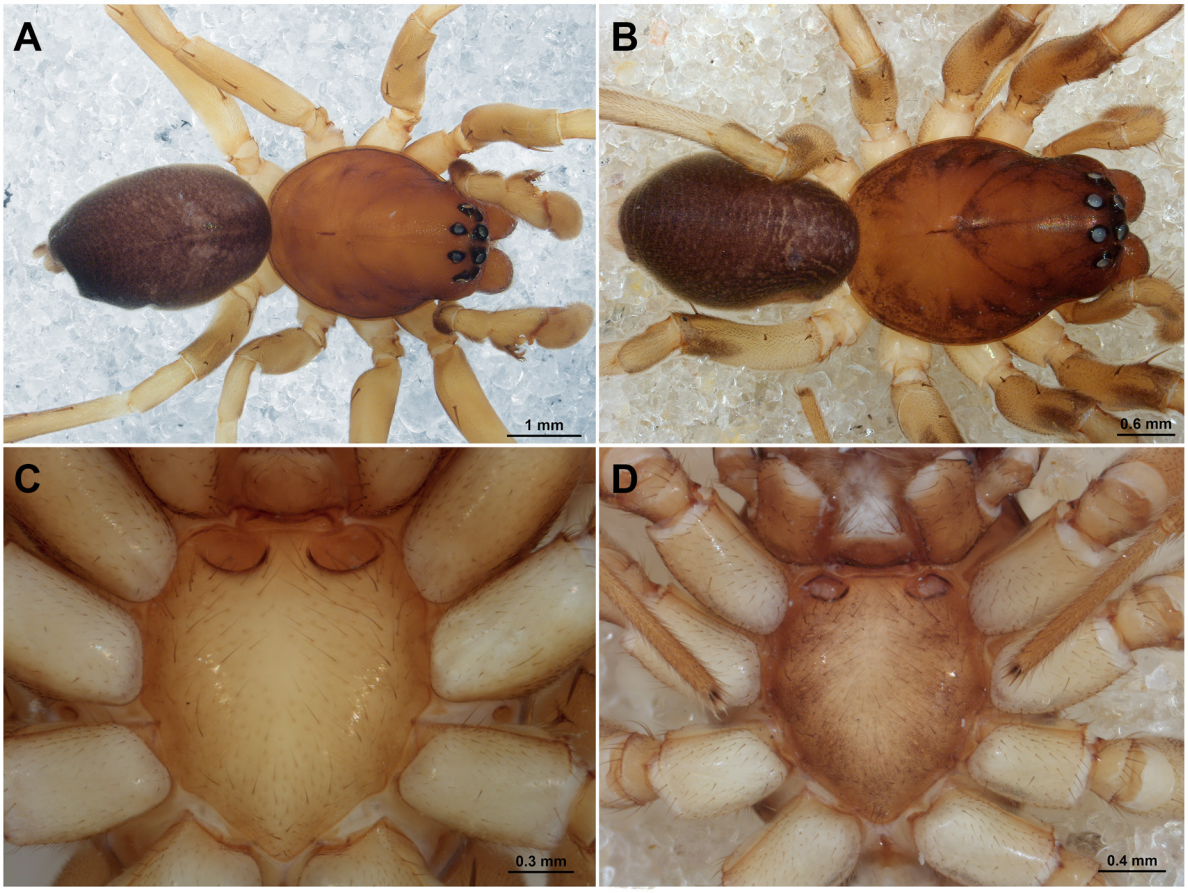

Fig. 15. *Stethorrhagus mandrillus* sp. nov. **A, C**. Holotype, ♂ (QCAZI 280515). **B, D**. Paratype, ♀ (MPEG 40002). **A–B**. Habitus, dorsal view. **C–D**. Sternum.

Etymology

The specific name is a noun in apposition in reference to the primate genus *Mandrillus* Ritgen, 1824, since the general conformation of the epigynum (as in Fig. 16D) resembles a mandrill monkey head in frontal view.

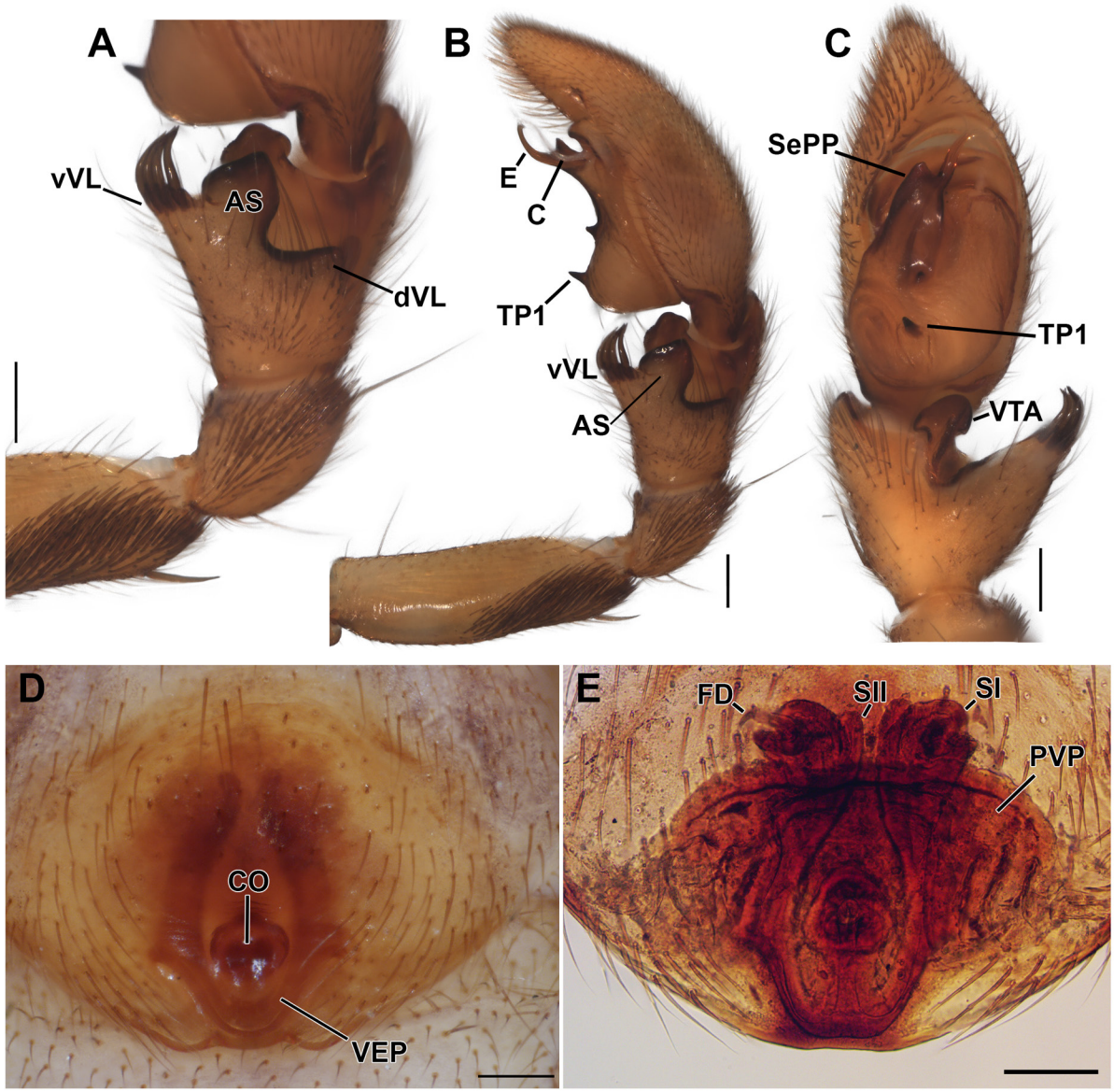

Fig. 16. *Stethorrhagus mandrillus* sp. nov., genitalia. **A–C**. Holotype, ♂ (QCAZI 280515), palp. **A**. Ventral view. **B**. Retrolateral view. **C**. Femur, patella and tibia; retrolateral view. **D–E**. Paratype, ♀ (MPEG 40002), epigynum. **D**. Ventral view. **E**. Dorsal view. Abbreviations: AS = apical spur; C = conductor; CO = copulatory opening; dVL = dorsal process of ventral lobe of RTA; E = embolus; FD = fertilization duct; PVP = posterior vulvar plate; SI = primary spermathecae; SII = secondary spermathecae; SePP = sub-embolic prolateral process; TP1 = tegular process 1; vVL = ventral process of ventral lobe of RTA; VEP = ventral epigynal plate; VTA = ventral tibial apophysis. Scale bars: A–D = 0.2 mm; E = 0.5 mm.

Material examined

Holotype

ECUADOR • ♂; Napo, Yanayacu, Cantón Quijos; 00°35′57.8″ S, 77°53′25.3″ W; elev. 2132 m; 23–30 Nov. 2009; A.B. Bonaldo leg.; QCAZI 280515.

Paratypes

ECUADOR • 1 ♂; same data as for holotype; MPEG 40001 • 1 ♀; same data as for holotype; QCAZI 280516 • 1 ♀; same data as for holotype; MPEG 40002.

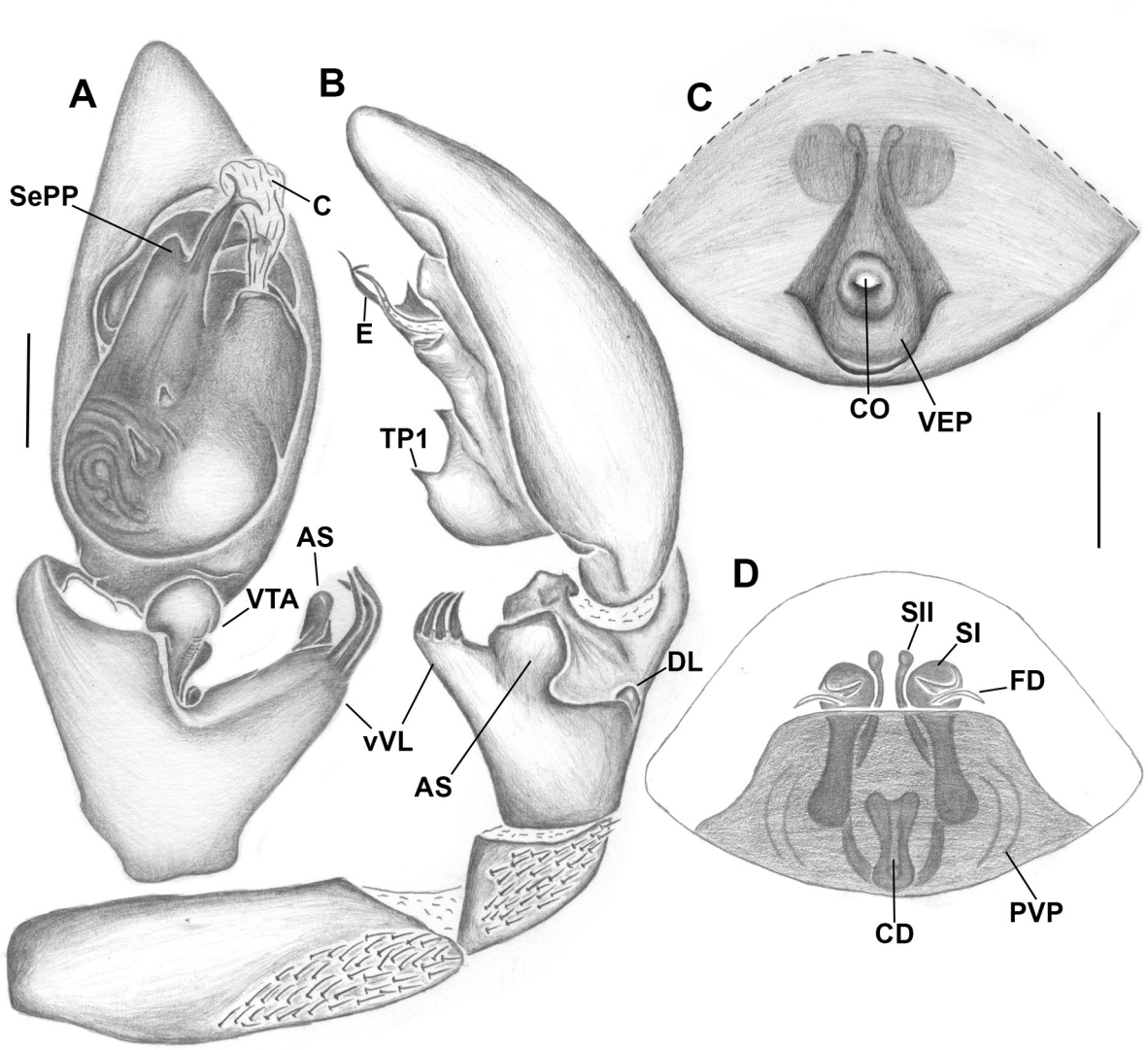

Fig. 17. *Stethorrhagus mandrillus* sp. nov. **A–B**. Holotype, ♂ (QCAZI 280515), palp. **A**. Ventral view. **B**. Retrolateral view. **C–D**. Paratype, ♀ (MPEG 40002), epigynum. **C**. Ventral view. **D**. Dorsal view. Abbreviations: AS = apical spur; C = conductor; CD = copulatory duct; CO = copulatory opening; DL = RTA dorsal lobe; E = embolus; FD = fertilization duct; PVP = posterior vulvar plate; SI = primary spermathecae; SII = secondary spermathecae; SePP = sub-embolic prolateral process; TP1 = tegular process 1; vVL = ventral process of ventral lobe of RTA; VEP = ventral epigynal plate; VTA = ventral tibial apophysis. Scale bars = 0.25 mm.

Description

Male (holotype – QCAZI 280515)

Coloration. Carapace orange-brown (Fig. 15A). Chelicerae orange. Endites, labium and sternum yellow. Legs yellow with distal area of patellae, tibiae and metatarsi gray. Abdomen dark gray dorsally and cream ventrally (Fig. 15A). Sternum with deep sternal excavations (Fig. 15C).

Measurements. Total length 6.00. Carapace 2.96 long, 2.25 wide. Clypeus 0.28. Leg measurements: I: femur 2.49/ patella 1.07/ tibia 2.07/ metatarsus 1.94/ tarsus 1.27/ total 8.84; II: 2.24/ 0.99/ 1.92/ 1.85/ 1.26/ 8.26; III: 1.78/ 0.82/ 1.48/ 1.87/ 1.03/ 6.98; IV: 2.55/ 1.02/ 2.13/ 2.64/ 1.18/ 9.52. Eye diameters: AME 0.19, ALE 0.17, PME 0.15, PLE 0.16. Chelicerae 1.31 long, with three promarginal teeth and four retromarginal denticles.

Leg spination. I – femur d1-1-0, p0-0-1, r0; tibia d0, p0, r0, v2-2-2; metatarsus d0, p0, r0, v2-2-0. II – femur d1-1-0, p0-0-1, r0; tibia d0, p0, r0, v0-1r-1r; metatarsus d0, p0, r0, v2-2-0. III – femur d1-1-1, p0, r0; tibia d0, p1-1-0, r0-0-1, v1p-2-2; metatarsus d0, p0-1-1, r0-1-1, v2-2-1. IV – femur d1-1-1, p0-0-1, r0-0-1; tibia d0, p1-1-0, r1-1-0, v1p-1p-2; metatarsus d0, p1-1-0, r1-1-0, v2-2-1.

Palp. Retrolateral surface of femur and patella with cluster of modified hairs, vVL with four modified hairs on apex, dVL glabrous and not protruding, AS diamond-shaped in retrolateral view and shifted dorsally, DL reduced, spermophor situated prolaterally, SeRP absent, TP1 short, conical, situated on distal fold of spermophor, TP2 absent, embolus short and slightly curved in retrolateral view, VTA longer than broad in ventral view (Figs 13A–C, 14A–B).

Female (paratype – MPEG 40002)

Coloration. As in male, except labium and endites orange, sternum yellow with brown borders (Fig. 15B). Sternum with sternal excavations smaller than the male (Fig. 15D).

Measurements. Total length 5.20. Carapace 2.82 long, 2.11 wide. Clypeus 0.24. Leg measurements: I: femur 2.26/ patella 0.88/ tibia 1.84/ metatarsus 1.80/ tarsus 1.20/ total 7.98; II: 2.21/ 0.85/ 1.78/ 1.74/ 1.16/ 7.74; III: 1.92/ 0.84/ 1.36/ 1.60/ 0.83/ 6.55; IV: 2.30/ 0.85/ 1.91/ 2.19/ 1.07/ 8.32. Eye diameters: AME 0.19, ALE 0.17, PME 0.16, PLE 0.16. Chelicerae 1.26 long, with three promarginal teeth and four retromarginal denticles.

Leg spination. I – femur d1-1-0, p0-0-1, r0; tibia d0, p0, r0, v1p-2-2-2; metatarsus d0, p0, r0, v2-2-0. II – femur d1-1-0, p0, r0; tibia d0, p0, r0, v1r-1r-0; metatarsus d0, p0, r0, v2-2-0. III – femur d1-1-0, p0, r0; tibia d0, p1-1-0, r1-1-0, v2-2-2; metatarsus d0, p0-1-1, r0-1-1, v2-2-1. IV – femur d1-1-0, p0, r0; tibia d0, p1-1-0, r1-1-0, v1p-2-2; metatarsus d0, p1-1-0, r1-1-0, v1p-2-1.

Epigynum. Copulatory opening circular, situated posteriorly in relation to spermathecae, anterior margin not delimited and depressed, depression anterior to CO deep, triangular, VEP present, PVP covering up the first half of SI, wider than long (Figs 13D–E, 14C–D).

Distribution

Known only from the type locality (Fig. 49).

Stethorrhagus loxodonta sp. nov.
urn:lsid:zoobank.org:act:B84568EA-9D11-4EF3-9E05-FDCF81C5D085
Figs 18–20, 51

Diagnosis

Males of *S. loxodonta* sp. nov. resemble those of *S. planada*, *S. hyula* and *S. sylvilagus* sp. nov. by the combined presence of a bifid VL and by the dVL not protruding, covered by long, thick modified hairs (Figs 19A–C, 20A–B, 21C–E, 22C–E, 25A–B, 26A–B; Bonaldo & Brescovit 1994: figs 16b, 19b), differing by the SePP and embolus geminated at the base (Figs 19A, 20A) (SePP and embolus separated at base in *S. planada*, *S. hyula* and *S. sylvilagus* – Figs 21C, 22C, 25A, 26A; Bonaldo & Brescovit 1994: figs 16a, 19a). Females resemble those of *S. tremarctos* sp. nov. and *S. maculatus* by the CO circular, disposed posteriorly in relation to SI, and the anterior margin of CO not delimited by a lip (Figs 13D–E, 19D–E, 14C–D, 20C–D, 46B–C). They differ from those of *S. tremarctos* by the depression anterior to the CO shallow, sub-triangular (Figs 19D, 20C) whereas it is deep, quadrangular in *S. tremarctos* (Figs 13D, 14C), and from those of *S. maculatus* by the VEP lateral margins curved, converging anteriorly, whereas it is straight, diverging anteriorly in *S. maculatus* (Fig. 46C).

Etymology

The specific name is a noun in apposition in reference to the Elephantidae Gray, 1821 genus *Loxodonta* Cuvier, 1825, since the general conformation of the epigynum (as in Fig. 19D) resembles an African elephant head in frontal view.

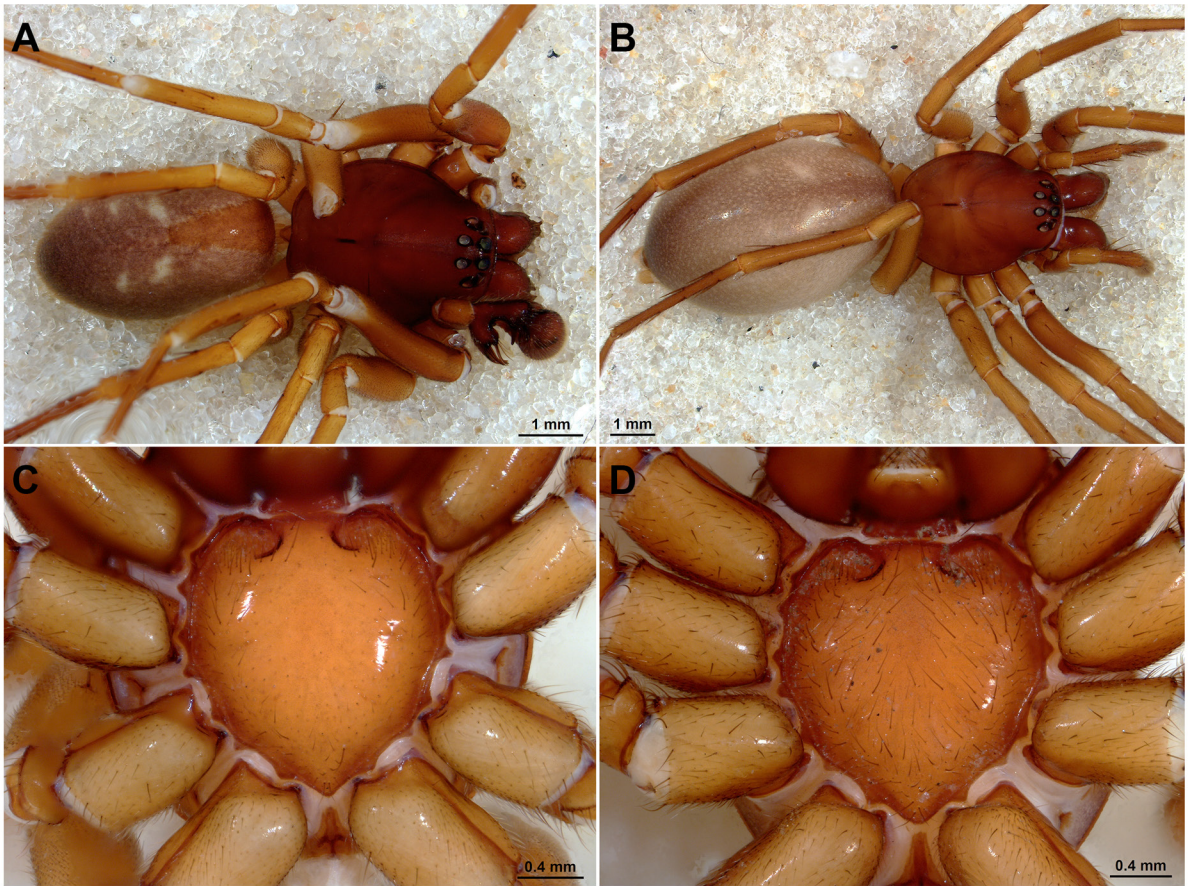

Fig. 18. *Stethorrhagus loxodonta* sp. nov. **A, C**. Holotype, ♂ (ICN Ar-1237). **B, D**. Paratype, ♀ (ICN Ar-13739). **A–B**. Habitus, dorsal view. **C–D**. Sternum.

Material examined

Holotype

COLOMBIA • ♂; Boiacá, SFF de Iguoque, Camisal; [5°43′11″ N, 73°27′42″ W]; elev. 2900 m; 9 Jun. 2001; E. Flórez and V. Rodríguez leg.; ICN-Ar 1237.

Paratypes

COLOMBIA – **Boiacá** • 1 ♀; same data as for holotype; ICN-Ar 13739 • 2 ♀♀; same data as for holotype; elev. 2810 m; 13 Jun. 2002; J. Vulpeda leg.; ICN-Ar 1902. – **Cundinamarca** • 1 ♂; Páramo

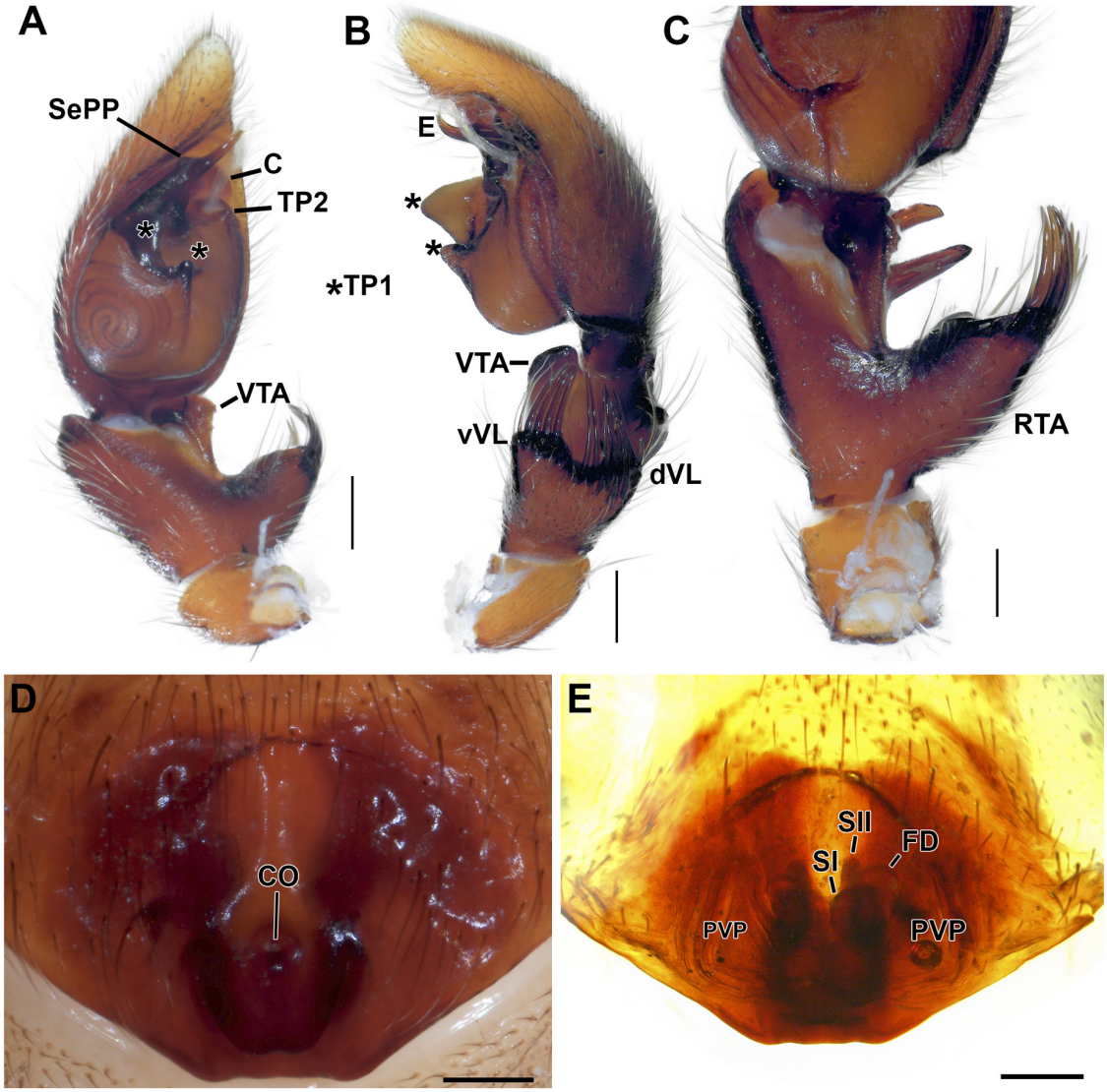

Fig. 19. *Stethorrhagus loxodonta* sp. nov. genitalia. **A–C**. Holotype, ♂ (ICN Ar-1237), palp. **A**. Ventral view. **B**. Tibia, ventral view. **C**. Retrolateral view. **D–E**. Paratypes, ♀♀, epigynum. **D**. Ventral view (ICN Ar-13739) **E**. Dorsal view (ICN Ar-1902). Abbreviations: C = conductor; CO = copulatory opening; dVL = dorsal process of ventral lobe of RTA; E = embolus; FD = fertilization duct; PVP = posterior vulvar plate; RTA = retrolateral tibial apophysis; SePP = sub-embolic prolateral process: SI = primary spermathecae; SII = secondary spermathecae; TP1 = tegular process 1; TP2 = tegular process 2; VTA = ventral tibial apophysis; vVL = ventral process of ventral lobe of RTA. Scale bars: A–B = 0.3 mm; C–E = 0.2 mm.

de Chingaza; [5°43′11″ N, 73°27′42″ W]; elev. 3100 m; 19 Oct. 2010; C. Valderrama leg.; MPEG 40003 • 1 ♂; same data as for preceding; 1 Oct. 1986; in a house; IBSP 345758.

Other material

COLOMBIA – **Cundinamarca** • 1 ♂; Bogotá, Embalse de Chisaco, El Hato, Usme; [6°32′31″ N, 73°18′27″ W]; Aug. 2008; J.E. Díaz leg; IBSP 221888.

Description

Male (holotype – ICN Ar-1237)

Coloration. Carapace, chelicerae, endites and labium brown (Fig. 18A). Sternum orange, darker at anterior border (Fig. 18C). Legs orange-brown. Abdomen dorsally brown, with four white central spots, ventrally gray (Fig. 18A). Sternum with deep sternal excavations (Fig. 18C).

Measurements. Total length 7.32. Carapace 3.25 long, 2.60 wide. Clypeus 0.31. Leg measurements: I: femur 2.74/ patella 1.12/ tibia 2.60/ metatarsus 2.43/ tarsus 1.47/ total 10.36; II: 2.67/ 1.12/ 2.34/ 2.33/ 1.36/ 9.82; III: 2.33/ 1.02/ 1.97/ 2.18/ 1.10/ 8.60; IV: 3.13/ 1.11/ 2.78/ 3.55/ 1.29/ 11.86. Eye diameters: AME 0.22, ALE 0.19, PME 0.17, PLE 0.19. Chelicerae 1.55 long, with three promarginal teeth and four retromarginal denticles.

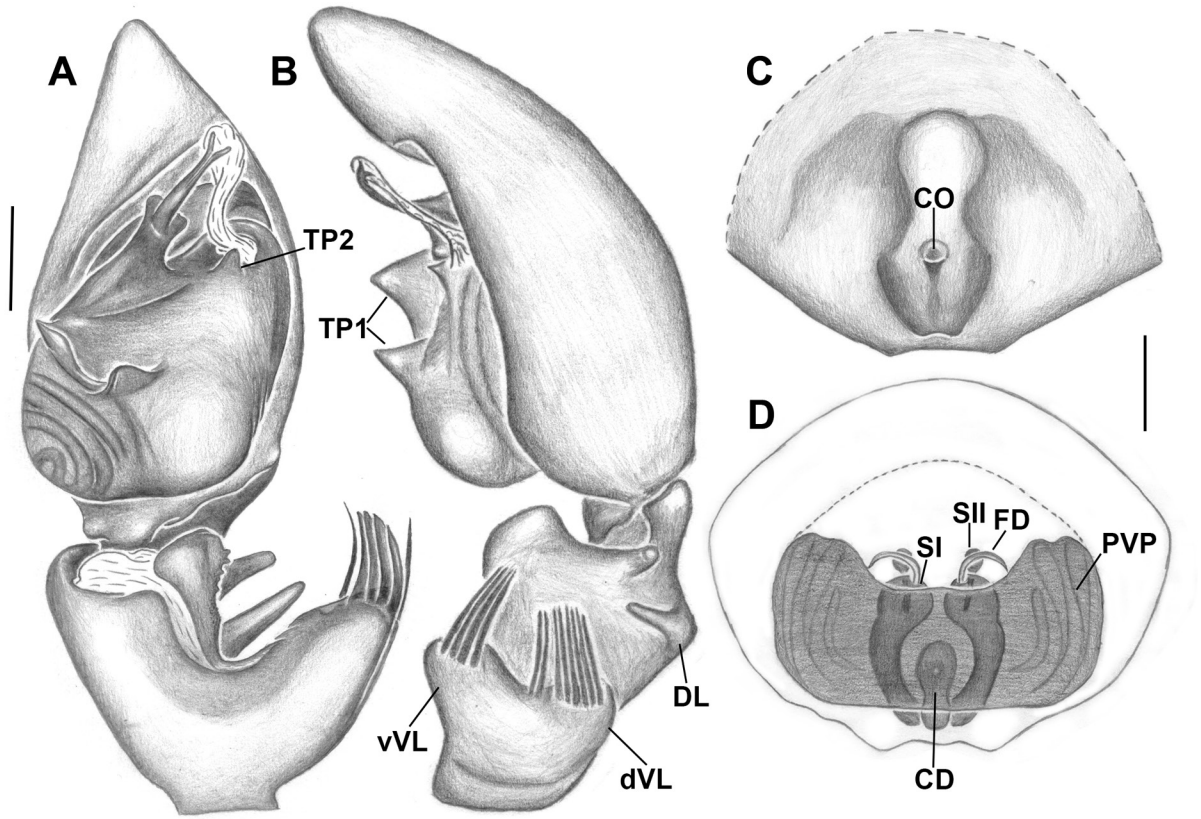

Fig. 20. *Stethorrhagus loxodonta* sp. nov. **A–B**. Holotype, ♂ (ICN Ar-1237), palp. **A**. Ventral view. **B**. Retrolateral view. **C–D**. Paratype, ♀ (ICN Ar-1902), epigynum. **C**. Ventral view. **D**. Dorsal view. Abbreviations: CD = copulatory duct; CO = copulatory opening; dVL = dorsal process of ventral lobe of RTA; DL = RTA dorsal lobe; FD = fertilization duct; PVP = posterior vulvar plate; SI = primary spermathecae; SII = secondary spermathecae; TP1 = tegular process 1; TP2 = tegular process 2; vVL = ventral process of ventral lobe of RTA. Scale bars = 0.25 mm.

Leg spination. I – femur d1-1-0, p0-1-1, r0; tibia d0, p0, r0, v2-2-2; metatarsus d0, p0, r0, v2-2-0. II – femur d1-1-0, p0-0-1, r0; tibia d0, p0, r0, v0-2-2; metatarsus d0, p0, r0, v2-2-0. III – femur d1-1-0, p0-0-1, r0-0-1; tibia d0, p1-1-0, r1-1-0, v2-2-2; metatarsus d0, p1-1-0, r1-1-0, v2-2-1. IV – femur d1-1-0, p0-0-1, r0-0-1; tibia d0, p1-1-0, r1-1-0, v2-2-2; metatarsus d0, p1-1-1, r1-1-1, v2-2-1.

Palp. RTA discreetly bilobed, noticeable by the tufts of modified setae at different apices (vVL and dVL), VTA longer than wide, with proximal surface about seven times smaller than distal surface, spermophor situated prolaterally, SePP and embolus geminated at base, embolus short, not curved, TP1 bilobated and projected (visible in retrolateral view), situated on distal fold of the spermophor, TP2 small and subtriangular (Figs 19A–C, 20A–B).

Female (paratype, MPEG 40003)

Coloration. As in male (Fig. 18B). Sternum with sternal excavations as in male (Fig. 18D).

Measurements. Total length 9.35. Carapace 3.57 long, 2.80 wide. Clypeus 0.27. Leg measurements: I: femur 2.78/ patella 1.23/ tibia 2.60/ metatarsus 2.25/ tarsus 1.47/ total 10.33; II: 2.76/ 1.30/ 2.33/ 2.25/ 1.37/ 10.01; III: 2.63/ 1.21/ 2.05/ 2.37/ 1.25/ 9.51; IV: 3.32/ 1.30/ 3.0/ 3.56/ 1.43/ 12.61. Eye diameters: AME 0.21, ALE 0.19, PME 0.18, PLE 0.19. Chelicerae 1.83 long, with three promarginal teeth and four retromarginal denticles.

Leg spination. I – femur d1-1-1, p0-0-1, r0; tibia d0, p0, r0, v2-2-2; metatarsus d0, p0, r0, v2-2-0. II – femur d1-1-0, p0-0-1, r0; tibia d0, p0, r0, v1r-2-2; metatarsus d0, p0, r0, v2-2-0. III – femur d1-1-0, p0-1-1, r0-1-1; tibia d0, p1-1-0, r1-1-0, v2-2-2; metatarsus d0, p1-1-1, r1-1-1, v2-2-1. IV – femur d1-1-0, p0-0-1, r0-0-1; tibia d0, p1-1-0, r1-1-0, v2-2-2; metatarsus d0, p1-1-0, r1-1-0, v2-2-1.

Epigynum. CO circular and disposed posteriorly in relation to SI, anterior margin of CO not delimited and depressed, depression anterior to CO shallow, subtriangular, VEP lateral margins curved, converging anteriorly, placed posteriorly on epigynal plate, PVP wider, two times the distance between the anterior and posterior margins, covering SI, copulatory duct relatively short, from CO to posterior margin of VEP (Figs 19D–E, 20C–D).

Distribution

Colombia (Fig. 51).

Stethorrhagus planada Bonaldo & Brescovit, 1994
Figs 21, 51

Stethorrhagus planada Bonaldo & Brescovit, 1994: 56, figs 17a–b, 18a–c, ♂♀.

Diagnosis

Males of *S. planada* resemble those of *S. loxodonta* sp. nov., *S. hyula* and *S. sylvilagus* sp. nov. by the combined presence of a bifid VL and by the dVL not protruding, covered by long, thick modified hairs (Fig. 21D–E; Bonaldo & Brescovit 1994: figs 17b, 19b), differing from those of *S. loxodonta* by the SePP and embolus separated at base (Fig. 21C) (SePP and embolus geminated at base in *S. loxodonta* – Fig. 20A) and from those of *S. hyula* and *S. sylvilagus* by the TP1 represented by a wide, serrated keel (Fig. 21C; Bonaldo & Brescovit 1994: fig. 17b) (TP1 tooth-like in *S. hyula* and *S. sylvilagus* – Figs 22D, 25A, 26A; Bonaldo & Brescovit 1994: fig. 19a). Females resemble those of *S. callithrix* sp. nov., *S. sylvilagus* and *S. sciurus* sp. nov. by the epigynum with VEP, CO disposed anteriorly in relation to SI, with U-shaped posterior margin, differing by the sub-rectangular VEP, placed medially on the epigynal plate (Bonaldo & Brescovit 1994: fig. 18a) (VEP gently procurved, placed posteriorly on the epigynal plate in *S. callithrix*, *S. sylvilagus* and *S. sciurus* – Figs 25C, 26C, 32C, 33C, 43C–D).

Type material

Holotype

COLOMBIA • ♂; Nariño, Ricaurte, Reserva Natural de La Planada; [01°09′14.10″ N, 77°58′47.16″ W]; elev. 1850 m; 6 Dec. 1991; C. Valderrama A. leg.; MCN 24050 (not re-examined).

Paratype

COLOMBIA • 1 ♀; same data as for holotype; MCN 24050 (not re-examined).

Description

Male and female, see Bonaldo & Brescovit (1994: 49). Additional documentation of the male in Fig. 21.

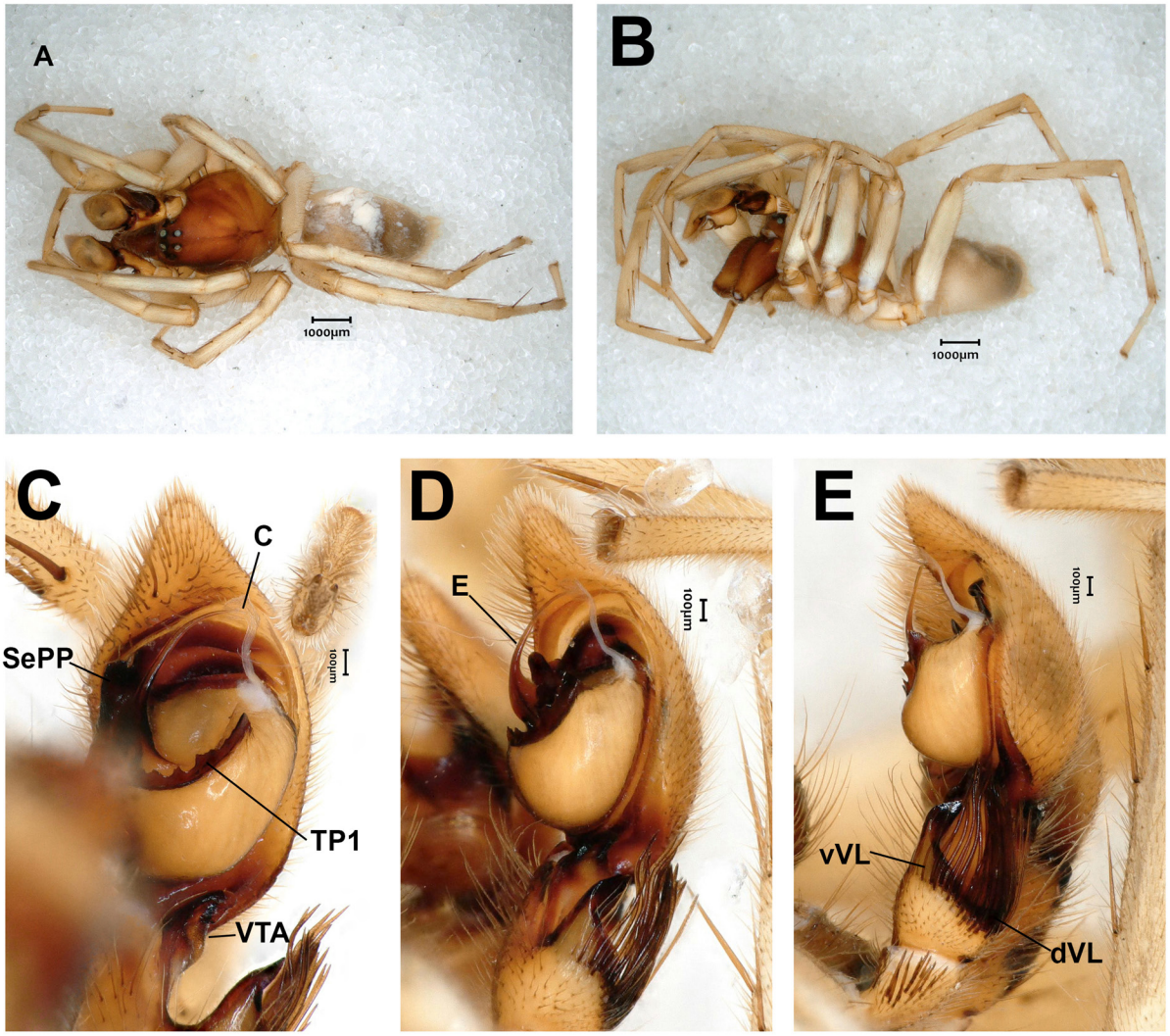

Fig. 21. *Stethorrhagus planada* Bonaldo & Brescovit, 1994, syntype, ♂ (MCZ 34654). **A**. Habitus, dorsal view. **B**. Habitus, lateral view. **C–E**. Palp. **C**. Ventral view. **D**. Ventral-retrolateral view. **E**. Retrolateral view. Photos by Ligia Benavides. Abbreviations: C = conductor; dVL = dorsal process of ventral lobe of RTA; E = embolus; SePP = sub-embolic prolateral process; TP1 = tegular process 1; VTA = ventral tibial apophysis; vVL = ventral process of ventral lobe of RTA.

Distribution

Colombia (Fig. 51).

Stethorrhagus hyula Bonaldo & Brescovit, 1994
Figs 22–23, 50

Stethorrhagus hyula Bonaldo & Brescovit, 1994: 57, fig. 19a–d, ♂♀.

Diagnosis

Males of *S. hyula* resemble those of *S. loxodonta* sp. nov., *S. planada* and *S. sylvilagus* sp. nov. by the presence of a bifid VL and by the dVL not protruding, covered by long, thick modified hairs (Figs 19B, 21E, 22E, 25B, 26B; Bonaldo & Brescovit 1994: figs 17b, 19b), differing from those of *S. loxodonta* by the SePP and embolus separated at base (Fig. 37C–D; Bonaldo & Brescovit 1994: fig. 19a) (SePP

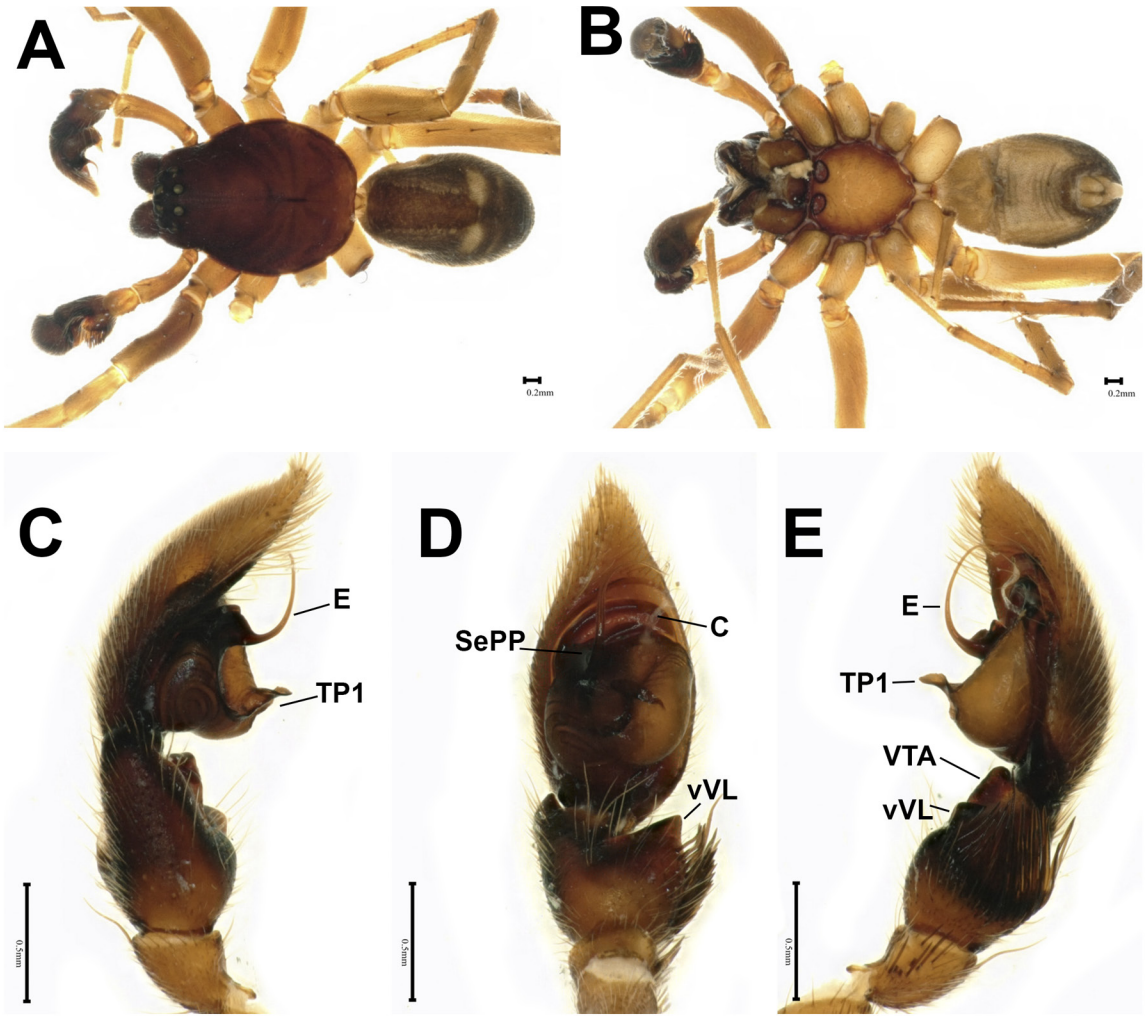

Fig. 22. *Stethorrhagus hyula* Bonaldo & Brescovit, 1994, holotype, ♂ (MCZ 34655). **A**. Habitus, dorsal view. **B**. Habitus, ventral view. **C–E**. Male palp. **C**. Prolateral view. **D**. Ventral view. **E**. Retrolateral view. Photos by Ligia Benavides. Abbreviations: C = conductor; E = embolus; SePP = sub-embolic prolateral process; TP1 = tegular process 1; VTA = ventral tibial apophysis; vVL = ventral process of ventral lobe of RTA.

and embolus geminated at base in *S. loxodonta* – Fig. 10A); from those of *S. planada* by the tooth-like TP1 (Fig. 21C–D; Bonaldo & Brescovit 1994: fig. 19a–b) (TP1 represented by a wide, serrated keel in *S. planada* – Fig. 21C; Bonaldo & Brescovit 1994: fig. 17a–b), and from those of *S. sylvilagus*, by the TP1 curved, pointing prolaterally (Bonaldo & Brescovit 1994: fig. 19a) (TP1 straight, pointing apically in *S. sylvilagus* – Figs 25A, 26A). Females are similar to those of *S. roraimae*, *S. nigrinus* and *S. papilio* sp. nov. by the epigynal plate without VEP, with CO disposed anteriorly in relation to SI (Figs 7C, 23C–D, 44C–D, 45C–F; Bonaldo & Brescovit 1994: figs 19a, 23a), differing by the presence of a posterior median half-moon-shaped sclerotization on the ventral epigynal plate (Bonaldo & Brescovit 1994: fig. 19c) (ventral epigynal plate without such a sclerotization in *S. roraimae*, *S. nigrinus* and *S. papilio* – Figs 7E–F, 44C–D, 45C–F; Bonaldo & Brescovit 1994: fig. 23s).

Type material

Holotype

COLOMBIA • ♂; Huila, Resina; 1°55′ N, 75°42′ W; elev. 1600 m; 8 Jun. 1956; H. Sturm leg.; MCZ 34655 (re-examined from photos).

Paratype

COLOMBIA • 1 ♀; same data as for holotype; MCZ 34656 (re-examined from photos).

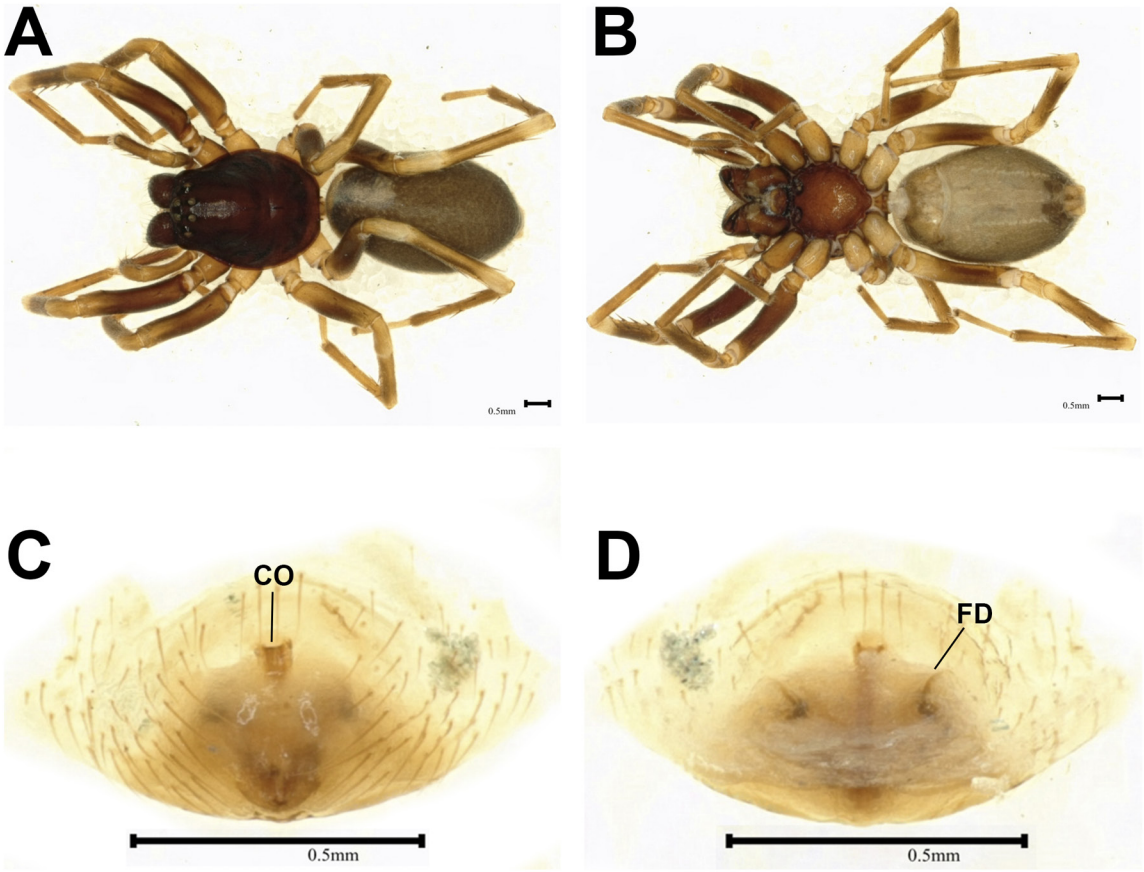

Fig. 23. *Stethorrhagus hyula* Bonaldo & Brescovit, 1994, paratype, ♀ (MCZ 34656). **A**. Habitus, dorsal view. **B**. Habitus, ventral view. **C**. Epigynum ventral view. **D**. Epigynum dorsal view. Photos by Ligia Benavides. Abbreviations: CO = copulatory opening; FD = fertilization duct.

Description

Male and female, see Bonaldo & Brescovit (1994: 49). Additional documentation in Figs 22–23.

Distribution

Colombia (Fig. 50).

Stethorrhagus sylvilagus sp. nov.
urn:lsid:zoobank.org:act:253618EB-1F11-4270-962F-FC31BAF8E73C
Figs 24–26, 51

Diagnosis

Males of *S. sylvilagus* sp. nov. resemble those of *S. loxodonta* sp. nov., *S. planada* and *S. hyula* by the presence of a bifid VL and by the dVL not protruding, covered by long, thick modified hairs (Figs 19B, 21E, 22E, 25B, 26B; Bonaldo & Brescovit 1994: figs 17b, 19b), differing by the presence of a mVL. Particularly, they differ from those of *S. loxodonta* by the SePP and embolus separated at the base (SePP and embolus geminated at base in *S. loxodonta* – Fig. 19A); from those of *S. planada* by the tooth-like TP1 (Figs 25A, 26A) (TP1 represented by a wide, serrated keel in *S. planada* – Fig. 21C; Bonaldo & Brescovit 1994: fig. 17a) and from those of *S. hyula*, by the TP1 straight, pointing apically (Figs 25A, 26A) (TP1 curved, pointing prolaterally in *S. hyula* – Fig. 22D; Bonaldo & Brescovit 1994: fig. 19a).

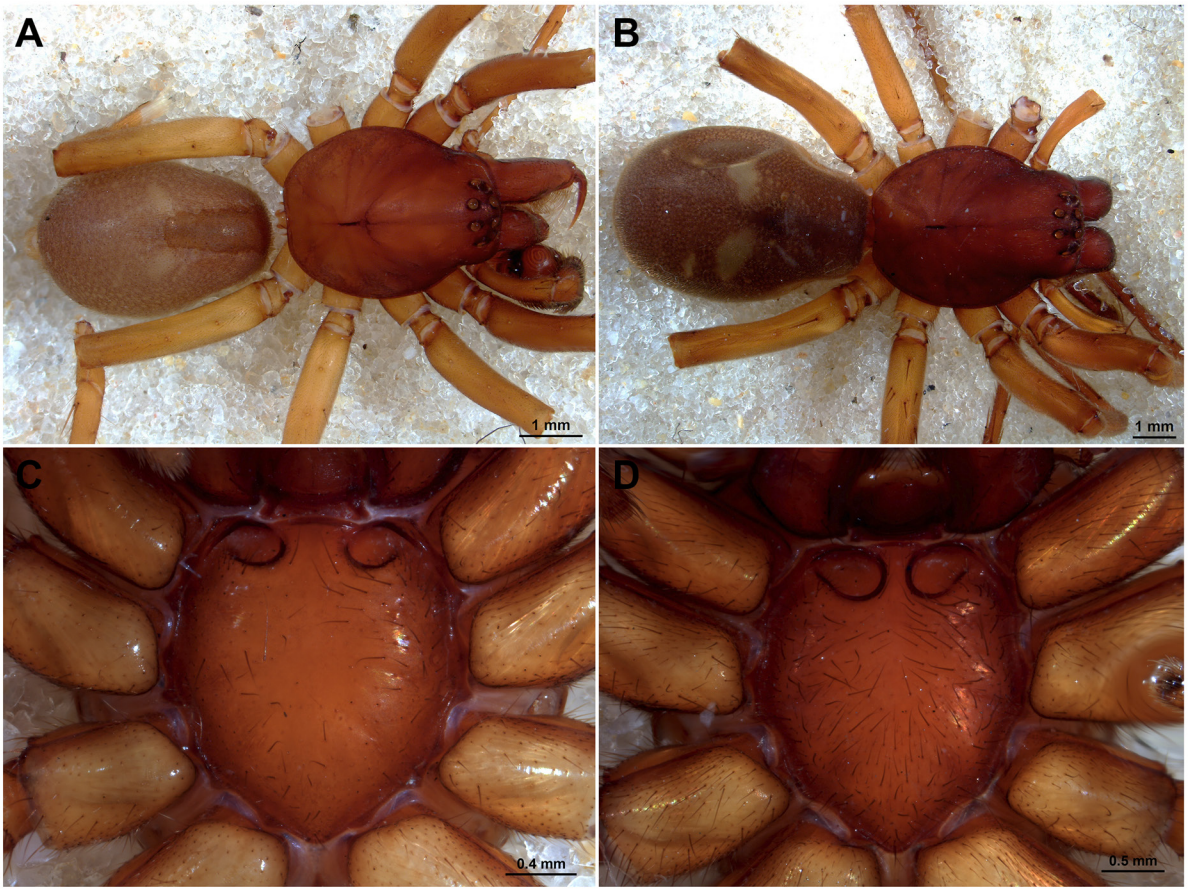

Fig. 24. *Stethorrhagus sylvilagus* sp. nov. **A, C**. Holotype, ♂ (ICN Ar-1648). **B, D**. Paratype, ♀ (ICN Ar-13740). **A–B**. Habitus, dorsal view. **C–D**. Sternum.

Females resemble those of *S. callithrix* sp. nov., *S. planada* and *S. sciurus* sp. nov. by the epigynum with VEP, CO disposed anteriorly in relation to SI, with a U-shaped posterior margin (Fig. 26C; Bonaldo & Brescovit 1994: fig. 18a). They differ from those of *S. planada* by the VEP gently procurved, placed posteriorly on epigynal plate (Fig. 25C) (VEP sub-rectangular, placed medially on epigynal plate in *S. planada* – Bonaldo & Brescovit 1994: fig. 18a); from those of *S. callithrix* by the CD relatively short (from CO to posterior margin of VEP, less than four times longer than the CO width – Fig. 25C) (in *S. callithrix*, long, more than six times longer than the CO width – Fig. 32C) and from those of *S. sciurus*

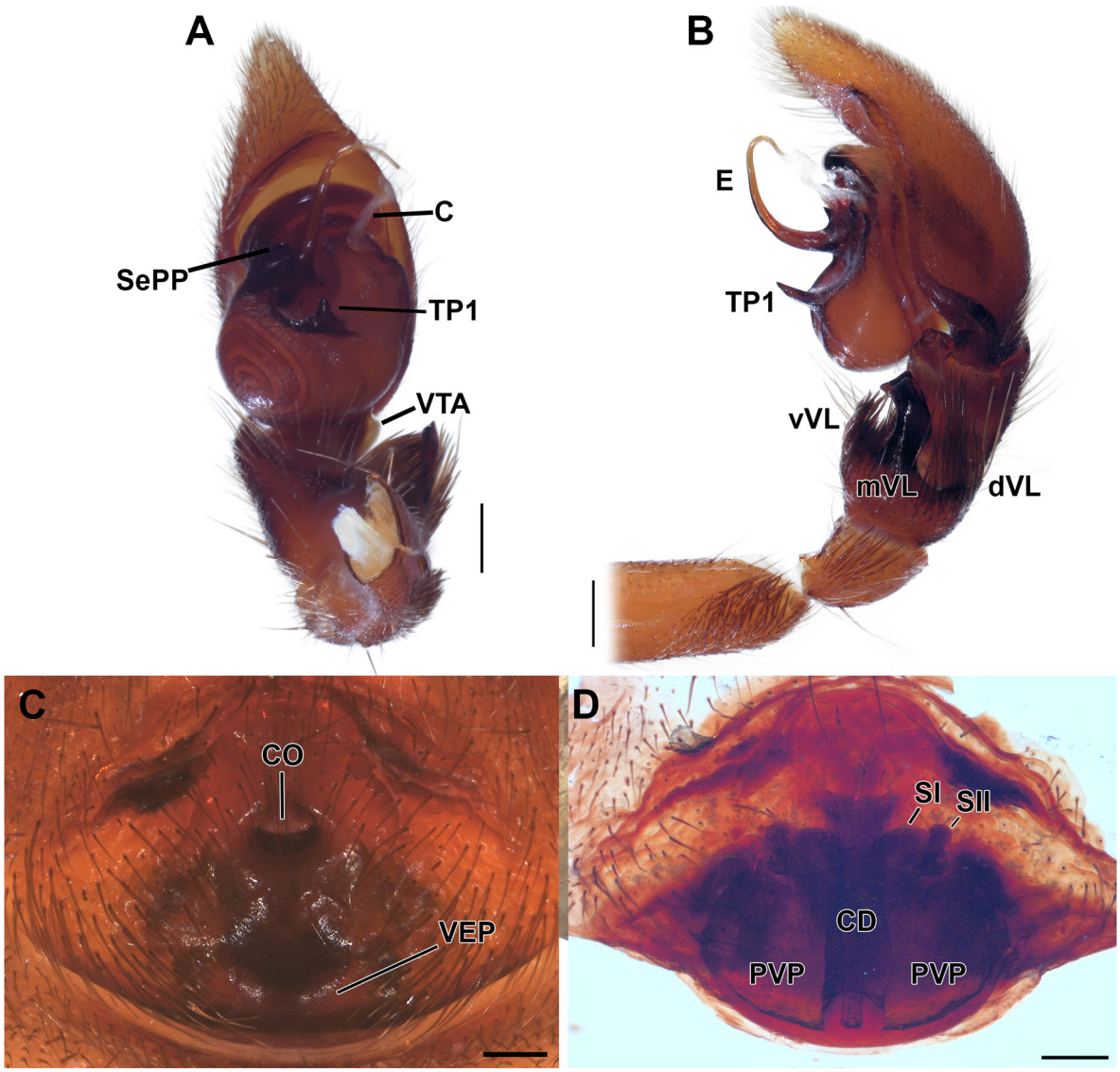

Fig. 25. *Stethorrhagus sylvilagus* sp. nov., genitalia. **A–B**. Holotype, ♂ (ICN Ar-1648), palp. **A**. Ventral view. **B**. Retrolateral view. **C–D**. Paratype, ♀ (ICN Ar-13740), epigynum. **C**. Ventral view. **D**. Dorsal view. Abbreviations: C = conductor; CD = copulatory duct; CO = copulatory opening; dVL = dorsal process of ventral lobe of RTA; E = embolus; mVL = median process of ventral lobe of RTA; PVP = posterior vulvar plate; SePP = sub-embolic prolateral process; SI = primary spermathecae; SII = secondary spermathecae; TP1 = tegular process 1; VEP = ventral epigynal plate; VTA = ventral tibial apophysis; vVL = ventral process of ventral lobe of RTA. Scale bars: A = 0.3 mm; B–D = 0.2 mm.

by the bulging area between the posterior margin of VEP and the posterior margin of the epigynal ventral plate (Fig. 25C) (depressed in *S. sciurus* – Fig. 43C).

Etymology

The specific name is a noun in apposition in reference to the lagomorph genus *Sylvilagus* Gray, 1867, since the general conformation of the epigynum (as in Fig. 25C) resembles a cottontail rabbit head in frontal view.

Material examined

Holotype

COLOMBIA • ♂; Huila, Parque Nacional Natural Nevado del Huila; [3°22′36”N, 74°48′08″ W]; elev. 3300 m; Sep. 1980; Páez leg., ICN-Ar 1648.

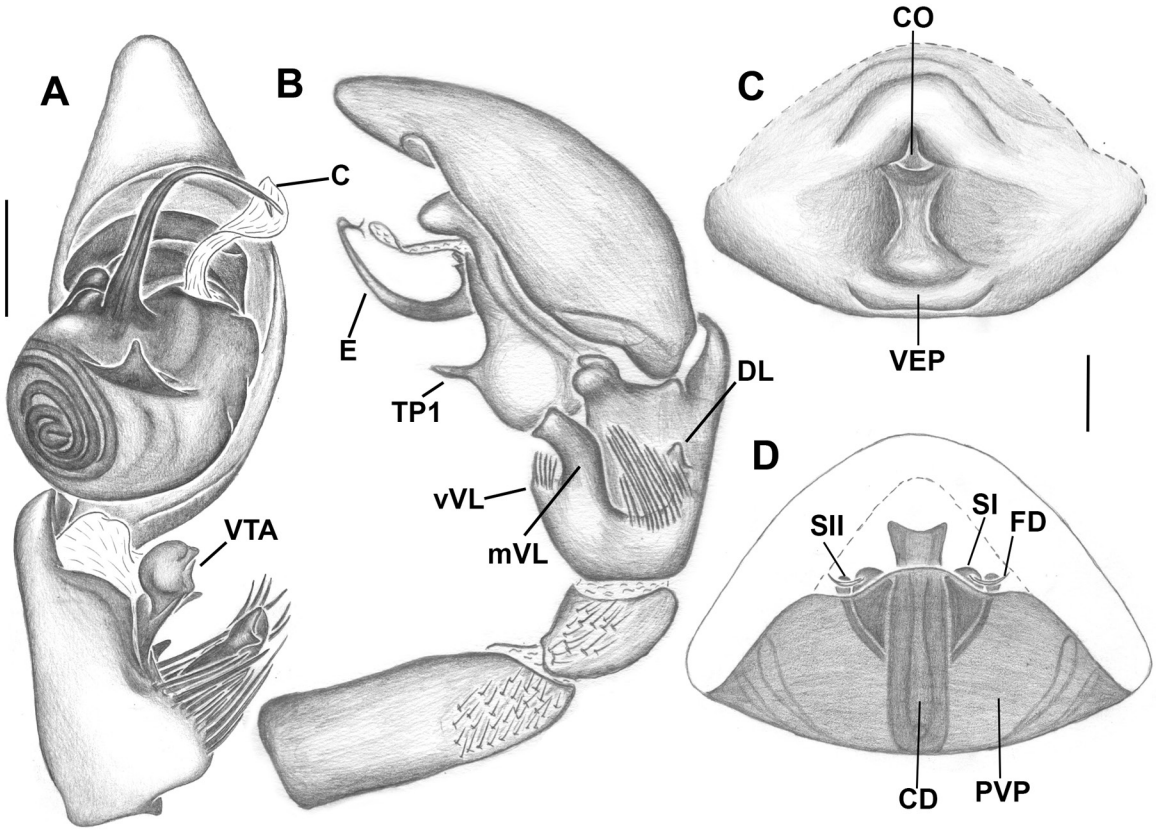

Fig. 26. *Stethorrhagus sylvilagus* sp. nov. **A–B**. Holotype, ♂ (ICN Ar-1648), palp. **A**. Ventral view. **B**. Retrolateral view. **C–D**. Paratype, ♀ (ICN Ar-13740), epigynum. **C**. Ventral view. **D**. Dorsal view. Abbreviations: C = conductor; CD = copulatory duct; CO = copulatory opening; DL = RTA dorsal lobe; E = embolus; mVL = median process of ventral lobe of RTA; PVP = posterior vulvar plate; SI = primary spermathecae; SII = secondary spermathecae; TP1 = tegular process 1; VEP = ventral epigynal plate; VTA = ventral tibial apophysis; vVL = ventral process of ventral lobe of RTA. Scale bars = 0.25 mm.

Paratypes

COLOMBIA – **Caldas** • 1 ♂; La Termal, Inderena, Belalcázar; elev. 2850 m; Oct. 1980; L. de Arévalo leg., IBSP 221891. – **Huila** • 1 ♀; same data as for holotype; ICN-Ar 13740.

Description

Male (holotype – ICN-Ar 1648)

Coloration. Cephalothorax and legs brown. Abdomen gray with two white central dorsal spots (Fig. 24A). Sternum with deep sternal excavations (Fig. 24C).

Measurements. Total length 7.36. Carapace 3.50 long, 2.72 wide. Clypeus 0.17. Leg measurements: I: femur 2.83/ patella 1.25/ tibia 2.64/ metatarsus 2.43/ tarsus 1.55/ total 10.70; II: 2.58/ 1.20/ 2.57/ 2.02/ 1.44/ 9.81; III: 2.37/ 1.01/ 1.84/ 2.14/ 1.20/ 8.26; IV: 2.95/ 1.05/ 2.65/ 3.15/ 1.39/ 11.19. Eye diameters: AME 0.19, ALE 0.16, PME 0.17, PLE 0.17. Chelicerae 1.75 long, with three promarginal teeth and four retromarginal denticles.

Leg spination. I – femur d1-1-0, p0-0-1, r0; tibia d0, p0, r0, v1p-2-2; metatarsus d0, p0, r0, v2-2-0. II – femur d1-1-0, p0-0-1, r0; tibia d0, p0, r0, v1r-2-0; metatarsus d0, p0, r0, v2-2-0. III – femur d1-1-0, p0-1-0, r0-0-1; tibia d0, p1-1-0, r1-1-0, v2-2-2; metatarsus d0, p1-1-0, r1-1-1, v2-2-1. IV – femur d1-1-0, p0-0-1, r0-0-1; tibia d0, p1-1-0, r1-1-0, v2-2-2; metatarsus d0, p1-1-0, r1-1-0, v2-2-1.

Palp. Retrolateral surface of femur and patellae with a cluster of modified hairs, tufts of modified hairs in vVL and dVL, median projection curved ventrally with subquadrangular tip between vVL and dVL, AS absent, DL reduced, VTA longer than wide, with distal surface C-shaped, spermophor situated prolaterally, TP1 straight, pointing apically, TP2 absent, SePP short, embolus long and curved prolaterally, prongs short (Figs 25A–B, 26A–B).

Female (paratype – ICN-Ar 13740)

Coloration. As in male, except dorsum of abdomen with four central dorsal spots, anterior pair twice the size of posterior pair (Fig. 24B). Sternum with sternal excavations as in male but larger (Fig. 24D).

Measurements. Total length 11.05. Carapace 4.76 long, 3.67 wide. Clypeus 0.30. Leg measurements: I: femur 4.19/ patella 1.74/ tibia 3.77/ metatarsus 3.25/ tarsus 2.00/ total 15.05; II: 3.77/ 1.79/ 3.43/ 3.40/ 1.97/ 14.36; III: 3.62/ 1.20/ 2.69/ 2.80/ 1.55/ 11.86; IV: 4.42/ 1.76/ 3.90/ 5.08/ 1.96/ 17.12. Eye diameters: AME 0.27, ALE 0.22, PME 0.26, PLE 0.22. Chelicerae 2.19 long, with three promarginal teeth and four retromarginal denticles.

Leg spination. I – femur d1-1-0, p0-0-1, r0; tibia d0, p0, r0, v1r-2-2; metatarsus d0, p0, r0, v2-2-0. II – femur d1-1-0, p0-0-1, r0; tibia d0, p0, r0, v1p-2-2-2; metatarsus d0, p0, r0, v2-2-0. III – femur d1-1-1, p0-1-1, r1-1-1; tibia d0, p1-1-0, r1-1-0, v2-2-2; metatarsus d0, p1-1-0, r1-1-0, v2-2-1. IV – femur d1-1-0, p0-0-1, r0; tibia d0, p1-1-0, r1-1-0, v2-2-2; metatarsus d0, p1-1-0, r1-1-0, v2-2-1.

Epigynum. Copulatory aperture U-shaped along posterior margin, CO disposed anteriorly in relation to spermathecae, VEP gently procurved, placed posteriorly on epigynal plate, area between posterior margin of VEP and posterior margin of epigynal plate bulging, PVP wider than long, covering SI, copulatory duct relatively short, from CO to posterior margin of VEP, less than four times longer than CO width (Figs 25C–D, 26C–D).

Distribution

Known only from the type locality (Fig. 51).

Stethorrhagus duidae Gertsch, 1942
Figs 27, 49

Stethorrhagus duidae Gertsch, 1942: 12, fig. 37, ♂.

Stethorrhagus duidae – Bonaldo & Brescovit 1994: 59, figs 20a–b, 21a.

Diagnosis

Males of *S. duidae* resemble those of *S. ovis* sp. nov. by the VL bifid, dVL protruding and both vVL and dVL glabrous, without thick modified hairs (Fig. 27B–D; Bonaldo & Brescovit 1994: fig. 20b). They differ by the vVL long, bifid in the distal third, the presence of AS, and by the embolus wide-based, with SePP not protruding, with reduced apical prongs (Fig. 27C–D; Bonaldo & Brescovit 1994: fig. 20a–b) (vVL short, entire, AS absent, embolus narrow-based, with protruding SePP and well-developed apical prongs in *S. ovis* – Figs 29A–B, 30A–B).

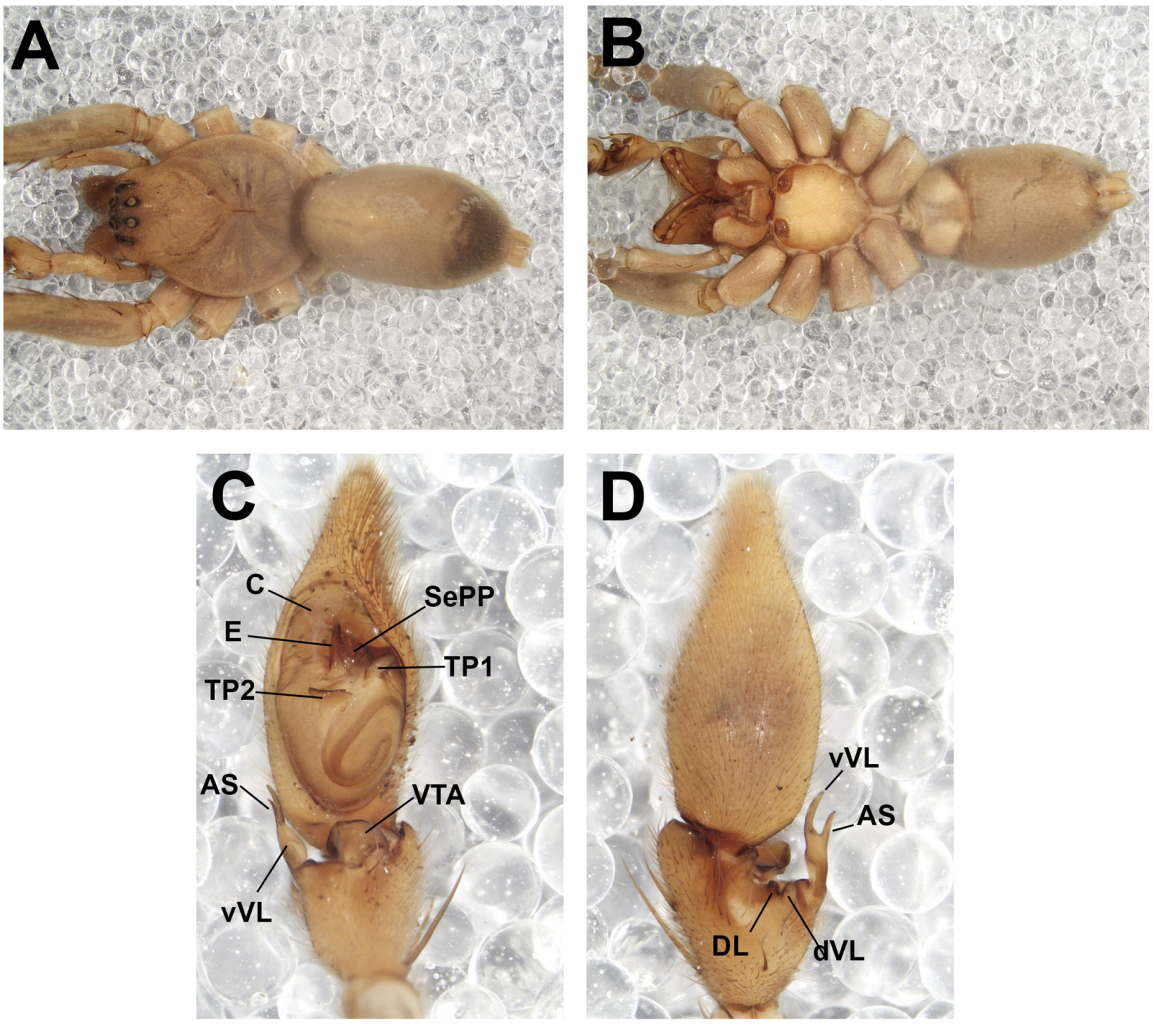

Fig. 27. *Stethorrhagus duidae* Gertsch, 1942 holotype, ♂ (AMNH). **A**. Habitus, dorsal view. **B**. Habitus, ventral view. **C**. Palp, ventral view. **D**. Palp, dorsal view. Photos by Paulo Pantoja. Abbreviations: AS = apical spur; C = conductor; DL = RTA dorsal lobe; dVL = dorsal process of ventral lobe of RTA; E = embolus; SePP = sub-embolic prolateral process; TP1 = tegular process 1; TP2 = tegular process 2; VTA = ventral tibial apophysis; vVL = ventral process of ventral lobe of RTA. Figure not to scale.

Type material

Holotype

VENEZUELA • ♂; Amazonas, summit of Mt Duida; [3°30′48″ N, 65°37′34″ W]; Tate leg.; AMNH (re-examined from photos).

Description

Male, see Bonaldo & Brescovit (1994: 59). Female unknown. Additional documentation of the male holotype in Fig. 27.

Distribution

Venezuela (Fig. 49).

Stethorrhagus ovis sp. nov.
urn:lsid:zoobank.org:act:8B57BFF7-EB80-4209-863E-D265249B961A
Figs 28–30, 51

Diagnosis

Males of *S. ovis* sp. nov. resemble those of *S. duidae* by the VL bifid, dVL protruding and both vVL and dVL glabrous, without thick modified hairs (Figs 27B–D, 29A–B, 30A–B; Bonaldo & Brescovit 1994: fig. 20b). They differ by the vVL short and entire AS absent, the embolus narrow-based, with

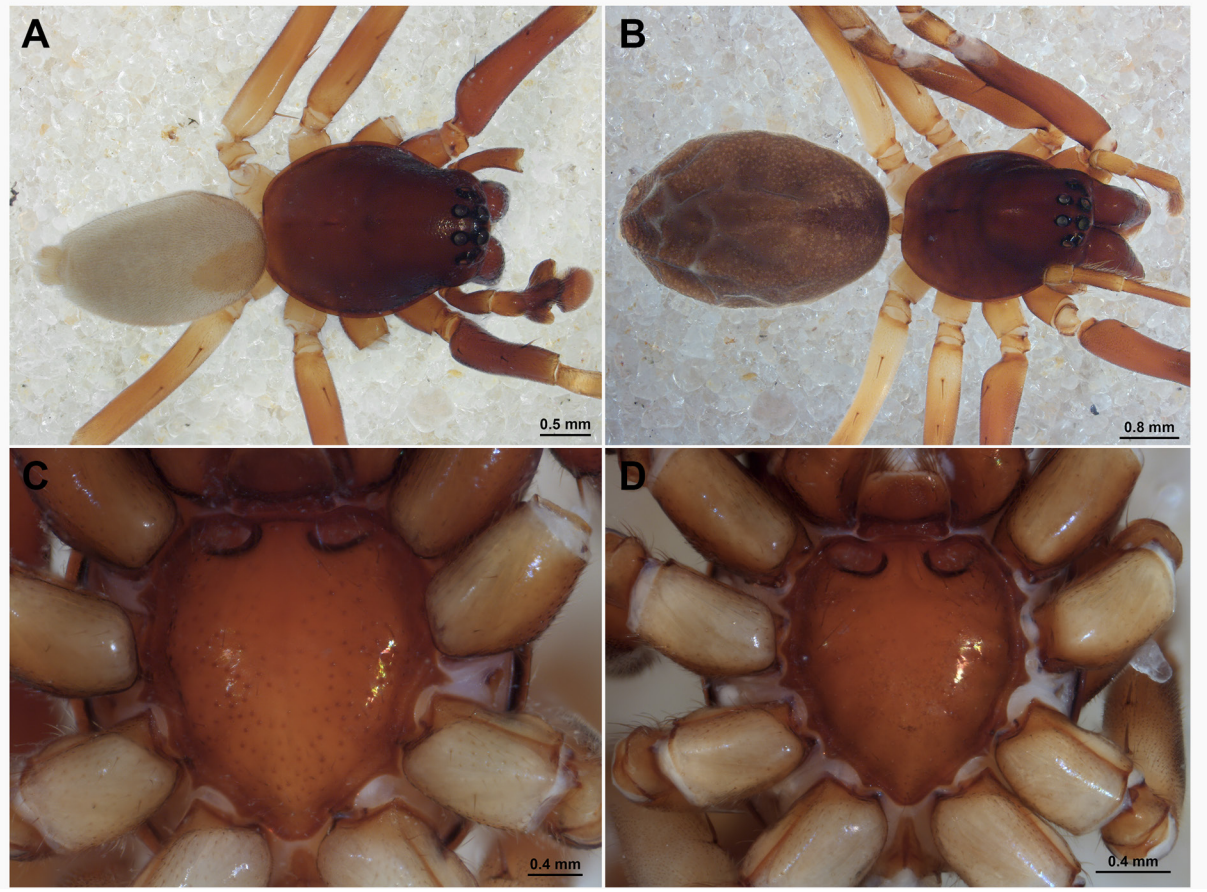

Fig. 28. *Stethorrhagus ovis* sp. nov. **A, C**. Holotype, ♂ (QCAZI 280517). **B, D**. Paratype, ♀ (MPEG 40708). **A–B**. Habitus, dorsal view. **C–D**. Sternum.

protruding SePP and well-developed apical prongs (Figs 29A–B, 30A–B) (vVL long, bifid in the distal third, AS present, and by the embolus wide-based, with SePP not protruding, with reduced apical prongs in *S. duidae* – Fig. 27C–D; Bonaldo & Brescovit 1994: fig. 20a–b). Females resemble those of *S. canis* sp. nov. and *S. felis* sp. nov. by the CO slit-shaped, disposed posteriorly in relation to SI (Figs 29C–D, 30C–D, 36C–D). They differ from those of *S. canis* by the CO relatively small (width five times smaller than the distance between CO and posterior margin of epigynal plate), placed on the anterior half of the epigynal plate (Figs 29C, 30C) (CO large, as wide as the distance between CO and posterior margin of

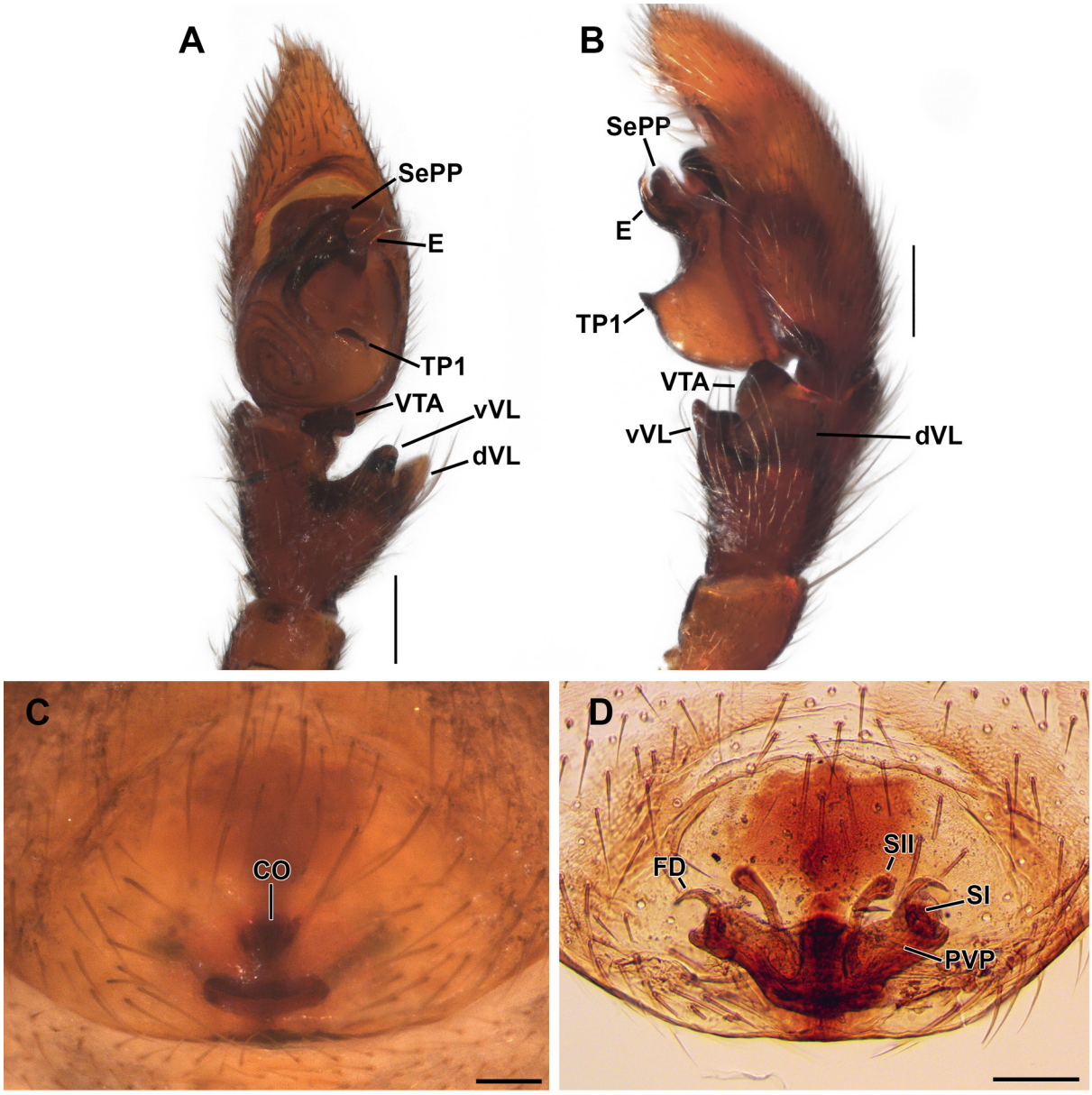

Fig. 29. *Stethorrhagus ovis* sp. nov., genitalia. **A–B**. Holotype, ♂ (QCAZI 280517), palp. **A**. Ventral view. **B**. Retrolateral view. **C–D**. Paratype, ♀ (MPEG 40708), epigynum. **C**. Ventral view. **D**. Dorsal view. Abbreviations: CO = copulatory opening; dVL = dorsal process of ventral lobe of RTA; E = embolus; FD = fertilization duct; PVP = posterior vulvar plate; SePP = sub-embolic prolateral process; SI = primary spermathecae; SII = secondary spermathecae; TP1 = tegular process 1; VTA = ventral tibial apophysis; vVL = ventral process of ventral lobe of RTA. Scale bars: A–C = 0.2 mm; D = 0.5 mm.

epigynal plate in *S. canis*, placed on the posterior half of the epigynal plate in *S. canis* – Fig. 47C, E) and from those of *S. felis* by the VEP posterior margin nearly straight (Figs 29C, 30C), whereas it is procurved in *S. felis* (Fig. 36C).

Etymology

The specific name is a noun in apposition in reference to the bovid genus *Ovis* Linnaeus, 1758, since the general conformation of the epigynum (as in Fig. 29C) resembles a sheep head in frontal view.

Material examined

Holotype

ECUADOR • ♂; Cotopaxi, Bosque Integral Otonga, 4.5 km S of San Francisco de Las Pampas; 0°25′8.0″ S, 78°59′51.5″ W; elev. 1625 m; 8 Dec. 2009; A.B. Bonaldo leg., QCAZI 280517.

Paratype

ECUADOR • 1 ♀; same data as for holotype; MPEG 40708.

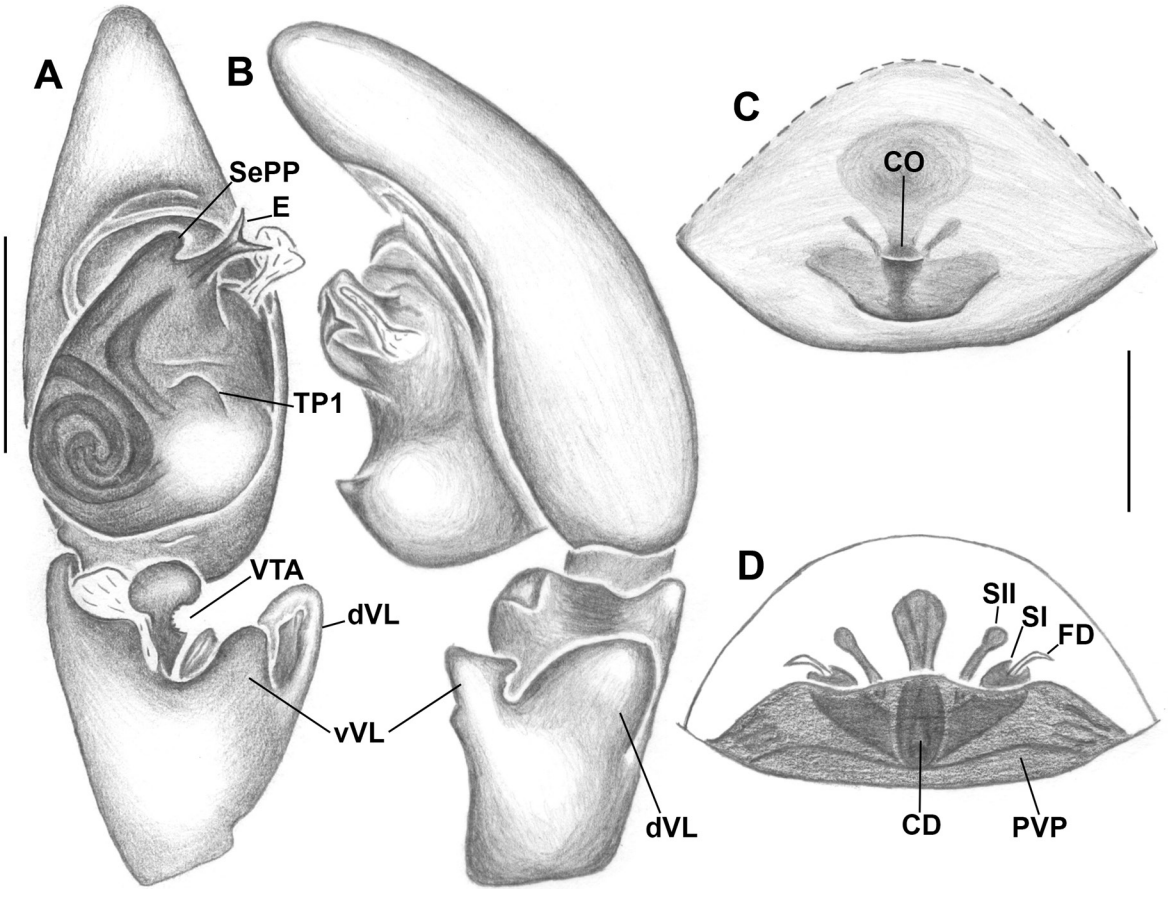

Fig. 30. *Stethorrhagus ovis* sp. nov. **A–B**. Holotype, ♂ (QCAZI 280517), palp. **A**. Ventral view. **B**. Retrolateral view. **C–D**. Paratype, ♀ (MPEG 40708), epigynum. **C**. Ventral view. **D**. Dorsal view. Abbreviations: CD = copulatory duct; CO = copulatory opening; dVL = dorsal process of ventral lobe of RTA; E = embolus; FD = fertilization duct; PVP = posterior vulvar plate; SePP = sub-embolic prolateral process; SI = primary spermathecae; SII = secondary spermathecae; TP1 = tegular process 1; VTA = ventral tibial apophysis; vVL = ventral process of ventral lobe of RTA. Scale bars = 0.25 mm.

Description

Male (holotype – QCAZI 280517)

Coloration. Cephalothorax red-brown. Legs red-brown with coxae and tarsi yellowish. Abdomen with orange muscular impressions (Fig. 28A). Sternum with deep sternal excavations (Fig. 28C).

Measurements. Total length 4.32. Carapace 2.18 long, 1.69 wide. Clypeus 0.16. Eye diameters: AME 0.15, ALE 0.14, PME 0.13, PLE 0.14. Chelicerae 0.85 long, with three promarginal teeth and four retromarginal denticles Leg measurements: I: femur 1.86/ patella 0.70/ tibia 1.62/ metatarsus 1.43/ tarsus 1.04/ total 6.65; II: absent; III: 1.53/ 0.57/ 1.20/ 1.44/ 0.89/ 5.63; IV: 1.93/ 0.64/ 1.60/ 2.20/ 0.98/ 7.35.

Leg spination. I – femur d1-1-0, p0-0-1, r0; tibia d0, p0, r0, v1p-2-2-2; metatarsus d0, p0, r0, v2-2-0. II – Missing. III – femur d1-1-1, p0, r0; tibia d0, p0, r0, v0-1p-1r; metatarsus d0, p1-1-0, r1-1-0, v2-0-1. IV – femur d1-1-1, p0, r0; tibia d0, p0, r0-0-1, v0-0-2; metatarsus d0, p1-1-1, r1-1-1, v2-0-1.

Palp. RTA with vVL and dVL glabrous, vVL apex straight in retrolateral view, dVL apex subtriangular in retrolateral view, AS absent, DL small, triangular, visible in dorsal view, VTA longer than wide, with narrowing between proximal and distal part visible in ventral view, spermophor situated prolaterally, TP1 small and rounded in ventral view, TP2 absent, SePP short, embolus short and slightly curved dorsally, visible in retrolateral view. (Figs 29A–B, 30A–B).

Female (paratype – MPEG 40708)

Coloration. As in male, except abdomen dark gray (Fig. 28B). Sternum with sternal excavations as in male but larger (Fig. 28D).

Measurements. Total length 6.40. Carapace 2.58 long, 2.06 wide. Clypeus 1.17. Leg measurements: I: femur 2.20/ patella 0.93/ tibia 2.02/ metatarsus 1.74/ tarsus 1.15/ total 8.04; II: 2.04/ 0.92/ 1.82/ 1.72/ 1.09/ 7.59; III: 1.98/ 0.67/ 1.48/ 1.66/ 1.01/ 6.80; IV: 2.31/ 0.94/ 2.12/ 2.54/ 1.06/ 8.97. Eye diameters: AME 0.19, ALE 0.18, PME 0.16, PLE 0.16. Chelicerae 1.17 long, with three promarginal teeth and four retromarginal denticles.

Leg spination. I – femur d1-1-1, p0-0-1, r0-0-1; tibia d0, p0, r0, v1p-2-2-3; metatarsus d0, p0, r0, v2-2-0. II – femur d1-1-1, p0, r0; tibia d0, p0, r0, v0-1r-2; metatarsus d0, p0, r0, v2-2-0. III – femur d1-1-0, p0-0-1, r0; tibia d0, p0-1-0, r0-1-1, v0-1-2; metatarsus d0, p0-1-2, r0-1-2, v2-2-1. IV – femur d1-1-0, p0-0-1, r0; tibia d0, p1-1-0, r1-1-0, v1p-1p-2; metatarsus d0, p1-1-0, r1-1-0, v2-2-1.

Epigynum. CO slit-shaped, disposed posteriorly in relation to spermathecae, PVP wider, three times the distance between the anterior and posterior margins, covering SI, SII elongated, copulatory duct relatively short, from CO to posterior margin of PVP (about four times smaller than the PVP width) (Figs 29C–D, 30C–D).

Distribution

Known only from the type locality (Fig. 51).

Stethorrhagus callithrix sp. nov.

urn:lsid:zoobank.org:act:E70E900E-0627-459D-A648-9BA96D0FD16C

Figs 31–33, 51

Diagnosis

Males of *S. callithrix* sp. nov. resemble those of *S. felis* sp. nov. and *S. bradypus* sp. nov. by the bifid VL, with thick modified hairs in both vVL and dVL, and dVL protruding (Fig. 33B), differing by the

SePP with a pointed tip directed retrolaterally (Figs 32A–B, 33A–B) (SePP with a blunt tip directed apically in both *S. felis* and *S. bradypus* – Figs 35A–C, 38A, 36A–B, 39A–C). Females resemble those of *S. sylvilagus* sp. nov., *S. planada* and *S. sciurus* sp. nov. by the epigynum with VEP, CO disposed anteriorly in relation to SI, with U-shaped posterior margin (Figs 32C, 33C; Bonaldo & Brescovit 1994: fig. 18a). They differ from those of *S. planada* by the VEP gently procurved, placed posteriorly on the epigynal plate (Fig. 33C) (VEP sub-rectangular, placed medially on the epigynal plate in *S. planada* – Bonaldo & Brescovit 1994: fig. 18a) and from those of *S. sylvilagus* and *S. sciurus* by the CD relatively long (from CO to posterior margin of VEP, more than six times longer than the CO width, Fig. 33D) (CD relatively short, from CO to posterior margin of VEP, less than four times longer than the CO width in both *S. sylvilagus* and *S. sciurus* – Figs 26D, 43F).

Etymology

The specific name is a noun in apposition in reference to the primate genus *Callithrix* Erxleben, 1777, since the posterior sector of the epigynum (as in Fig. 32C) resembles a marmoset head in frontal view.

Material examined

Holotype

COLOMBIA • ♂; Cauca, Huila, Parque Nacional Natural Nevado de Huila; [3°03′26″ N, 75°55′23″ W]; elev. 3300 m; Sep. 1980; Páez leg.; ICN-Ar 13741.

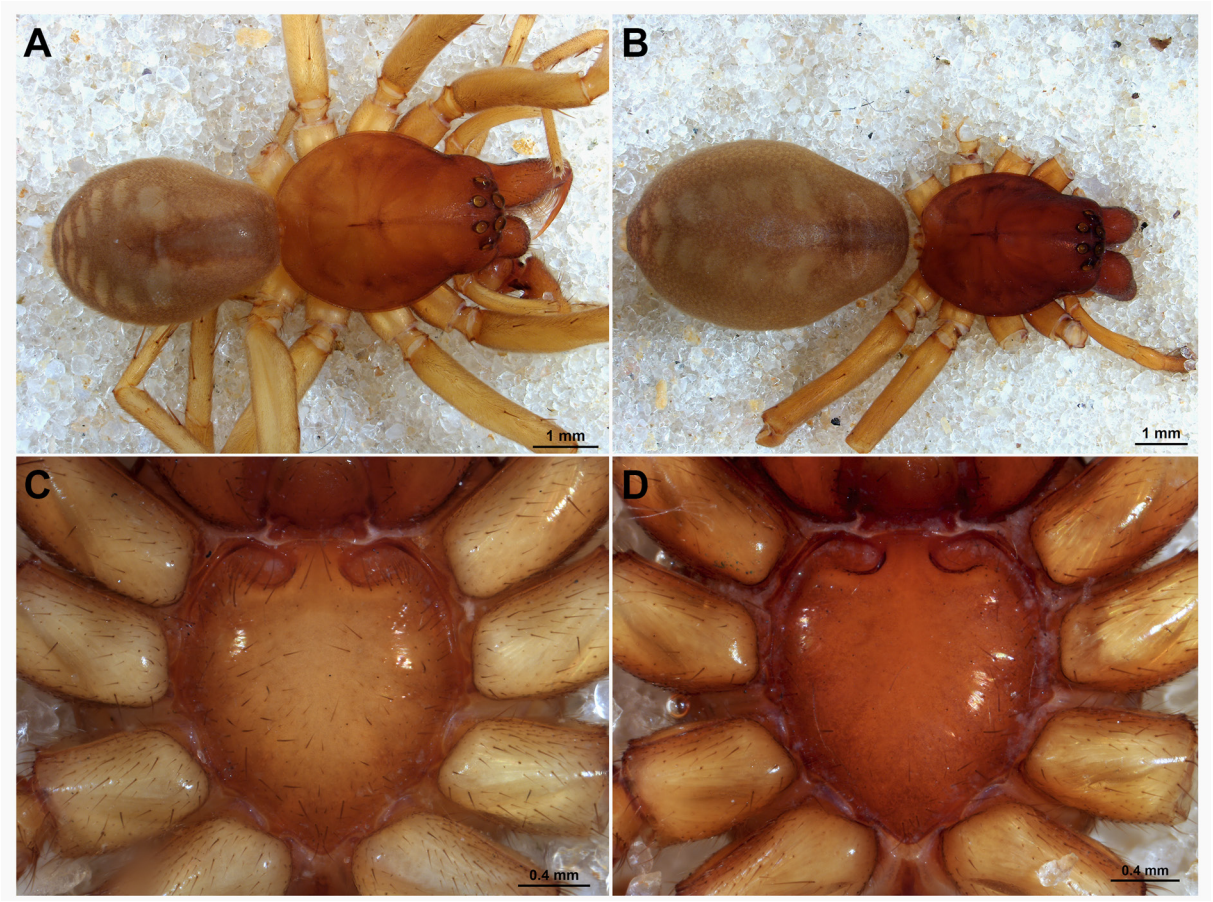

Fig. 31. *Stethorrhagus callithrix* sp. nov. **A, C**. Holotype, ♂ (ICN Ar-13741). **B**. Paratype, ♀ (ICN Ar-13742). **A–B**. Habitus, dorsal view. **C–D**. Sternum.

Paratype

COLOMBIA • 1 ♀; same data as for holotype; ICN-Ar 13742.

Description

Male (holotype – ICN-Ar 13741)

Coloration. Carapace, chelicerae, endites and labium red-brown (Fig. 31A). Sternum yellow with orange borders, and deep sternal excavations (Fig. 31C). Legs yellow-brown. Abdomen brown with two rows of dorsal white paramedian spots (Fig. 31A).

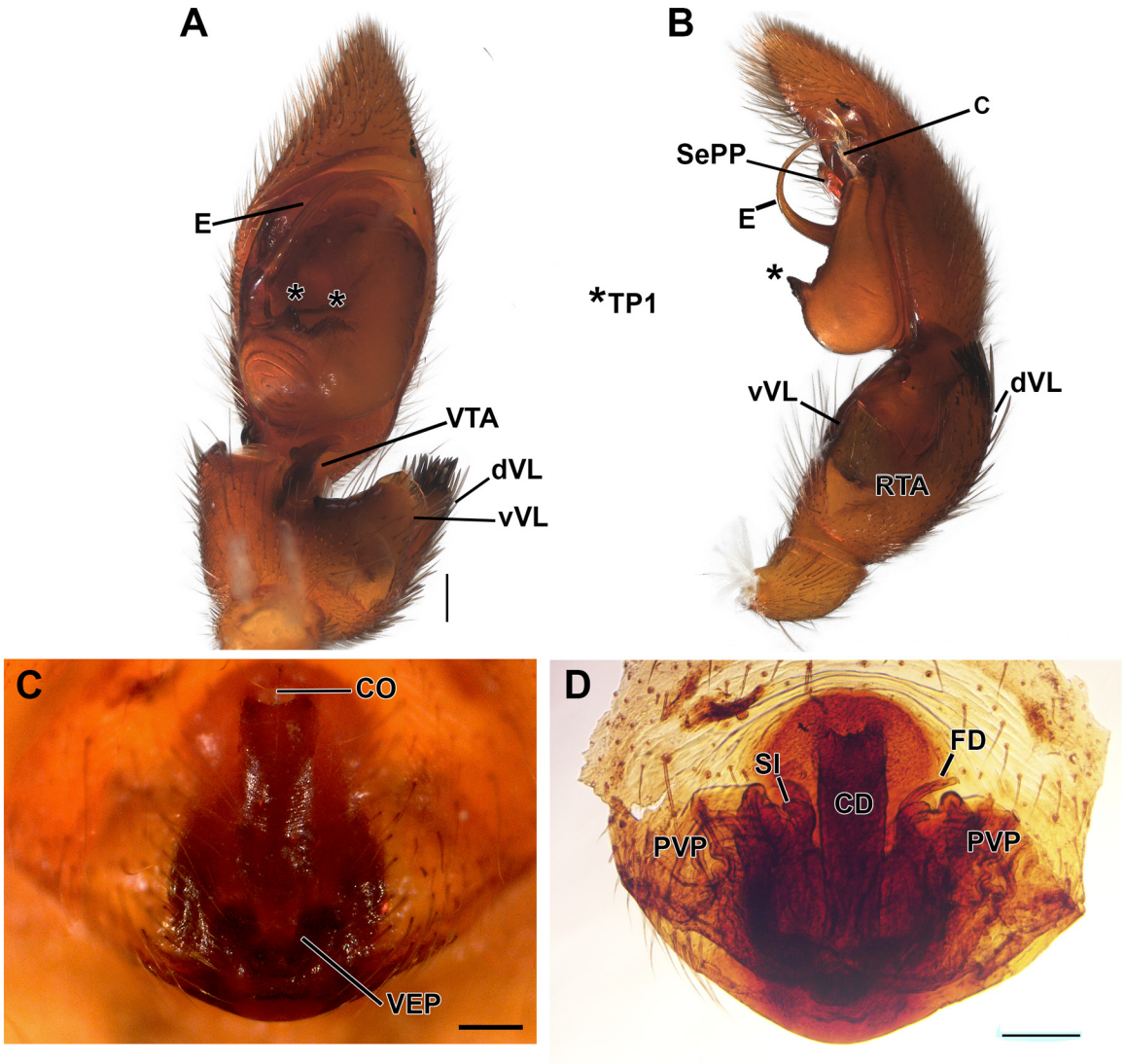

Fig. 32. *Stethorrhagus callithrix* sp. nov., genitalia. **A–B**. Holotype, ♂ (ICN-Ar 13741), palp. **A**. Ventral view. **B**. Retrolateral view. **C–D**. Paratype, ♀ (ICN-Ar 13742), epigynum. **C**. Ventral view. **D**. Dorsal view. Abbreviations: C = conductor; CD = copulatory duct; CO = copulatory opening; dVL = dorsal process of ventral lobe of RTA; E = embolus; FD = fertilization duct; PVP = posterior vulvar plate; RTA = retrolateral tibial apophysis; SePP = sub-embolic prolateral process; SI = primary spermathecae; TP1 = tegular process 1; VEP = ventral epigynal plate; VTA = ventral tibial apophysis; vVL = ventral process of ventral lobe of RTA. Scale bars = 0.2 mm.

Measurements. Total length 6.94. Carapace 3.36 long, 2.71 wide. Clypeus 0.15. Leg measurements: I: femur 2.84/ patella 1.21/ tibia 2.81/ metatarsus 2.47/ tarsus 1.7/ total 11.03; II: 2.70/ 1.11/ 2.32/ 2.28/ 1.68/ 10.09; III: 2.56/ 1.10/ 1.90/ 2.33/ 1.17/ 9.06; IV: 3.35/ 1.18/ 2.81/ 3.47/ 1.61/ 12.42. Eye diameters: AME 0.20, ALE 0.19, PME 0.19, PLE 0.18. Chelicerae 1.81 long, with three promarginal teeth and five retromarginal denticles.

Leg spination. I – femur d1-1-0, p0-0-1, r0; tibia d0, p0, r0, v1p-2-2-2; metatarsus d0, p0, r0, v2-2-0. II – femur d1-1-0, p0-0-1, r0; tibia d0, p0, r0, v0-2-2; metatarsus d0, p1-1-1, r1-1-1, v2-1p-2. III – femur d1-1-1, p1-1-1, r0-1-1; tibia d0, p1-1-0, r1-1-0, v2-2-2; metatarsus d0, p1-1-0, r1-1-0, v2-2-2. IV – femur d1-1-1, p0-0-1, r0-0-1; tibia d0, p1-1-0, r1-1-0, v2-2-2; metatarsus d0, p1-1-0, r1-1-0, v2-2-1.

Palp. RTA with vVL and dVL with modified hairs, dVL longer than vVL, AS present and separated from VL, DL reduced, VTA longer than wide, spermophor situated prolaterally, TP1 bilobated and serrated, situated abovedistal fold of spermophor, TP2 absent, SePP with pointed tip directed retrolaterally, embolus long, curved prolaterally in ventral view and curved dorsally in retrolateral view, prongs long and curved apically (Figs 32A–B, 33A–B).

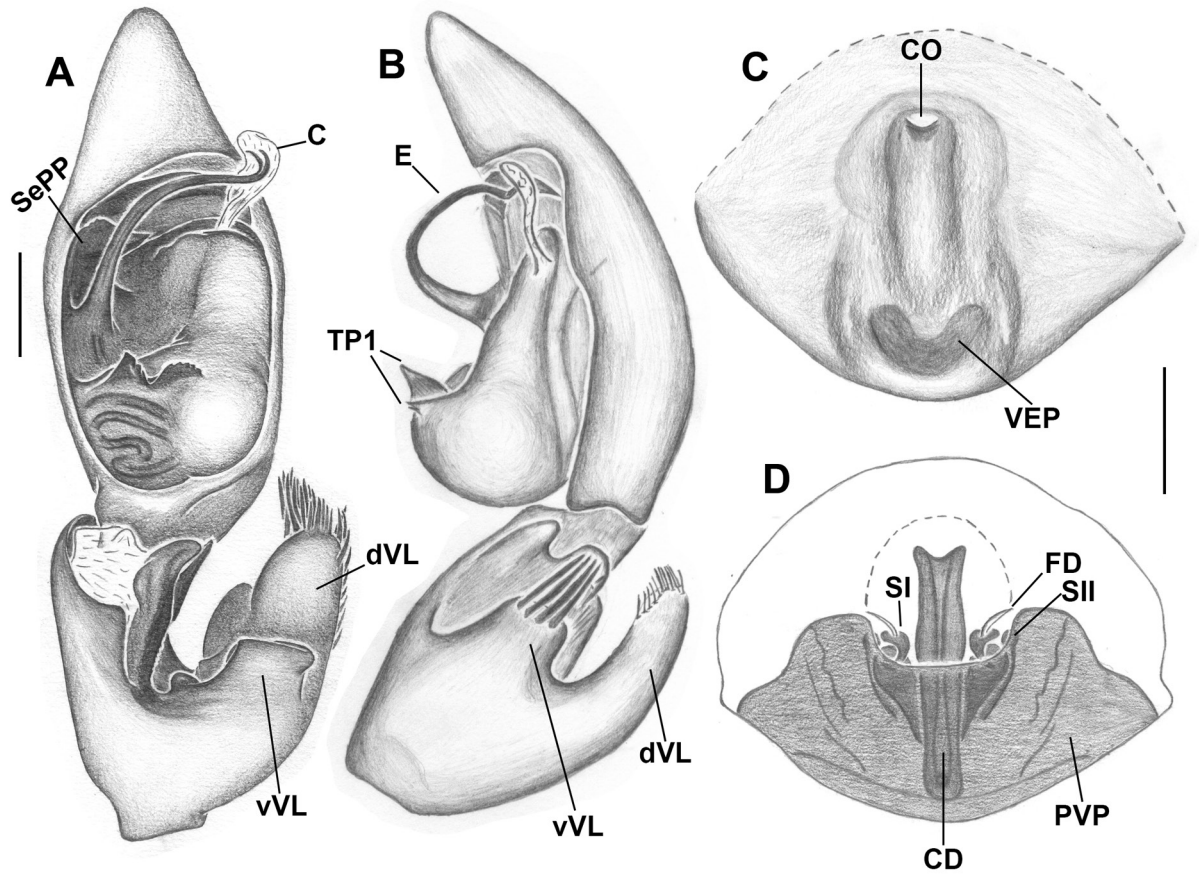

Fig. 33. *Stethorrhagus callithrix* sp. nov. **A–B**. Holotype, ♂ (ICN-Ar 13741), palp. **A**. Ventral view. **B**. Retrolateral view. **C–D**. Paratype, ♀ (ICN-Ar 13742), epigynum. **C**. Ventral view. **D**. Dorsal view. Abbreviations: C = conductor; CD = copulatory duct; CO = copulatory opening; dVL = dorsal process of ventral lobe of RTA; E = embolus; FD = fertilization duct; PVP = posterior vulvar plate; SePP = subembolic prolateral process; SI = primary spermathecae; SII = secondary spermathecae; TP1 = tegular process 1; VEP = ventral epigynal plate; VTA = ventral tibial apophysis; vVL = ventral process of ventral lobe of RTA. Scale bars = 0.25 mm.

Female (paratype – ICN-Ar 13742)

Coloration. As in male (Fig. 31B). Sternum with sternal excavations as in male (Fig. 31D).

Measurements. Total length 9.02. Carapace 3.43 long, 2.65 wide. Clypeus 0.19. femur 2.89/ patella 1.26/ tibia 2.57/ metatarsus 2.36/ tarsus 1.52/ total 10.60; II: 2.88/ 1.18/ 2.35/ 2.12/ 1.50/ 9.95; III: 2.68/ 1.08/ 1.93/ 2.19/ 1.26/ 9.14; IV: 3.41/ 1.28/ 3.01/ 3.63/ 1.43/ 12.76. Eye diameters: AME 0.23, ALE 0.2, PME 0.20, PLE 0.21. Chelicerae 1.48 long, with three promarginal teeth and five retromarginal denticles.

Leg spination. I – femur d1-1-0, p0-0-1, r0; tibia d0, p0, r0, v1p-2-2-2; metatarsus d0, p0, r0, v2-2-0. II – femur d1-1-0, p0-0-1, r0; tibia d0, p0, r0, v1r-2-2; metatarsus d0, p0, r0, v2-2-0. III – IV - femur d1-1-1, p0-0-1, r0-0-1; tibia d0, p1-1-0, r1-1-0, v2-2-2; metatarsus d0, p1-1-1, r1-1-1, v2-2-1.

Epigynum. CO disposed anteriorly in relation to spermathecae, copulatory aperture U-shaped along posterior margin, VEP gently procurved, placed posteriorly on epigynal plate, PVP wider than long, covering ⅔ of SI, PVP with slightly procurved notch along anterior margin, copulatory duct relatively long, with reinforcement rods anterior to CO (Figs 32C–D, 33C–D).

Distribution

Known only from the type locality (Fig. 51).

Stethorrhagus felis sp. nov.

urn:lsid:zoobank.org:act:522B0411-CBC9-4F56-B0EC-D4D10DE8878D

Figs 34–36, 50

Diagnosis

Males of *S. felis* sp. nov. resemble those of *S. callithrix* sp. nov. and *S. bradypus* sp. nov. by the bifid VL, with thick modified hairs in both vVL and dVL, and dVL protruding (Figs 32A–B, 33A–B, 35A–C, 36A–B, 38A–C, 39A–C). They differ from those of *S. callithrix* by the SePP with a blunt tip directed apically (Figs 35A–C, 36A–B) (SePP with a pointed tip directed retrolaterally in *S. callithrix* – Figs 32A–B, 33A–B) and from those of *S. bradypus* by the tibia with a DL and tegulum with TP1 (both DL and TP1 absent in *S. bradypus* – Figs 38A–C, 39A–C). Females resemble those of *S. canis* sp. nov. and *S. ovis* sp. nov. by the CO slit-shaped, disposed posteriorly in relation to SI (Figs 35D–E, 36C–D). They differ from those of *S. canis* by the CO relatively small (as wide as five times the distance between CO and posterior margin of the epigynal plate), placed on the anterior half of the epigynal plate (Figs 35D, 36C) (CO large, as wide as the distance between CO and posterior margin of epigynal plate, placed on the posterior half of the epigynal plate in *S. canis* – Fig. 47C–F) and from those of *S. ovis* by the VEP posterior margin procurved (Figs 35D, 36C) (VEP posterior margin nearly straight in *S. ovis* – Figs 29C, 30C).

Etymology

The specific name is a noun in apposition in reference to the carnivore genus *Felis* Linnaeus, 1758, since the general conformation of the epigynum (as in Fig. 35D) resembles a cat head in frontal view.

Material examined

Holotype

ECUADOR • ♂; Napo, Yanayacu, Cantón Quijos; 00°35′57.8″ S, 77°53′25.3″ W; elev. 2132 m; 23–30 Nov. 2009; A.B. Bonaldo leg.; QCAZI 280518.

Paratypes

ECUADOR • 1 ♀; same data as for holotype; QCAZI 280519 • 1 ♂, 1 ♀; same data as for holotype; QCAZI 280520 • 1 ♂; same data as for holotype; MPEG 40144 • 1 ♀; same data as for holotype; MPEG 40145.

Description

Male (holotype – QCAZI 280518)

Coloration. Carapace, chelicerae, endites and labium red-brown. Legs yellow. Abdomen brown with two rows of six white spots in the dorsal posterior third (Fig. 34A). Ventrally cream with longitudinal brownish band. Sternum brown with deep sternal excavations (Fig. 34C).

Measurements. Total length 6.07. Carapace 2.84 long, 2.30 wide. Clypeus 0.26. Leg measurements: I: femur 2.57/ patella 1.10/ tibia 2.33/ metatarsus 2.25/ tarsus 1.34/ total 9.59; II: 2.28/ 1.03/ 1.87/ 1.92/ 1.17/ 8.27; III: 1.80/ 0.86/ 1.47/ 1.70/ 0.93/ 6.76; IV: 2.60/ 0.99/ 2.15/ 2.65/ 1.08/ 9.47. Eye diameters: AME 0.16, ALE 0.15, PME 0.15, PLE 0.15. Chelicerae 1.46 long, with three promarginal teeth and five retromarginal denticles.

Leg spination. I – femur d1-1-0, p0-0-1, r0; tibia d0, p0, r0, v1p-2-2-2; metatarsus d0, p0, r0, v2-2-0. II – femur d1-1-0, p0, r0; tibia d0, p0, r0, v0-2-2; metatarsus d0, p0, r0, v2-2-0. III – femur d1-1-0, p0,

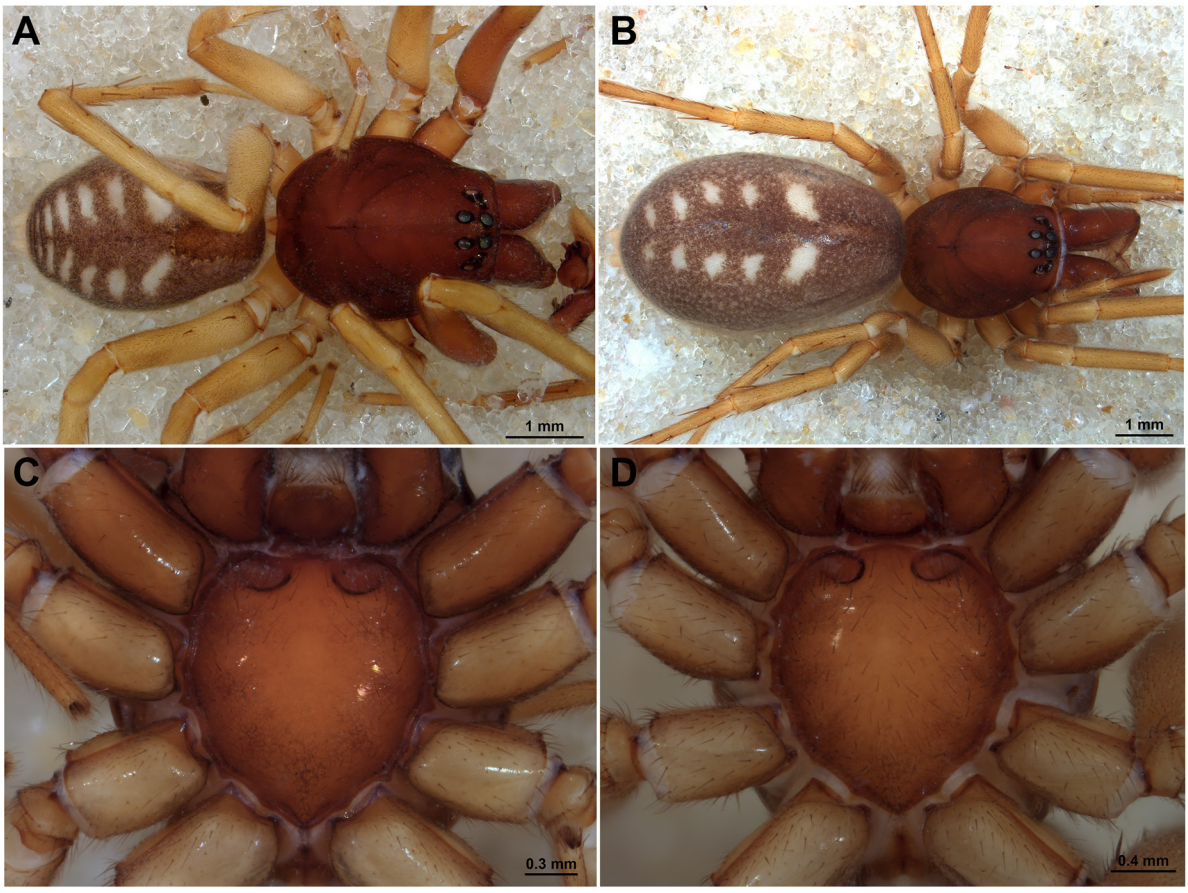

Fig. 34. *Stethorrhagus felis* sp. nov. **A, C**. Holotype, ♂ (QCAZI 280518). **B, D**. Paratype, ♀ (QCAZI 280519). **A–B**. Habitus, dorsal view. **C–D**. Sternum.

r0; tibia d0, p1-1-0, r1-1-0, v2-2-2; metatarsus d0, p0-1-0, r0-1-0, v2-2-1. IV – femur d1-1-0, p0, r0; tibia d0, p1-1-0, r1-1-0, v1p-2-2; metatarsus d0, p1-1-0, r1-1-0, v2-2-1.

Palp. RTA with vVL and dVL with modified hairs, dVL and vVL almost the same size in retrolateral view, AS absent, DL reduced, VTA longer than wide, with distal surface about ten times longer than proximal surface, spermophor situated ventro-prolaterally, TP1 small, situated prolaterally in distal fold

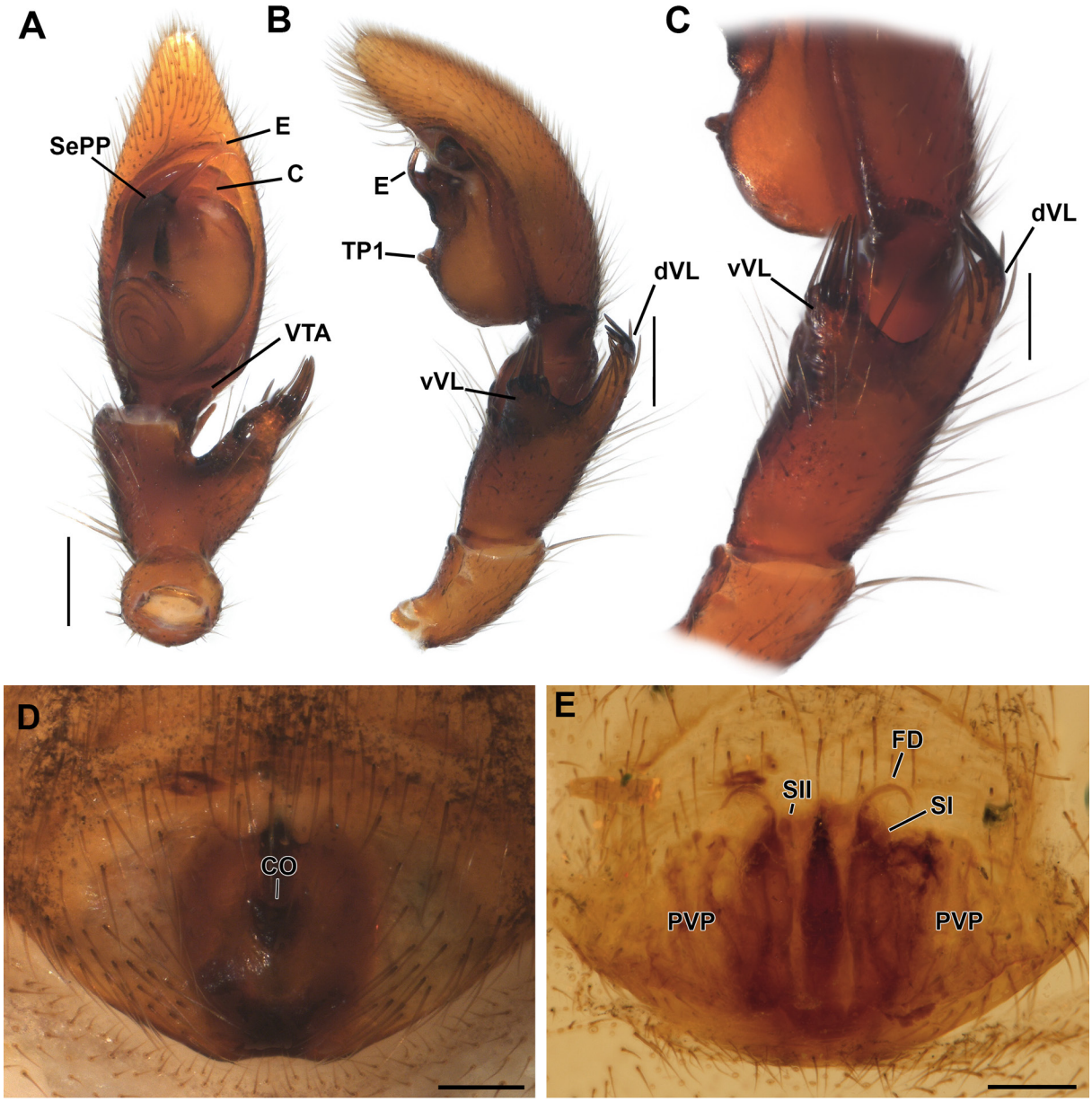

Fig. 35. *Stethorrhagus felis* sp. nov., genitalia. **A–C**. Holotype, ♂ (QCAZI 280518), palp. **A**. Ventral view. **B**. Retrolateral view. **C**. Tibia, retrolateral view. **D–E**. Paratype, ♀ (MPEG 40145), epigynum. **D**. Ventral view. **E**. Dorsal view. Abbreviations: C = conductor; CO = copulatory opening; dVL = dorsal process of ventral lobe of RTA; E = embolus; FD = fertilization duct; PVP = posterior vulvar plate; SePP = sub-embolic prolateral process; SI = primary spermathecae; SII = secondary spermathecae; TP1 = tegular process 1; VTA = ventral tibial apophysis; vVL = ventral process of ventral lobe of RTA. Scale bars = 0.2 mm.

of the spermophor, TP2 absent, SePP with blunt tip directed apically, embolus long and not curved. RTA bilobated with modified setae on the apex of both lobes, VTA longer than wide (Figs 35A–C, 36A–B).

Female (paratype – QCAZI 280519)

Coloration. As in male, except abdomen totally gray ventrally (Fig. 34B). Sternum with sternal excavations as in male (Fig. 34D).

Measurements. Total length 8.18. Carapace 2.90 long, 2.30 wide. Clypeus 0.23. Leg measurements: I: femur 2.33/ patella 1.13/ tibia 2.07/ metatarsus 1.88/ tarsus 1.18/ total 8.59; II: 2.32/ 0.99/ 1.83/ 1.79/ 1.09/ 8.02; III: 1.76/ 0.97/ 1.46/ 1.78/ 0.96/ 7.93; IV: 2.56/ 1.13/ 2.19/ 2.57/ 1.14/ 9.59. Eye diameters: AME 0.17, ALE 0.14, PME 0.15, PLE 0.14. Chelicerae 1.65 long, with three promarginal teeth and five retromarginal denticles.

Leg spination. I – femur d1-1-0, p0-0-1, r0; tibia d0, p0, r0, v1p-2-2-2; metatarsus d0, p0, r0, v2-2-0. II – femur d1-0-0, p0, r0, tibia d0, p0, r0, v1r-2-2-0; metatarsus d0, p0, r0, v2-2-0. III – femur d1-1-0,

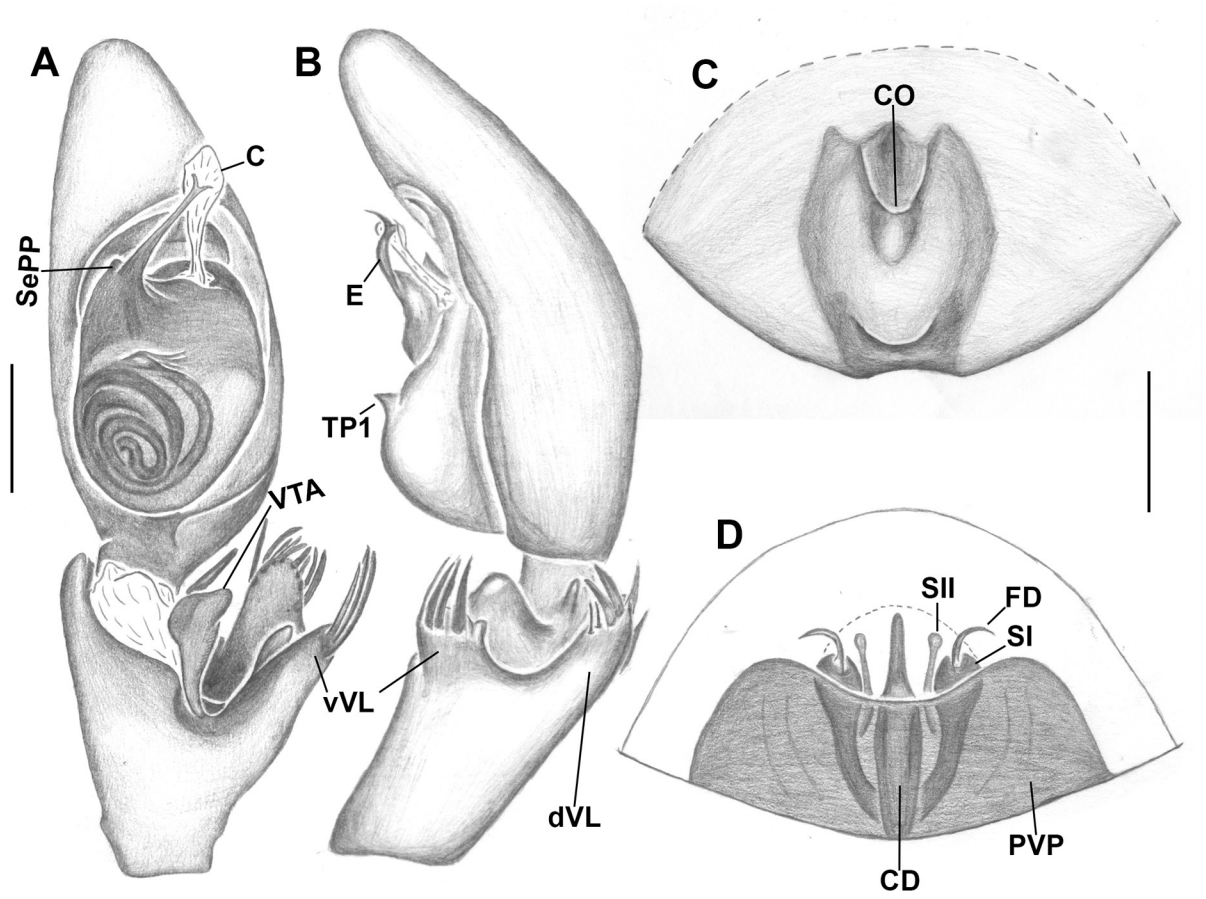

Fig. 36. *Stethorrhagus felis* sp. nov. **A–B**. Holotype, ♂ (QCAZI 280518), palp. **A**. Ventral view. **B**. Retrolateral view. **C–D**. Paratype, ♀ (MPEG 40145), epigynum. **C**. Ventral view. **D**. Dorsal view. Abbreviations: C = conductor; CD = copulatory duct; CO = copulatory opening; dVL = dorsal process of ventral lobe of RTA; E = embolus; FD = fertilization duct; PVP = posterior vulvar plate; SePP = subembolic prolateral process; SI = primary spermathecae; SII = secondary spermathecae; TP1 = tegular process 1; VTA = ventral tibial apophysis; vVL = ventral process of ventral lobe of RTA. Scale bars = 0.25 mm.

p0, r0; tibia d0, p1-1-0, r1-1-0, v2-2-2; metatarsus d0, p0-1-0, r0-1-0, v2-2-1. IV – femur d1-1-0, p0, r0; tibia d0, p1-1-0, r1-1-0, v1p-2-2; metatarsus d0, p1-1-0, r1-1-0, v2-2-1.

Epigynum. CO disposed anteriorly in relation to spermathecae, CO U-shaped along posterior margin, VEP gently procurved, placed posteriorly on epigynal plate, PVP wider than long, covering ⅔ of SI, PVP two times the distance between anterior and posterior margins, PVP with slightly procurved notch on anterior margin, copulatory duct relatively long, with reinforcement nods anteriorly to CO (Figs 35D–E, 36C–D).

Distribution

Known only from the type locality (Fig. 51).

Stethorrhagus bradypus sp. nov.
urn:lsid:zoobank.org:act:6FDB40FD-2AEC-431D-A75B-665D8B5ED9F6
Figs 37–39, 50

Diagnosis

Males of *S. bradypus* sp. nov. resemble those of *S. callithrix* sp. nov. and *S. felis* sp. nov. by the bifid VL, with thick modified hairs in both vVL and dVL, and dVL protruding (Figs 32A–B, 33A–B, 35A–C, 36A–B, 38A–C, 39A–C). They differ from those of *S. callithrix* by the SePP with a blunt tip directed

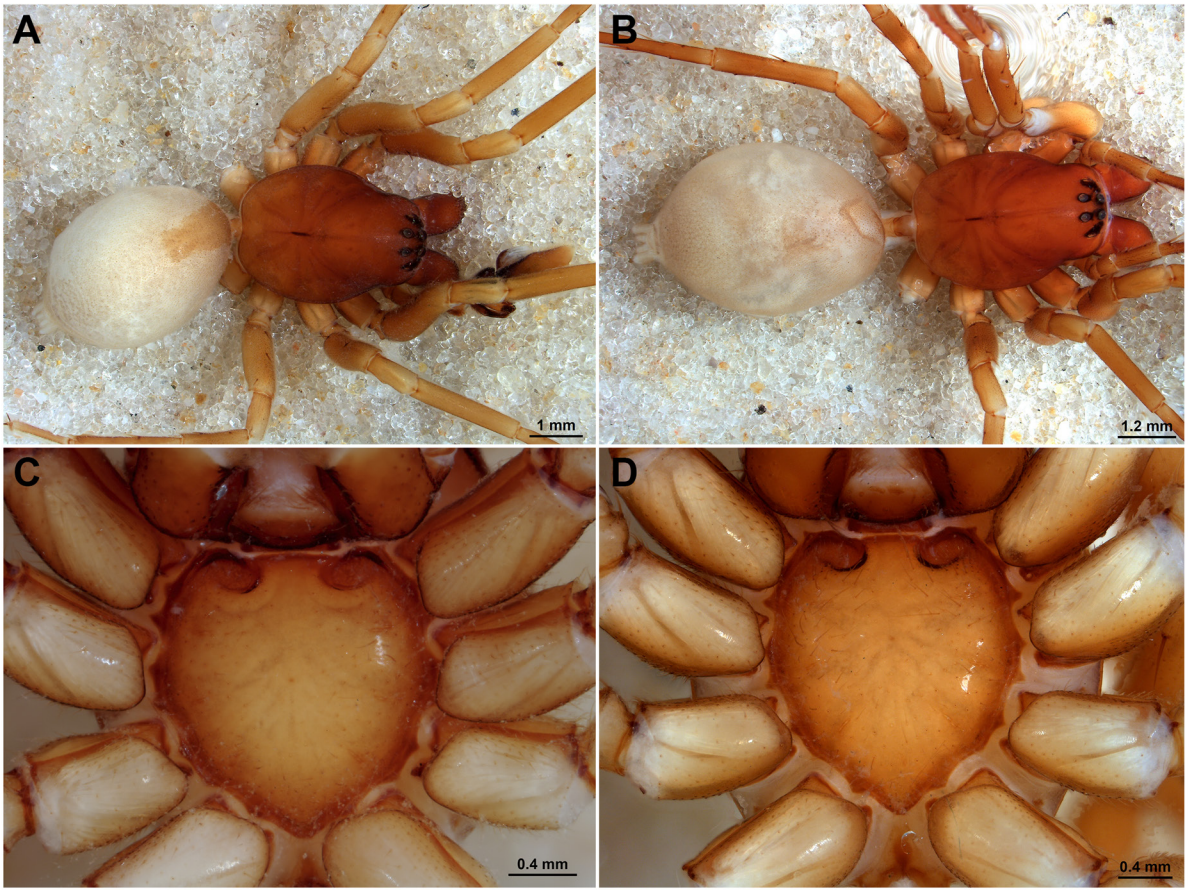

Fig. 37. *Stethorrhagus bradypus* sp. nov. **A, C**. Holotype, ♂ (MCZ-IZ 170622). **B, D**. Paratype, ♀ (MCZ-IZ 170623). **A–B**. Habitus, dorsal view. **C–D**. Sternum.

apically (Figs 38A–B, 39A–C) (SePP with a pointed tip directed retrolaterally in *S. callithrix* – Figs 32A–B, 33A–B) and from those of *S. felis* by the absence of both DL on the RTA and TP1 in the tegulum (RTA with a dorsal lobe and tegulum with TP1 in *S. felis* – Figs 35A–C, 36A–B). Females resemble those of *S. naja* sp. nov. by the epigynum with VEP, CO disposed anteriorly in relation to SI, with a straight posterior margin (Figs 38D–E, 39D–E), differing by the VEP placed medially on the epigynal plate; SI extended anteriorly, with long FDs inserted on the SI's extension, beyond the level of the CO (Figs 38D–E, 39D–E) (VEP placed posteriorly on the epigynal plate; SI not extended anteriorly, below the level of the CO in *S. naja* – Fig. 42D–E).

Etymology

The specific name is a noun in apposition in reference to the bradypodid genus *Bradypus* Linnaeus, 1758, since the general conformation of the epigynum (as in Fig. 38D) resembles a sloth head in frontal view.

Material examined

Holotype

COLOMBIA • ♂; Quindío, Valle del Cauca, 21 km E of Calcara; [4°21′11″ N, 75°47′37″ W]; elev. 10000 feet; 6–11 Feb. 1974; S.J. Peck. leg.; MCZ-IZ 170622.

Paratypes

COLOMBIA • 1 ♀; same data as for holotype; MCZ-IZ 170623 • 1 ♂; same data as for holotype; MCZ-IZ 170624 • 1 ♂; same data as for holotype; MCZ-IZ 170625 • 1 ♀; same data as for holotype; MCZ-IZ 170626.

Description

Male (holotype – MCZ-IZ 170622)

Coloration. Carapace and chelicerae red-brown (Fig. 37A). Endites, labium, sternum and legs deep orange. Abdomen gray with dark anterior stain (Fig. 37A). Sternum with deep sternal excavations (Fig. 37C).

Measurements. Total length 7.02. Carapace 3.29 long, 2.65 wide. Clypeus 0.27. Leg measurements: I: femur 2.75/ patella 1.19/ tibia 2.44/ metatarsus 2.27/ tarsus 1.45/ total 10.10; II: 2.65/ 1.25/ 2.17/ 2.11/ 1.42/ 9.60; III: 2.57/ 1.07/ 1.81/ 2.04/ 1.17/ 8.66; IV: 2.93/ 1.24/ 2.54/ 3.27/ 1.38/ 11.36. Eye diameters: AME 0.19, ALE 0.20, PME 0.21, PLE 0.19. Chelicerae 1.84 long, with three promarginal teeth and four retromarginal denticles.

Leg spination. I – femur d1-1-0, p0-0-1, r0; tibia d0, p0, r0, v1p-2-2-2; metatarsus d0, p0, r0, v2-2-0. II – femur d1-1-0, p0-0-1, r0; tibia d0, p0, r0, v1r-2-1r; metatarsus d0, p0, r0, v2-2-0. III – femur d1-1-0, p0-0-1, r0-0-1; tibia d0, p1-1-0, r1-1-0, v2-2-2-2; metatarsus d0, p1-0-0, r1-0-0, v2-2-1. IV – femur d1-1-0, p0-0-1, r0-0-1; tibia d0, p1-1-0, r1-1-0, v2-2-2; metatarsus d0, p1-1-0, r1-1-0, v2-2-1.

Palp. Retrolateral surface of femur and patella with cluster of modified hairs, RTA with vVL and dVL with modified hairs, vVL larger than dVL, AS absent, DL absent, VTA slightly larger than long in ventral view, spermophor situated ventrally, TP1 and TP2 absent, SePP with blunt tip directed apically, embolus long, gently curved prolaterally in ventral view, prongs long (Figs 38A–C, 39A–C).

Female (paratype – MCZ-IZ 170623)

Coloration. As in male (Fig. 37B). Sternum with sternal excavations as in male (Fig. 37D).

Measurements. Total length 9.18. Carapace 4.02 long, 3.02 wide. Clypeus 0.24. Leg measurements: I: femur 3.26/ patella 1.45/ tibia 2.83/ metatarsus 2.46/ tarsus 1.63/ total 11.63; II: 3.18/ 1.37/ 2.62/ 2.36/

1.57/ 11.10; III: 2.67/ 1.28/ 2.16/ 2.48/ 1.35/ 9.94; IV: 3.53/ 1.39/ 3.03/ 3.78/ 1.59/ 13.32. Eye diameters: AME 0.22, ALE 0.21, PME 0.22, PLE 0.22. Chelicerae 2.09 long, with three promarginal teeth and four retromarginal denticles.

Leg spination. I – femur d1-1-0, p0-0-1, r0; tibia d0, p0, r0, v1p-2-2-2; metatarsus d0, p0, r0, v2-2-0. II – femur d1-1-0, p0-0-1, r0; tibia d0, p0, r0, v2-2-1r; metatarsus d0, p0, r0, v2-2-0. III – femur d1-1-0,

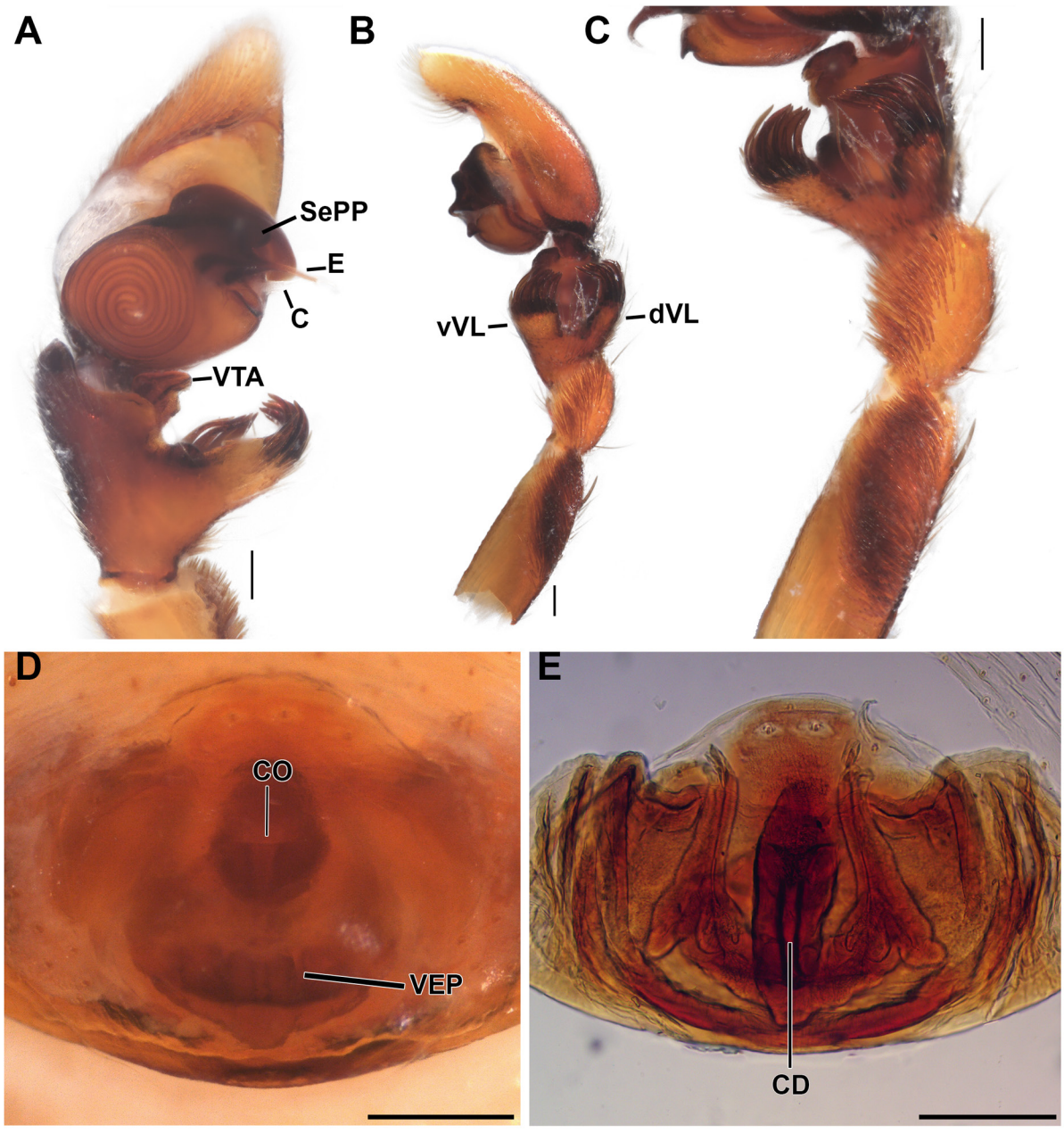

Fig. 38. *Stethorrhagus bradypus* sp. nov. genitalia. **A–C**. Holotype, ♂ (MCZ-IZ 170622), palp. **A**. Ventral view. **B**. Retrolateral view. **C**. Femur, patella and tibia; retrolateral view. **D–E**. Paratype, ♀ (MCZ-IZ 170623), epigynum. **D**. Ventral view. **E**. Dorsal view. Abbreviations: C = conductor; CD = copulatory duct; CO = copulatory opening; dVL = dorsal process of ventral lobe of RTA; E = embolus; SePP = sub-embolic prolateral process; VEP = ventral epigynal plate; VTA = ventral tibial apophysis; vVL = ventral process of ventral lobe of RTA. Scale bars: A–C = 0.2 mm; D–E = 0.5 mm.

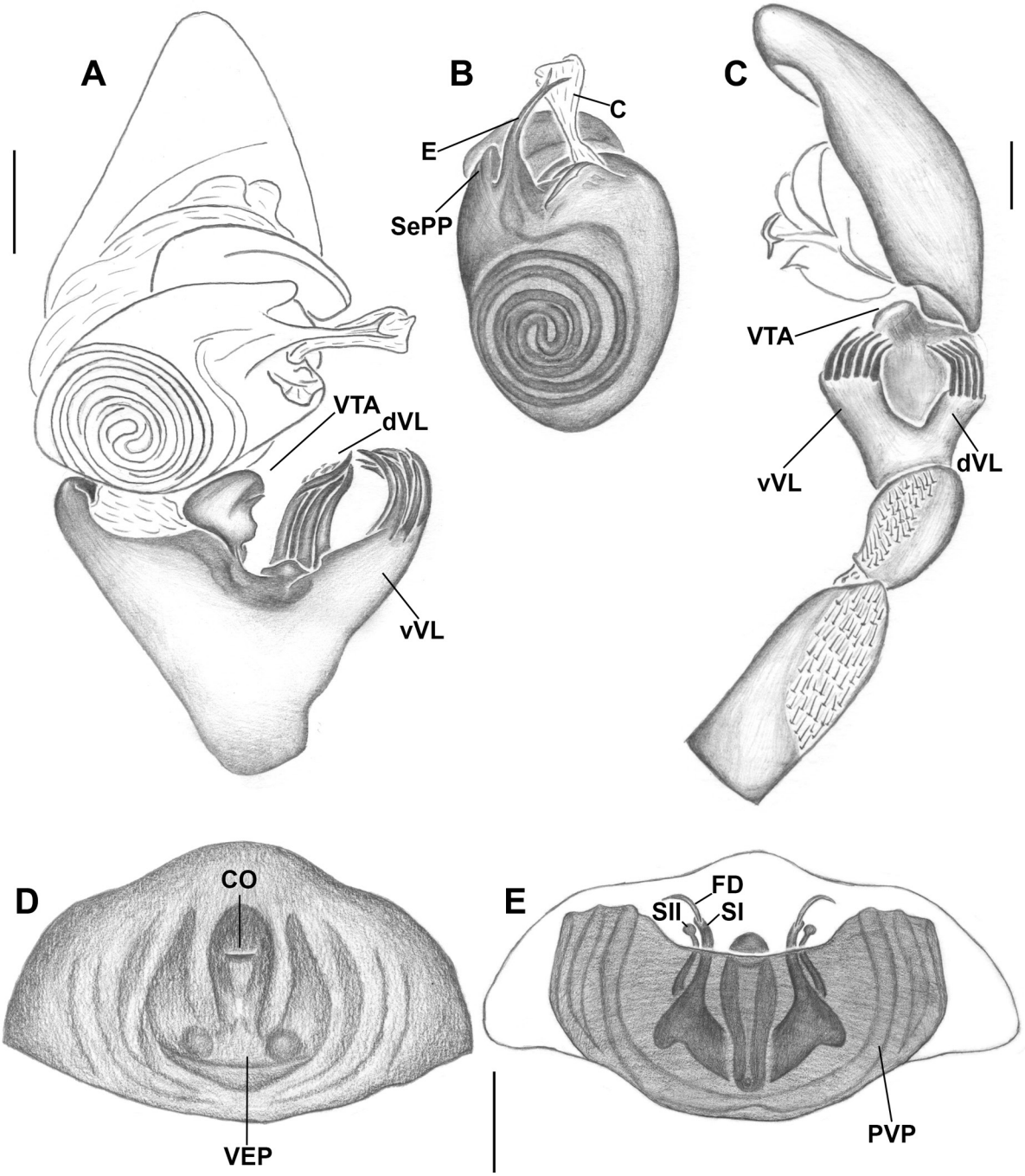

Fig. 39. *Stethorrhagus bradypus* sp. nov. **A–C**. Holotype, ♂ (MCZ-IZ 170622), palp. **A**. Ventral view. **B**. Bulb, ventral view. **C**. Bulb, retrolateral view. **D–E**. Paratype, ♀ (MCZ-IZ 170623), epigynum. **D**. Ventral view. **E**. Dorsal view. Abbreviations: C = conductor; CO = copulatory opening; dVL = dorsal process of ventral lobe of RTA; E = embolus; FD = fertilization duct; PVP = posterior vulvar plate; SePP = sub-embolic prolateral process; SI = primary spermathecae; SII = secondary spermathecae; VEP = ventral epigynal plate; VTA = ventral tibial apophysis; vVL = ventral process of ventral lobe of RTA. Scale bars = 0.25 mm.

p0-1-1, r0; tibia d0, p1-1-0, r1-1-0, v2-2-2; metatarsus d0, p1-0-0, r1-0-0, v2-2-1. IV – femur d1-1-0, p0, r0-0-1; tibia d0, p0-1-0, r1-1-0, v1r-2-2; metatarsus d0, p1-0-0, r1-1-0, v2-2-1.

Epigynum. CO disposed anteriorly to SI, CO with straight posterior margin, VEP placed medially on epigynal plate, PVP wider than long, covering almost entire SI, SI extended anteriorly, long FDs inserted on SI extension beyond CO level, PVP two times the distance between anterior and posterior margins, PVP with slightly procurved notch on anterior margin, CD relatively long, with large reinforcement rods from CO to posterior margin of PVP (Figs 38D–E, 39D–E).

Distribution

Known only the type locality (Fig. 50).

Stethorrhagus naja sp. nov.
urn:lsid:zoobank.org:act:5DC82360-F963-408B-B00B-E0673F637CE2
Figs 40–42, 50

Diagnosis

Males of *S. naja* sp. nov. resemble those of *S. chalybeius* by the bifid VL, with dVL protuding and thick modified hairs only present on the vVL, dVL glabrous (Fig. 41B–C), differing by the large finger-shaped SePP as long as the embolus, with a blunt tip (Fig. 41A) (SePP smaller than the embolus, comma-shaped, tip pointed in *S. chalybeius* – Bonaldo & Brescovit 1994: fig. 16a). Females resemble those of *S. bradypus* sp. nov. by the epigynum with VEP, CO disposed anteriorly in relation to SI, with straight posterior margin (Fig. 41D), differing by the VEP placed posteriorly on the epigynal plate; SI not extended anteriorly, below the level of CO (Figs 41D–E, 42E–F) (VEP placed medially on epigynal plate; SI extended anteriorly, with long FDs inserted on the SI's extension, (beyond the level of the CO in *S. bradypus* – Figs 38D–E, 39D–E).

Etymology

The specific name is a noun in apposition in reference to the elapid genus *Naja* Laurenti, 1768, since the anterior sector of the epigynum (as in Fig. 41D) resembles a cobra with spread hood.

Material examined

Holotype

COLOMBIA • ♂; Cundinamarca, Parque Nacional Natural de Chingaza; [4°0′ N, 73°30′ W]; elev. 3150 m; 16 Dec. 1997; E. Niao leg.; pitfall; ICN-Ar 6477.

Paratypes

COLOMBIA – **Cundinamarca** • 1 ♀; same data as for holotype; ICN-Ar 13743 • 1 ♂; same data as for holotype; 24 Jan. 1998; Guarda Bosques leg.; ICN-Ar 6470.

Description

Male (holotype – ICN-Ar 6477)

Coloration. Carapace, chelicerae, endites and sternum red-brown (Fig. 40A). Labium orange. Legs brown. Abdomen gray with dorsal muscular impression orange (Fig. 40A). Sternum with deep sternal excavations (Fig. 40C).

Measurements. Total length 5.40. Carapace 2.47 long, 1.85 wide. Clypeus 0.22. Leg measurements: I: femur 1.93/ patella 0.77/ tibia 1.53/ metatarsus 1.49/ tarsus 1.19/ total 6.91; II: 1.80/ 0.76/ 1.35/ 1.42/ 1.09/ 6.42; III: 1.55/ 0.64/ 1.08/ 1.40/ 0.82/ 5.49; IV: 2.07/ 0.80/ 1.65/ 2.09/ 0.93/ 7.54. Eye diameters:

AME 0.13, ALE 0.11, PME 0.12, PLE 0.11. Chelicerae 1.15 long, with three promarginal teeth and five retromarginal denticles.

Leg spination. I – femur d1-1-0, p0-0-1, r0; tibia d0, p0, r0, v0-2-0; metatarsus d0, p0, r0, v2-2-0. II – femur d1-1-0, p0-0-1, r0; tibia d0, p0, r0, v0-2-0; metatarsus d0, p0, r0, v2-2-0. III – femur d1-1-0, p0, r0; tibia d0, p1-1-0, r1-1-0, v1p-1p-2; metatarsus d0, p0-1-0, r0-1-0, v2-2-1. IV – femur d1-1-0, p0, r0-0-1; tibia d0, p1-1-0, r1-1-0, v1p-1p-2; metatarsus d0, p1-1-0, r1-1-0, v2-2-1.

Palp. Retrolateral surface of femur with a cluster of modified hairs, vVL with modified hairs, dVL glabrous, well-developed, subrectangular, vVL larger than dVL, AS absent, DL absent, VTA slightly broader than long in ventral view, spermophor situated prolaterally, TP1 small, triangular, TP2 absent, SePP well-developed, finger-shaped, tip blunt, pointed retrolaterally, embolus long, not curved, prongs short, not curved (Figs 41A–C, 42A–C).

Female (paratype – ICN-Ar 13743)

Coloration. As in male, except abdomen totally dark gray (Fig. 40B). Sternum with sternal excavations as in male (Fig. 40D).

Measurements. Total length 6.97. Carapace 2.70 long, 2.00 wide. Clypeus 0.22. Leg measurements: I: femur 1.99/ patella 0.94/ tibia 1.50/ metatarsus 1.49/ tarsus 1.08/ total 7.00; II: 1.92/ 0.90/ 1.34/ 1.45/

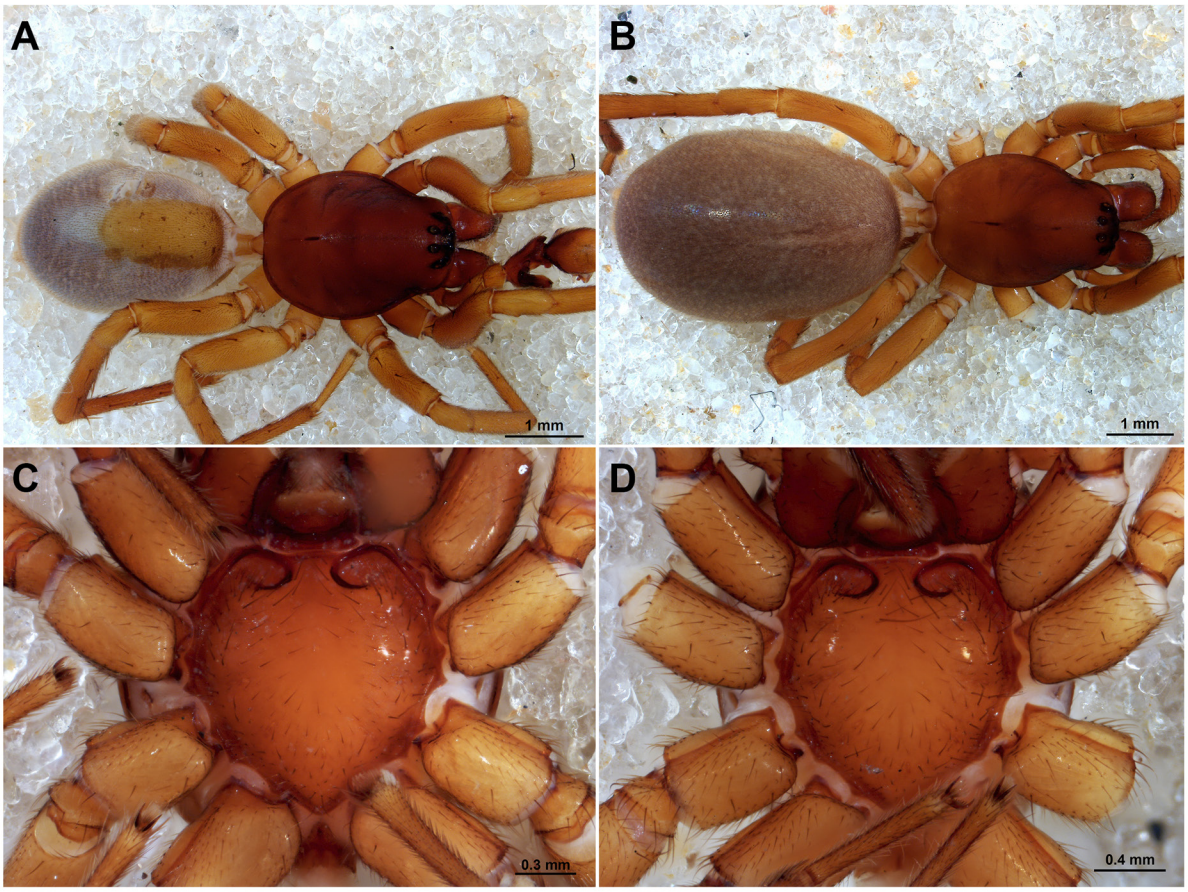

Fig. 40. *Stethorrhagus naja* sp. nov. **A, C**. Holotype, ♂ (ICN Ar-6477). **B, D**. Paratype, ♀ (ICN Ar-13743). **A–B**. Habitus, dorsal view. **C–D**. Sternum.

1.14/ 6.75; III: 1.65/ 0.79/ 1.15/ 1.36/ 0.88/ 5.83; IV: 2.21/ 0.91/ 1.86/ 2.24/ 0.96/ 8.18. Eye diameters: AME 0.13, ALE 0.11, PME 0.11, PLE 0.12. Chelicerae 1.34 long, with three promarginal teeth and five retromarginal denticles.

Leg spination. I – femur d1-1-0, p0-0-1, r0; tibia d0, p0, r0, v0-2-0; metatarsus d0, p0, r0, v2-2-0. II – femur d1-1-0, p0, r0; tibia d0, p0, r0, v0-1p-0; metatarsus d0, p0, r0, v2-2-0. III – femur d1-1-0, p0,

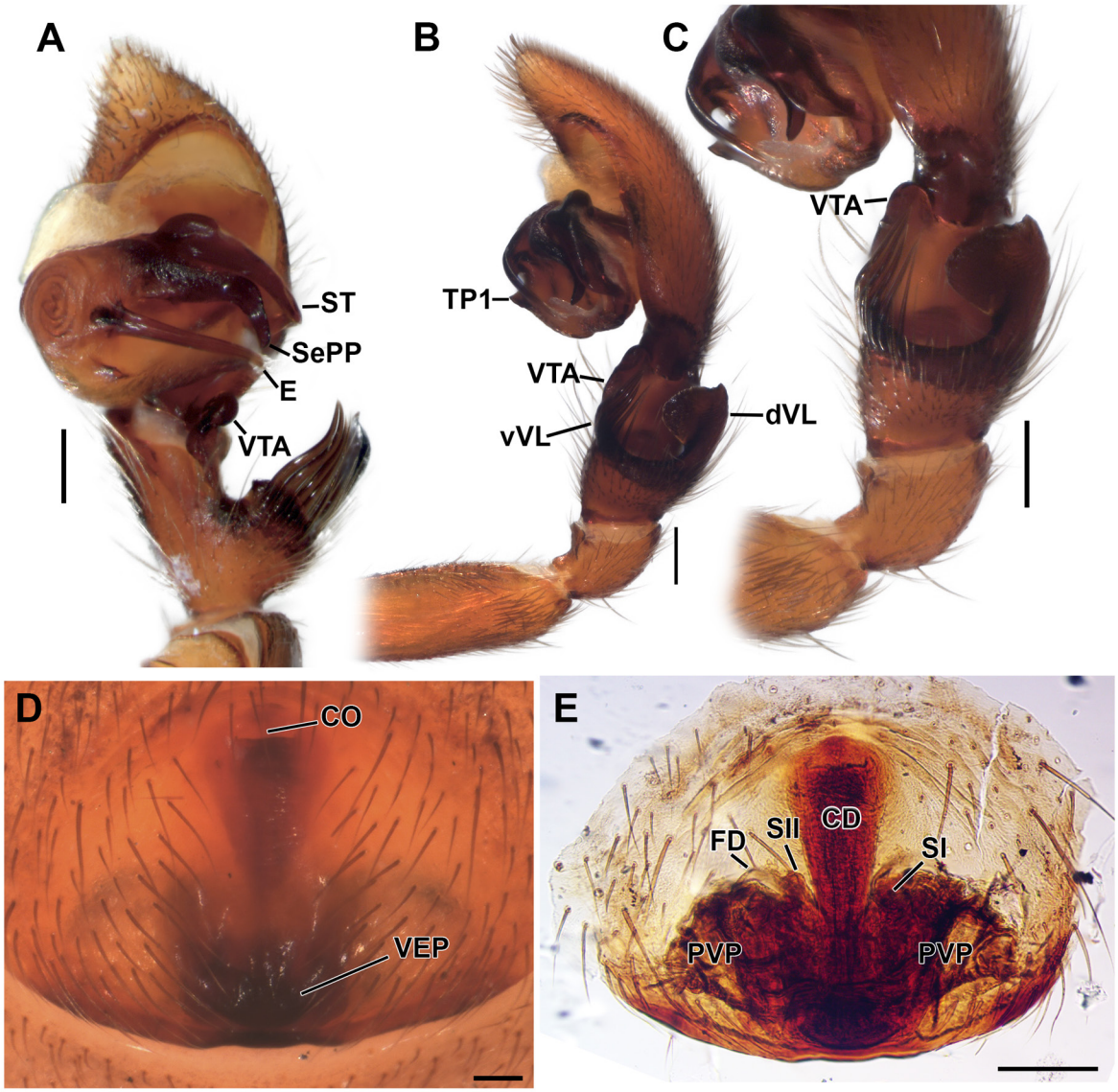

Fig. 41. *Stethorrhagus naja* sp. nov., genitalia. **A–C**. Holotype, ♂ (ICN-Ar 6477), palp. **A**. Ventral view. **B**. Retrolateral view. **C**. Femur, patella and tibia; retrolateral view. **D–E**. Paratype, ♀ (ICN-Ar 13743), epigynum. **D**. Ventral view. **E**. Dorsal view. Abbreviations: CD = copulatory duct; CO = copulatory opening; dVL = dorsal process of ventral lobe of RTA; E = embolus; FD = fertilization duct; PVP = posterior vulvar plate; SI = primary spermathecae; SII = secondary spermathecae; SePP = sub-embolic prolateral process; ST = subtegulum; TP1 = tegular process 1; VEP = ventral epigynal plate; VTA = ventral tibial apophysis; vVL = ventral process of ventral lobe of RTA. Scale bars: A–D = 0.2 mm; E = 0.5 mm.

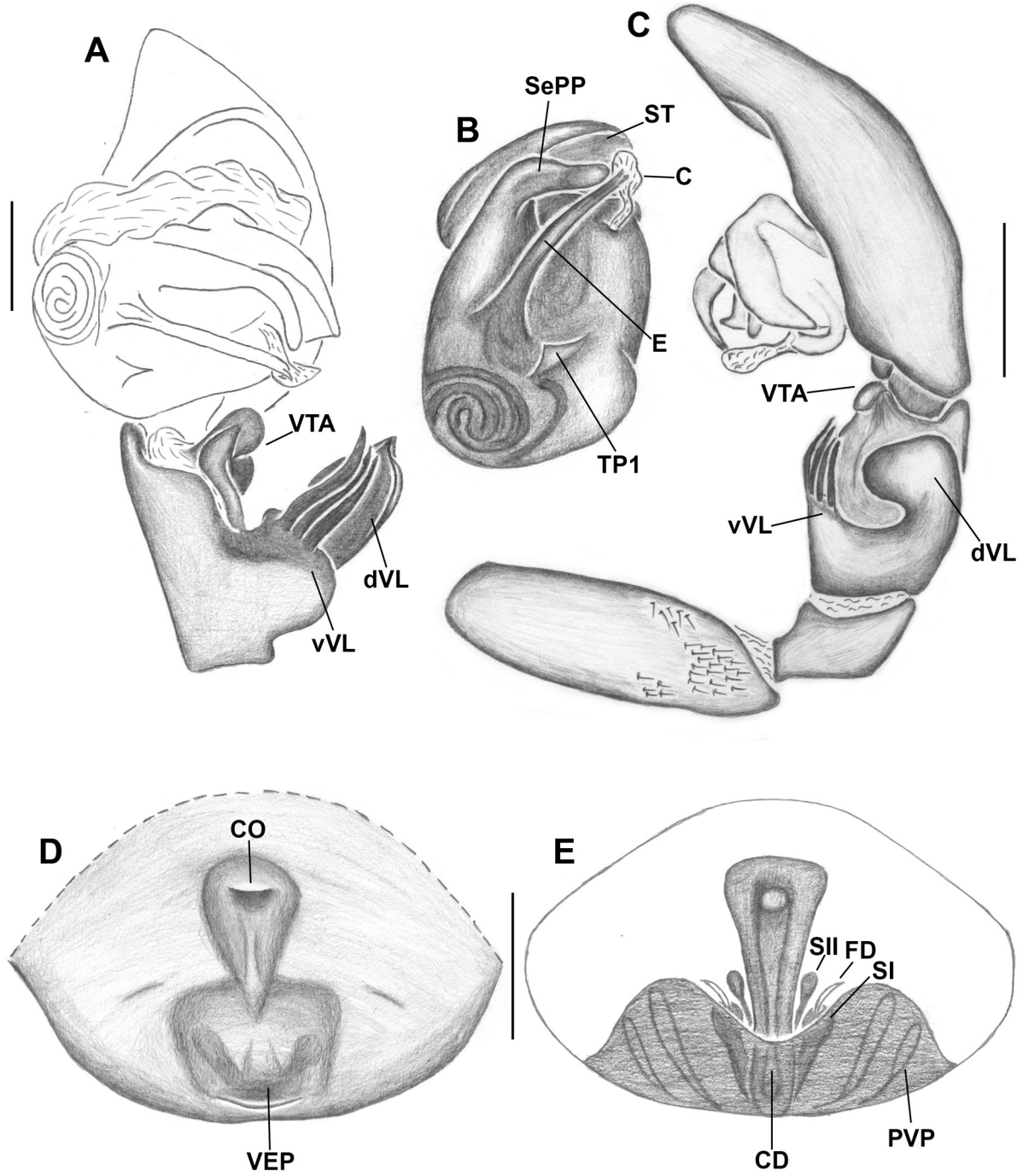

Fig. 42. *Stethorrhagus naja* sp. nov. **A–B**. Holotype, ♂ (ICN Ar-6477), palp. **A**. Ventral view. **B**. Bulb, ventral view. **C**. Bulb, retrolateral view. **D–E**. Paratype, ♀ (ICN Ar-13743), epigynum. **D**. Ventral view. **E**. Dorsal view. Abbreviations: CD = copulatory duct; CO = copulatory opening; dVL = dorsal process of ventral lobe of RTA; E = embolus; FD = fertilization duct; PVP = posterior vulvar plate; SI = primary spermathecae; SII = secondary spermathecae; SePP = sub-embolic prolateral process; ST = subtegulum; TP1 = tegular process 1; VEP = ventral epigynal plate; VTA = ventral tibial apophysis; vVL = ventral process of ventral lobe of RTA. Scale bars = 0.25 mm.

r0; tibia d0, p0-1-0, r0-1-0, v1p-2-2; metatarsus d0, p1-1-0, r1-1-0, v2-2-1. IV – femur d1-1-0, p0, r0; tibia d0, p1-1-0, r1-1-0, v1p-1p-2; metatarsus d0, p1-1-1, r1-1-1, v2-2-1.

Epigynum. CO disposed anteriorly in relation to SI, CO with straight posterior margin, VEP placed posteriorlly on epigynal plate, PVP wider than long, covering entire SI, PVP as wide as four times the distance between anterior and posterior margins, PVP with slightly procurved notch along anterior margin, copulatory duct as long as two times the distance between anterior and posterior margins of PVP (Figs 41D–E, 42D–E).

Distribution

Known only from the type locality (Fig. 50).

Stethorrhagus chalybeius (L. Koch, 1866)
Fig, 51

Hypsinotus chalybeius L. Koch, 1866: 280: pl. 11 figs 179–181, ♂.

Corinna chalybeia – Petrunkevitch 1911: 465.
Stethorrhagus chalybeius – Bonaldo & Brescovit 1994: 54, figs 1a–d, 2a–e, 3d–f, 4a–f, 5a–d, 6f, 7a–c, 16a–e, ♂♀ (transferred from *Corinna*).

Diagnosis

Males of *S. chalybeius* resemble those of *S. naja* sp. nov. by the bifid VL, with dVL protruding and thick modified hairs present only in vVL, dVL glabrous, differing by the smaller than the embolus, comma-shaped SePP, with a pointed tip (Bonaldo & Brescovit 1994: fig. 16a) (SePP larger, as long as the embolus, finger-shaped, tip blunt in *S. naja* – Fig. 42B). Females resemble those of *S. mandrillus* sp. nov. by the anterior margin of the CO delimited by a protruding lip (Bonaldo & Brescovit 1994: fig. 16d), differing by the lip being divided into two humps (Bonaldo & Brescovit 1994: fig. 16d) (lip entire in *S. mandrillus* – Figs 16D, 17C).

Type material

Lectotype of *Hypsinotus chalybeius* L. Koch, 1866
COLOMBIA • ♂; New Granada (probably Colombia); BMNH 1890.7.I.1241-1242 (examined).

Description

Male and female, see Bonaldo & Brescovit (1994: 49).

Distribution

Colombia (Fig. 51).

Stethorrhagus sciurus sp. nov.
urn:lsid:zoobank.org:act:AC0B278B-B104-42F6-8C00-85222472A373
Figs. 43, 49, 51

Diagnosis

Females of *S. sciurus* sp. nov. resembles those of *S. callithrix* sp. nov. and *S. sylvilagus* sp. nov. by the epigynal plate and CO U-shaped, disposed anteriorly in relation to SI, with VEP gently procurved, placed posteriorly on the epigynal plate (Fig. 43C–F), differing from *S. callithrix* by the CD being relatively short (from CO to posterior margin of VEP, less than four times longer than the CO width) (Fig. 43C–F) (CD relatively long, from CO to posterior margin of VEP, more than six times longer than the CO width

in *S. callithrix* – Figs 32C–D, 33C–D) and from those of *S. sylvilagus* sp. nov. by the area between the posterior margin of VEP and the posterior margin of the epigynal ventral plate depressed (Fig. 43C) (area between the posterior margin of VEP and the posterior margin of the epigynal ventral plate bulging in *S. sylvilagus* – Figs 25C–D, 26C–D).

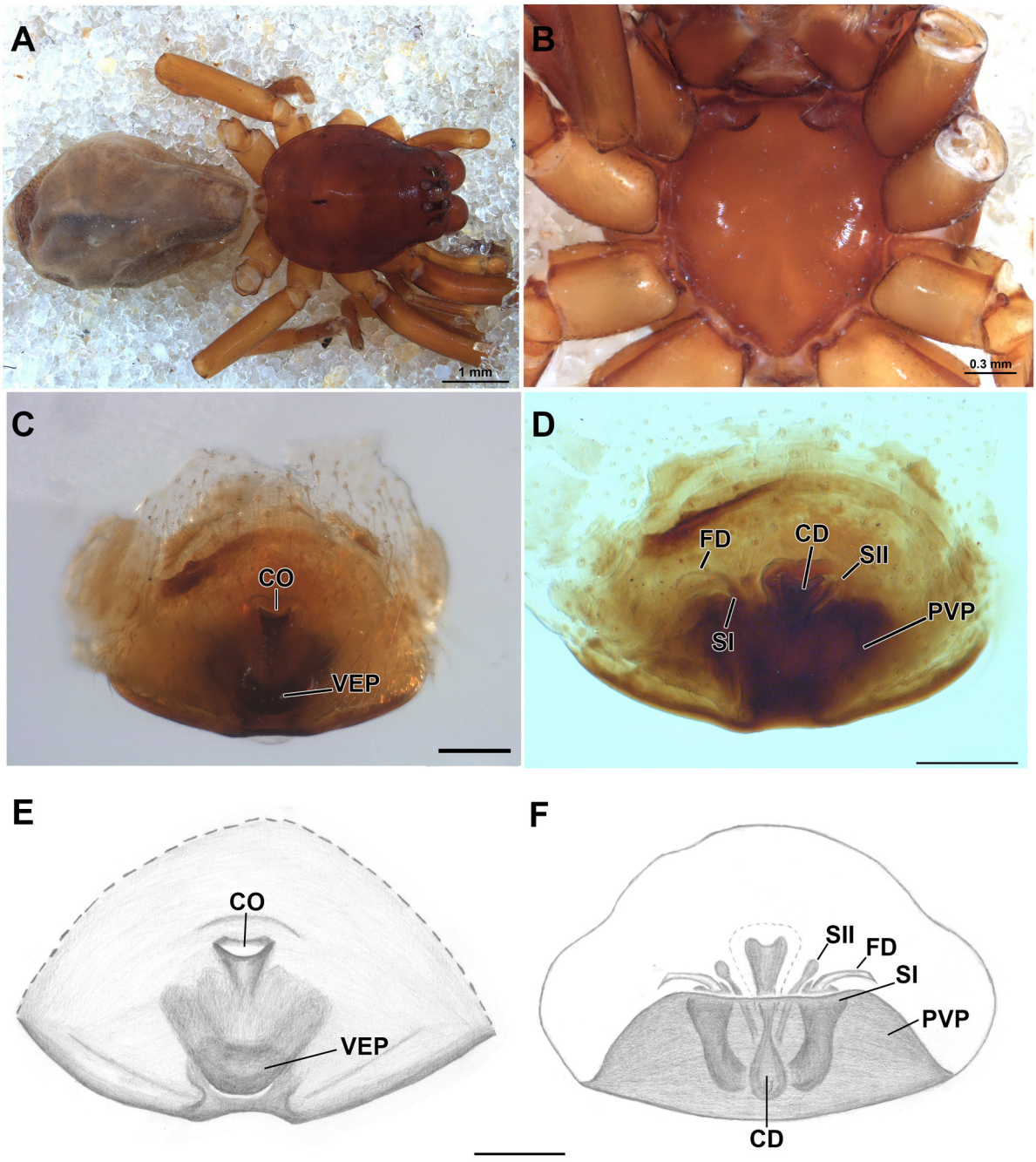

Fig. 43. *Stethorrhagus sciurus* sp. nov., holotype, ♀ (SMF). **A**. Habitus, dorsal view. **B**. Sternum. **C–F**. Epigynym. **C, E**. Ventral view. **D, F**. Dorsal view. Abbreviations: CO = copulatory opening; CD = copulatory duct; FD = fertilization duct; PVP = posterior vulvar plate; SI = primary spermathecae; SII = secondary spermathecae; VEP = ventral epigynal plate. Scale bars: C–D = 0.5 mm; E–F = 0.25 mm.

Etymology

The specific name is a noun in apposition in reference to the rodent genus *Sciurus* Linnaeus, 1758, since the general conformation of the epigynum (as in Fig. 43C) resembles a squirrel head in frontal view.

Material examined

Holotype

COLOMBIA • ♀; Cundinamarca, Sabana de Bogotá; [4°45′16″ N, 74°10′31″ W]; elev. 3000 m; Oct. 1956; Noguel-Maier leg.; SMF.

Description

Male

Unknown.

Female (holotype – SMF)

Coloration. Cephalothorax red-brown. Legs yellow-brown. Abdomen gray dorsally and cream ventrally (Fig. 43A). Sternum with deep sternal excavations (Fig. 43B).

Measurements. Total length 6.35. Carapace 2.73 long, 2.19 wide. Clypeus 0.26. Leg measurements: I: femur 2.05/ patella 0.92/ tibia 1.80/ metatarsus 1.47/ tarsus 1.08/ total 7.32; II: 1.86/ 0.92/ 1.63; III: 1.77/ 0.85/ 1.31/ 1.42/ 0.72/ 6.07; IV: 2.44/ 0.94/ 2.18/ 2.40/ 1.00/ 8.96. Eye diameters: AME 0.17, ALE 0.15, PME 0.14, PLE 0.14. Chelicerae 1.15 long, with three promarginal teeth and five retromarginal denticles.

Leg spination. I – femur d1-0-0, p0, r0; tibia d0, p0, r0, v0-1p-1p; metatarsus d0, p0, r0, v2-2-0. II – femur d1-0-0, p0, r0; tibia missing; metatarsus missing. III – femur d1-0-0, p0, r0; tibia d0, p1-1-0, r0-0-1, v1p-2-2; metatarsus d0, p1-1-1, r1-1-1, v2-2-1. IV – femur d1-1-0, p0, r0; tibia d0, p1-1-0, r1-1-0, v1p-1p-2; metatarsus d0, p1-1-1, r1-1-1, v2-2-1.

Epigynum. CO posterior margin U-shaped, CO disposed anteriorly in relation to SI, VEP gently procurved, placed posteriorly on epigynal plate, area between posterior margin of VEP and posterior margin of epigynal plate depressed, PVP subrectangular, covering SI, CD relatively short, from CO to posterior margin of VEP, less than four times longer than CO width, narrowed in median portion (Fig. 43).

Distribution

Known only from the type locality (Fig. 49).

Stethorrhagus roraimae Gertsch, 1942
Figs 7A–C, 49

Stethorrhagus roraimae Gertsch, 1942: 13, fig. 36, ♀.

Stethorrhagus roraimae – Bonaldo & Brescovit 1994: 61, fig. 23a–b, ♀.

Diagnosis

Females are similar to those of *S. hyula*, *S. nigrinus* and *S. papilio* sp. nov. by the epigynal plate without VEP and with the CO disposed anteriorly in relation to SI (Figs 7B–C, 23C–D, 44C–D, 45C–F; Bonaldo & Brescovit 1994: figs 19c–d, 21b–c, 23a). They differ from those of *S. hyula* by the epigynal plate without a posterior median half-moon-shaped sclerotization (Fig. 7C; Bonaldo & Brescovit 1994: fig. 23a) (present in *S. hyula* – Bonaldo & Brescovit 1994: fig. 19c); from those of *S. nigrinus* and *S. papillio* by the small CO, with its width nearly 12 times smaller than the distance between the CO and

the posterior margin of the epigynal plate (Figs 44C–D, 45C–F; Bonaldo & Brescovit 1994: fig. 23a) (relatively large CO, with width four times smaller than the distance between the CO and the posterior margin of epigynal plate in *S. nigrinus* and *S. papillio* – Figs 44C–D, 45C–F).

Type material

Holotype

BRAZIL • ♀; Roraima, Ireng River; [3°45′31.45″ N, 59°40′47.02″ W]; 15 Aug. 1911; AMNH (re-examined from photos).

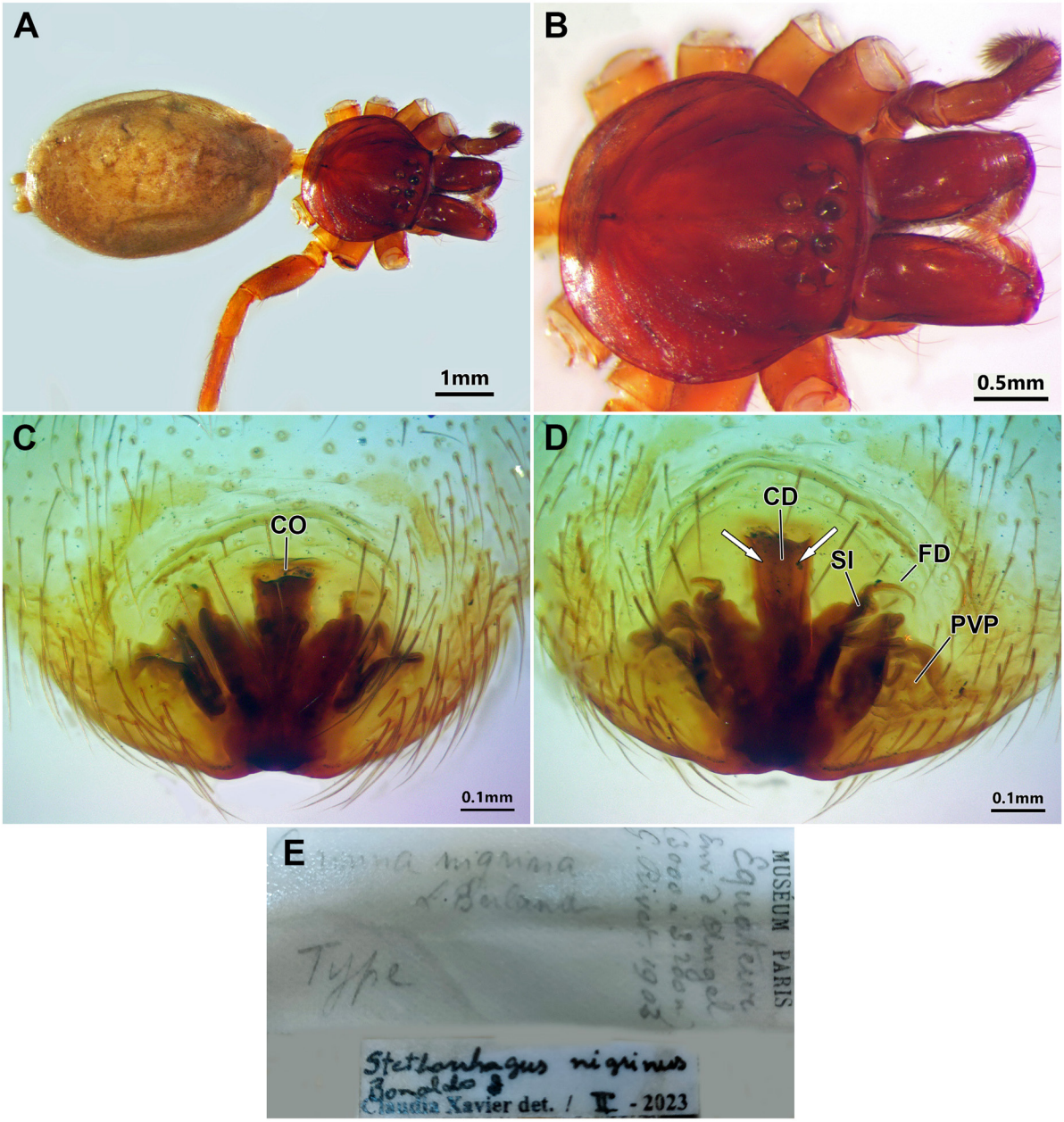

Fig. 44. *Stethorrhagus nigrinus* (Berland, 1913), ♀ (MNHN). **A**. Habitus, dorsal view. **B**. Prosoma dorsal view. **C–D**. Female epigynum. **C**. Ventral view. **D**. Dorsal view; arrows pointing to reinforcement rods. **E**. Labels. Photos A–D by Yvan Montardi. Abbreviations: CO = copulatory opening; CD = copulatory duct; FD = fertilization duct; PVP = posterior vulvar plate; SI = primary spermathecae.

Description

Female, see Bonaldo & Brescovit (1994: 61); male unknown. Additional documentation of the female holotype in Fig. 7A–C.

Distribution

Known only from the type locality (Fig. 49).

Stethorrhagus nigrinus (Berland, 1913)
Figs 44, 50

Corinna nigrina Berland, 1913: 99, ♀.

Stethorrhagus nigrinus – Bonaldo & Brescovit 1994: 59, fig. 21b–c (transferred from *Corinna*).

Diagnosis

Females are similar to those of *S. hyula*, *S. roraimae* and *S. papilio* sp. nov. by the epigynal plate without VEP, with CO disposed anteriorly in relation to SI (Figs 7B–C, 23B–D, 44C–D, 45C–F; Bonaldo & Brescovit 1994: figs 19c–d, 21b–c, 23a). They differ from those of *S. hyula* by the epigynal plate without a posterior median half-moon-shaped sclerotization (Fig. 44C–D; Bonaldo & Brescovit 1994: fig. 21b–c) (present in *S. hyula* – Bonaldo & Brescovit 1994: fig. 19c); from those of *S. roraimae* by the relatively large CO, with width four times smaller than the distance between the CO and the posterior margin of epigynal plate (Fig. 44C–D) (small CO, with width nearly 12 times smaller than the distance between the CO and the posterior margin of the epigynal plate in *S. roraimae* (Bonaldo & Brescovit 1994: fig. 23a); and from those of *S. papillio* by the posterior border of the CO sinuous; CD's dorsal reinforcement rods not surpassing CO anteriorly (Fig. 44C–D; Bonaldo & Brescovit 1994: fig. 21b) (posterior border of CO straight; CD's dorsal reinforcement rods surpassing CO anteriorly in *S. papillio* – Fig. 45C–F).

Type material

Holotype

ECUADOR • ♀; El Ángel [Carchi]; [0°37′05.93″ N, 77°56′32.83″ W]; elev. 3000–3200 m; Rivet leg.; MNHN (examined).

Description

See Bonaldo & Brescovit (1994: 59). Additional documentation of the habitus and copulatory organs is provided in Fig. 44.

Distribution

Known only from the type locality (Fig. 50).

Stethorrhagus papilio sp. nov.
urn:lsid:zoobank.org:act:04E89F12-3F4B-414B-9D6A-D79DBE8797CF
Figs 45, 51

Diagnosis

Females are similar to those of *S. hyula*, *S. roraimae* and *S. nigrinus* by the epigynal plate without VEP, with CO disposed anteriorly in relation to SI (Figs 7C, 23C–D, 44C–D, 45C–F; Bonaldo & Brescovit 1994: figs 19c–d, 21b–c, 23a–b). They differ from those of *S. hyula* by the epigynal plate without a posterior median half-moon-shaped sclerotization (Fig. 45C–F) (present in *S. hyula* Bonaldo & Brescovit 1994: fig. 19c); from those of *S. roraimae* by the relatively large CO, with its width four times smaller

than the distance between the CO and the posterior margin of the epigynal plate (Fig. 45C–F) (small CO, with width nearly 12 times smaller than the distance between the CO and the posterior margin of the epigynal plate in *S. roraimae* (Fig. 7C; Bonaldo & Brescovit 1994: fig. 23a) and from those of *S. nigrinus* by the posterior border of CO straight; CD's dorsal reinforcement rods surpassing CO

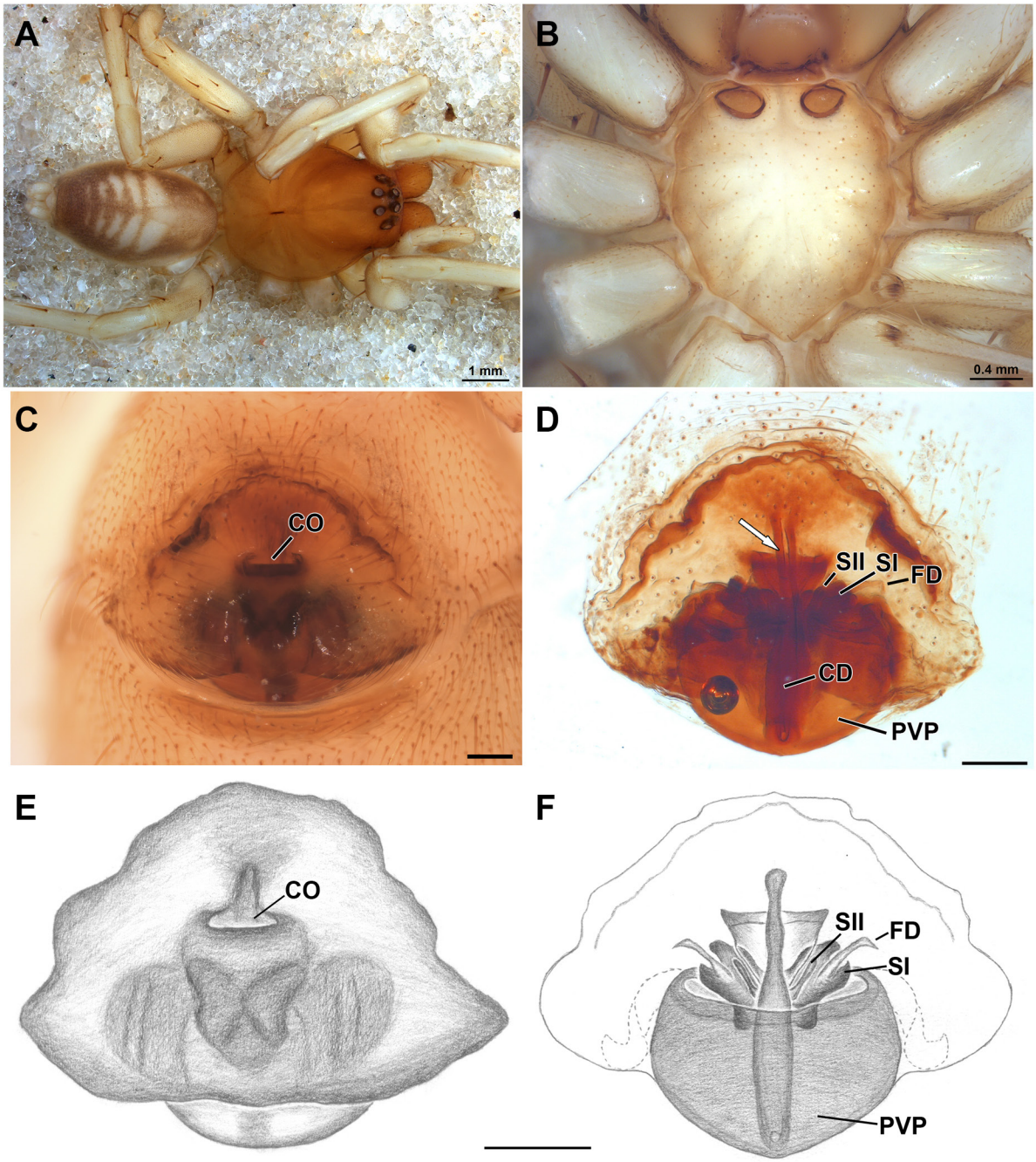

Fig. 45. *Stethorrhagus papilio* sp. nov., paratype, ♀ (CASENT9119043). **A**. Habitus, dorsal view. **B**. Sternum. **C–F**. Epigynym. **C, E**. Ventral view. **D, F**. Dorsal view. Abbreviations: CD = copulatory duct; CO = copulatory opening; FD = fertilization duct; PVP = posterior vulvar plate; SI = primary spermathecae; SII = secondary spermathecae; arrow pointing to reinforcement rods. Scale bars: C–D = 0.5 mm; E–F = 0.25 mm.

anteriorly (Fig. 45C–F) (posterior border of CO sinuous; CD's dorsal reinforcement rods not surpassing CO anteriorly *S. nigrinus* (Fig. 44C–D; Bonaldo & Brescovit 1994: fig. 21b).

Etymology

The specific name is a noun in apposition in reference to the lepidopteran genus *Papilio* Linnaeus, 1758, since the median sector of the epigynum (as in Fig. 45C) resembles a butterfly in dorsal view.

Material examined

Holotype

COLOMBIA • ♀; Nariño, from 25 mi. SW of Mocoa; [1°08′45″ N, 76°38′16″ W]; 3 Mar. 1955; E.S. Shinger and E.S. Ross leg.; CAS 9119043.

Description

Male

Unknown.

Female (holotype – CASENT9119043)

Coloration. Carapace orange-brown, dark in cephalic area. Sternum, endites, labium and legs yellow. Chelicerae brown. Abdomen gray with white dorsal spots (Fig. 45A) venter and spinnerets cream. Sternum with deep sternal excavations (Fig. 45B).

Measurements. Total length 7.71, prosoma length 3.76, width 2.88. Clypeus 0.30. I: femur 3.25/ patella 1.22/ tibia 2.88/ metatarsus 2.67/ tarsus 1.60/ total 11.62; II: 3.20/ 1.29/ 2.75/ 2.65/ 1.50/ 11.39; III: 2.90/ 1.30/ 2.29/ 2.61/ 1.31/ 10.41; IV: 3.61/ 1.30/ 3.18/ 3.94/ 1.54/ 13.57. Eye diameters: AME 0.20, ALE 0.19, PME 0.19, PLE 0.18. Chelicerae 1.68 long, with three promarginal teeth and five retromarginal denticles.

Leg spination. I – femur d1-1-0, p0-0-1, r0; tibia d0, p0, r0, v2-1p-2-2; metatarsus d0, p0, r0, v2-2-0. II – femur d1-1-0, p0-1-1, r; tibia d0, p0, r0, v1r-2-2-0; metatarsus d0, p0, r0, v2-2-0. III – femur d1-1-1, p0-0-1, r0-0-1; tibia d0, p1-1-0, r1-1-0, v2-2-2; metatarsus d0, p1-1-1, r1-1-1, v2-2-1. IV – femur d1-1-1, p0-1-1, r0-1-1; tibia d0-1-0, p1-1-0, r1-1-0, v2-2-2; metatarsus d0, p1-1-1, r1-1-1, v2-2-2.

Epigynum. CO slit-shaped, disposed anteriorly in relation to SI, posterior border of CO straight, CD's dorsal reinforcement rods surpassing CO anteriorly, VEP absent, PVP almost as wide as long, covering almost entire SI, posterior margin of PVP rounded and protruding (Fig. 45C–F).

Distribution

Known only from the type locality (Fig. 51).

Stethorrhagus maculatus (L. Koch, 1866)
Figs 46, 50

Hypsinotus maculatus L. Koch, 1866: 283, pl. 12 fig. 182, ♀ (original description)

Corinna maculata – Petrunkevitch 1911: 467.
Stethorrhagus maculatus – Bonaldo 2000: 125 (transferred from *Corinna*).

Diagnosis

Females resemble those of *S. tremarctos* sp. nov. and *S. loxodonta* sp. nov. by the CO circular, disposed posteriorly in relation to the SI, and the anterior margin of the CO not delimited by a lip (Fig. 46C). They

differ from those of *S. tremarctos* by the depression anterior to the CO shallow, sub-triangular (Fig. 46C) (depression anterior to the CO deep, quadrangular in *S. tremarctos* – Figs 13D, 14C) and from those of *S. loxodonta* by the VEP lateral margins straight, diverging anteriorly (Fig. 46C) (VEP lateral margins curved, converging anteriorly in *S. loxodonta* – Figs 19D, 20C).

Type material

Holotype

COLOMBIA • ♀; [Cundinamarca], Santa Fé de Bogotá; Keyserling leg.; BMNH 1890.7.1.1234-H0 (examined).

Description

See L. Koch (1866: 283). Additional documentation of the habitus and copulatory organ is provided in Fig. 46.

Distribution

Known only from the type locality (Fig. 50).

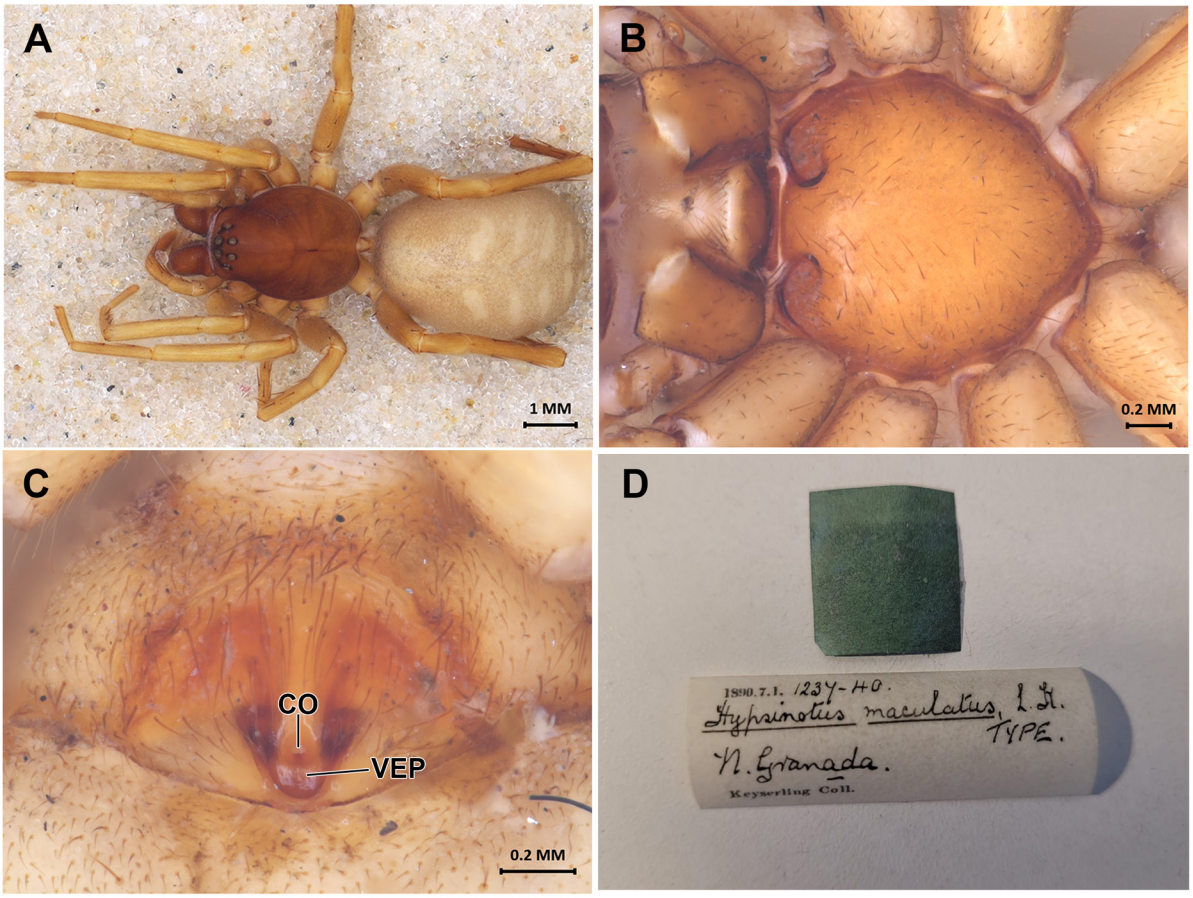

Fig. 46. *Stethorrhagus maculatus* (L. Koch, 1866), syntype, ♀ (BMNH). **A**. Habitus, dorsal view. **B**. Sternum. **C**. Epigynum ventral view. **D**. Labels. Abbreviations: CO = copulatory opening; VEP = ventral epigynal plate.

Stethorrhagus canis sp. nov.
urn:lsid:zoobank.org:act:9B0CE66C-3675-4EA9-911D-41E8DA950DC4
Figs 47, 49–50

Diagnosis

Females resemble those of *S. felis* sp. nov. and *S. ovis* sp. nov. by the CO slit-shaped, disposed posteriorly in relation to SI (Figs 29C–D, 30C–D, 35D–E, 36C–D), differing by the CO large, as wide as the

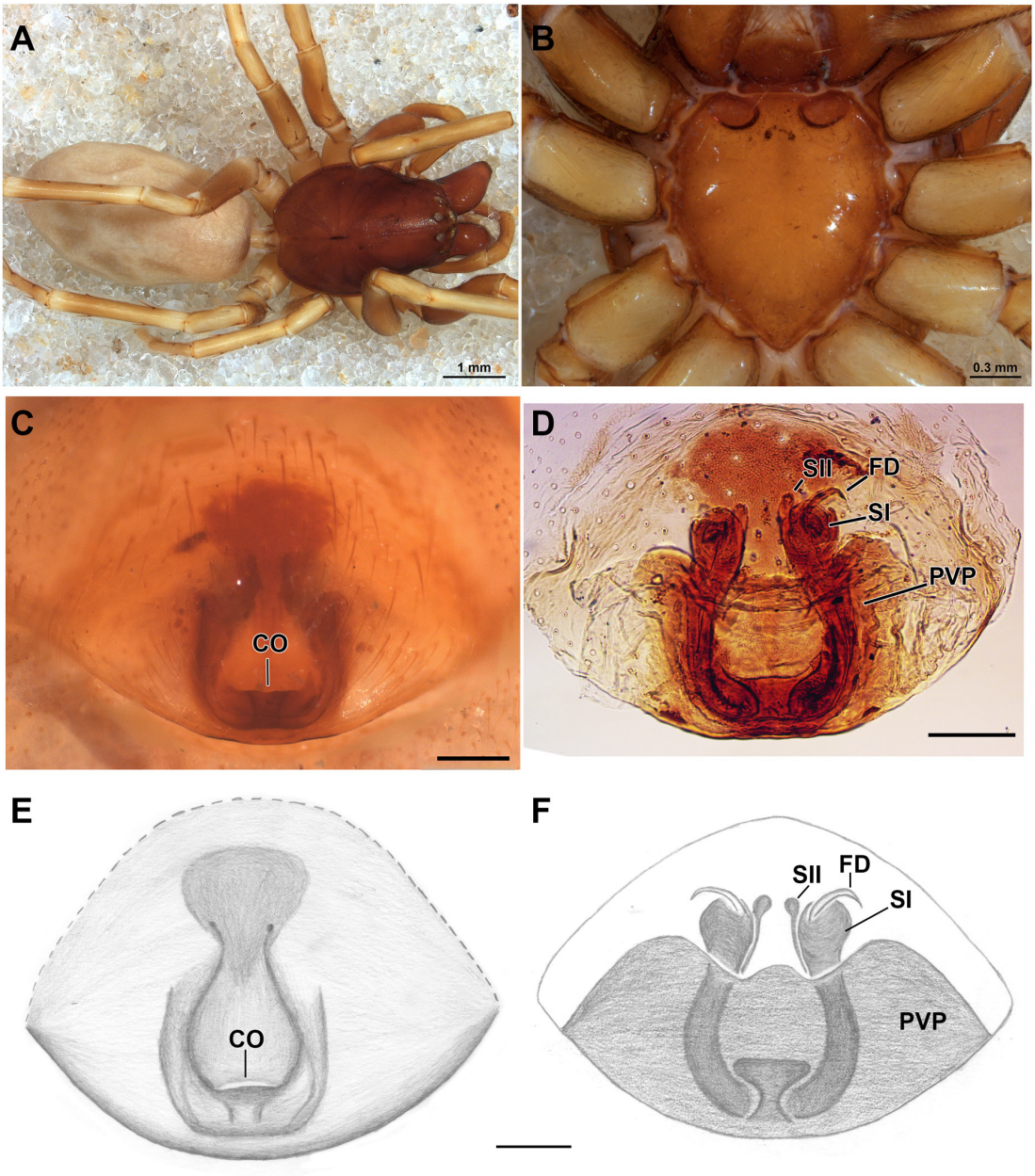

Fig. 47. *Stethorrhagus canis* sp. nov., holotype, ♀ (CASENT9119044). **A**. Habitus, dorsal view. **B**. Sternum. **C–F**. Epigynum. **C, E**. Ventral view. **D, F**. Dorsal view. Abbreviations: CO = copulatory opening; FD = fertilization duct; PVP = posterior vulvar plate; SI = primary spermathecae; SII = secondary spermathecae. Scale bars: C–D = 0.5 mm; E–F = 0.25 mm.

distance between the CO and the posterior margin of the epigynal plate, located on the posterior half of the epigynal plate (Fig. 47C–F) (CO relatively small, as wide as five times the distance between the CO and the posterior margin of the epigynal plate, located on the anterior half of the epigynal plate in both *S. felis* and *S. ovis* – Figs 29C–D, 30C–D, 36C–D, 35D–E).

Etymology

The specific name is a noun in apposition in reference to the carnivor genus *Canis* Linnaeus, 1758, since the general conformation of the epigynum (as in Fig. 47C) resembles a basset hound head in frontal view.

Material examined

Holotype

ECUADOR • ♀; 6–8 mi. SE of Baños, N slope of Mt Tungurahua; [1°24′59″ S, 78°25′33″ W]; 13 Feb. 1955; E.S. Schlinger and E.S. Ross leg.; CAS9119044.

Paratype

ECUADOR • 1 ♀; same data as for holotype; CAS9119045.

Description

Female (holotype – CASENT9119044)

Coloration. Cephalothorax brown. Legs red-brown with tibiae, metatarsi and tarsi yellow. Abdomen gray with dorsal anterior border brown (Fig. 47A). Sternum with deep sternal excavations (Fig. 47B).

Measurements. Total length 6.70. Carapace 2.69 long, 2.07 wide. Clypeus 0.21. Leg measurements: I: femur 2.13/ patella 0.91/ tibia 1.94/ metatarsus 1.76/ tarsus 1.00/ total 7.74; II: 2.03/ 0.92/ 1.77/ 1.61/ 0.96/ 7.29; III: 1.95/ 0.82/ 1.53/ 1.70/ 0.93/ 6.93; IV: 2.43/ 0.99/ 2.26/ 2.58/ 1.05/ 9.31. Eye diameters: AME 0.19, ALE 0.17, PME 0.15, PLE 0.17. Chelicerae 1.19 long, with four promarginal teeth and five retromarginal denticles.

Leg spination. I – femur d1-1-0, p0-0-1, r0; tibia d0, p0, r0, v2-2-2; metatarsus d0, p0, r0, v2-2-0. II – femur d1-1-0, p0, r0; tibia d0, p0, r0, v2-2-2; metatarsus d0, p0, r0, v2-2-0. III – femur d1-1-0, p0, r0; tibia d0, p1-1-0, r1-1-0, v1p-2-2; metatarsus d0, p1-1-0, r1-1-0, v2-2-1. IV – femur d1-1-1, p0-1-1, r0; tibia d0, p1-1-0, r1-1-0, v1p-2-2; metatarsus d0, p1-1-0, r1-1-0, v2-2-1.

Epigynum. CO slit-shaped, disposed posteriorly in relation to spermathecae, CO large (as wide as the distance between the CO and the posterior margin of the epigynal plate), placed on the posterior half of the epigynal plate, VEP absent, PVP as wide as two times the distance between the anterior and posterior margins, PVP not covering SI, copulatory duct relatively short with large branches pointed anteriorly (Fig. 47C–F).

Distribution

Known only from the type locality (Fig. 50).

Discussion

Stethorrhagus is a Neotropical genus with a significant diversity in Colombia, Brazil, and Ecuador, being mainly distributed in the Andean and Amazon regions (except for *S. oxossi*, which occurs mainly in the Atlantic Forest of Northeast Brazil, Fig. 49). As mentioned before, *Stethorrhagus* shares with *Parachemmis* and *Tupirinna* the presence of a pair of excavations on the anterior margin of the sternum. However, species of *Stethorrhagus* are readily identified by the embolus with a bifid tip on the male palp, with the ejaculatory duct opening at the bifurcation (Figs 3D, 10E, 14A), and, in females, by the single

copulatory opening leading to a single copulatory duct, along with the presence of a developed posterior vulvar plate (PVP), covering at least the posterior half of the vulva (Figs 2C–D, 4C–D, 11C–E).

The presence of modified bristles on the femur, patella, and/or tibia of the male palp, previously documented in eight of the 12 males previously described, has also been identified in most of the species described here. *Stethorrhagus loxodonta* sp. nov., *S. callithrix* sp. nov., *S. felis* sp. nov., *S. lupulus*, *S. oxossi* and *S. archangelus* share the presence of modified bristles in the retrolateral tibial apophysis. *Stethorrhagus bradypus* sp. nov., *S. sylvilagus* sp. nov., *S. naja* sp. nov., *S. tremarctos* sp. nov., *S. mandrillus* sp. nov., *S. latoma*, *S. penai*, *S. chalybeius* and *S. planada* present modified setae in the RTA but also possess clusters of modified setae on the retrolateral faces of the patellae and tibiae. These modified bristles are absent in *S. limbatus*, *S. duidae*, *S. tridentatus*, *S. peckorum* and *S. ovis* sp. nov.

As discussed by Bonaldo (2000), the type species, *S. limbatus*, is particularly intriguing due to several unique characteristics, making it probably the easiest species to identify among those currently comprising the genus. This species differs from all others in the genus by presenting two darker lateral stripes on the edges of the carapace (Figs 9A–B, 11A). However, here we report the occurrence of this character as an intraspecific variation in *S. lupulus*, which may be interpreted as homoplastic. The male

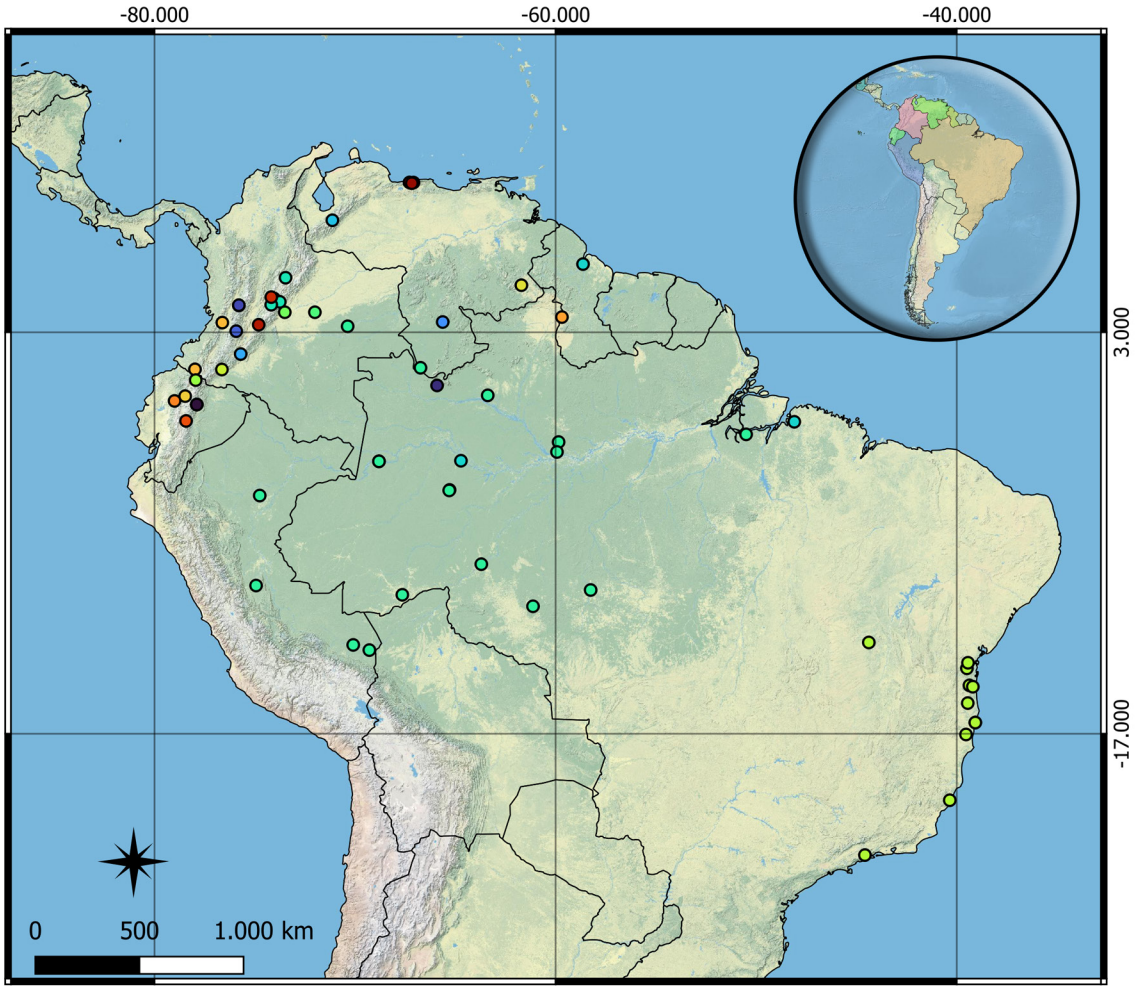

Fig. 48. Distribution records of all species of the genus *Stethorrhagus* Simon, 1896.

palp of *S. limbatus*, as those of all other species in the genus, features the apex of the embolus bifurcated, but the RTA is simpler with an undivided VL. This distinguishes *S. limbatus* from all other species, as the bifurcated VL appears to be the standard condition of this structure in males of the genus.

Bonaldo & Brescovit (1994) interpreted the female genitalia of *S. limbatus* as having two copulatory ducts converging into a large common copulatory opening. However, after re-analyzing the type material deposited in the MNHN and comparing it with other species of the genus, we have concluded that the female of *S. limbatus* possesses a single copulatory duct. What was previously interpreted as distinct copulatory ducts are, in fact, cuticular reinforcements within the duct itself (Fig. 11D). This character is also observed in *S. papilio* sp. nov. and *S. bradypus* sp. nov., *S. oxossi* and *S. tridentatus* (Figs 4D, 38E, 45D; Bonaldo & Brescovit 1994: figs 11d, 14e). This finding reinforces the presence of a single copulatory opening and a single copulatory duct as a diagnostic feature for females of the

Fig. 49. Distribution records of nine species of *Stethorrhagus* Simon, 1896.

genus. Nevertheless, *S. limbatus* differs from all other species in the genus by possessing the widest copulatory opening among all females known to date.

In Bonaldo & Brescovit (1994), all females were described as having the copulatory opening situated anteriorly on the epigynal plate, except for *S. chalybeius*, which has the opening situated medially. In the present study, the pattern of an anteriorly situated copulatory opening is also observed in *S. papilio* sp. nov., *S. bradypus* sp. nov., *S. sylvilagus* sp. nov., *S. callithrix* sp. nov., *S. naja* sp. nov., and *S. sciurus* sp. nov. However, the copulatory opening is situated medially in *S. loxodonta* sp. nov., *S. tremarctos* sp. nov., *S. mandrillus* sp. nov., and *S. felis* sp. nov., and is positioned posteriorly in *S. canis* sp. nov.

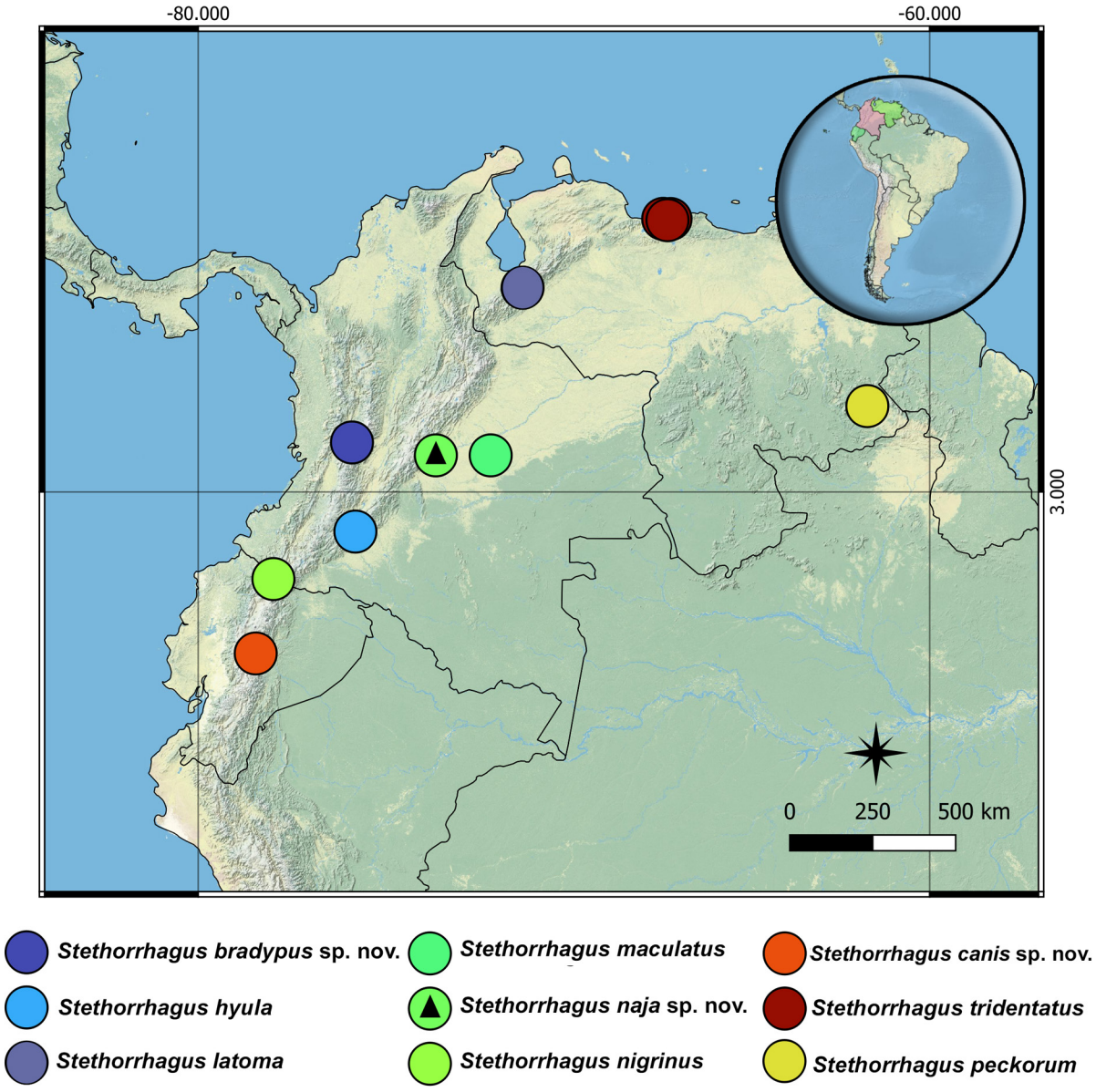

Fig. 50. Distribution records of nine species of *Stethorrhagus* Simon, 1896 from northwestern South America.

Despite the diversity of species documented here, specimens of *Stethorrhagus* are not commonly found in collections (except for *S. lupulus* and *S. oxossi*) and are rarely observed in vivo. As a result, most of the species described, including those in this paper, are known only from the type material. Nonetheless, the morphological complexity of the group's genitalia holds great potential for the survey of characters which could significantly contribute to the development of a phylogenetic framework for the subfamily Corinninae.

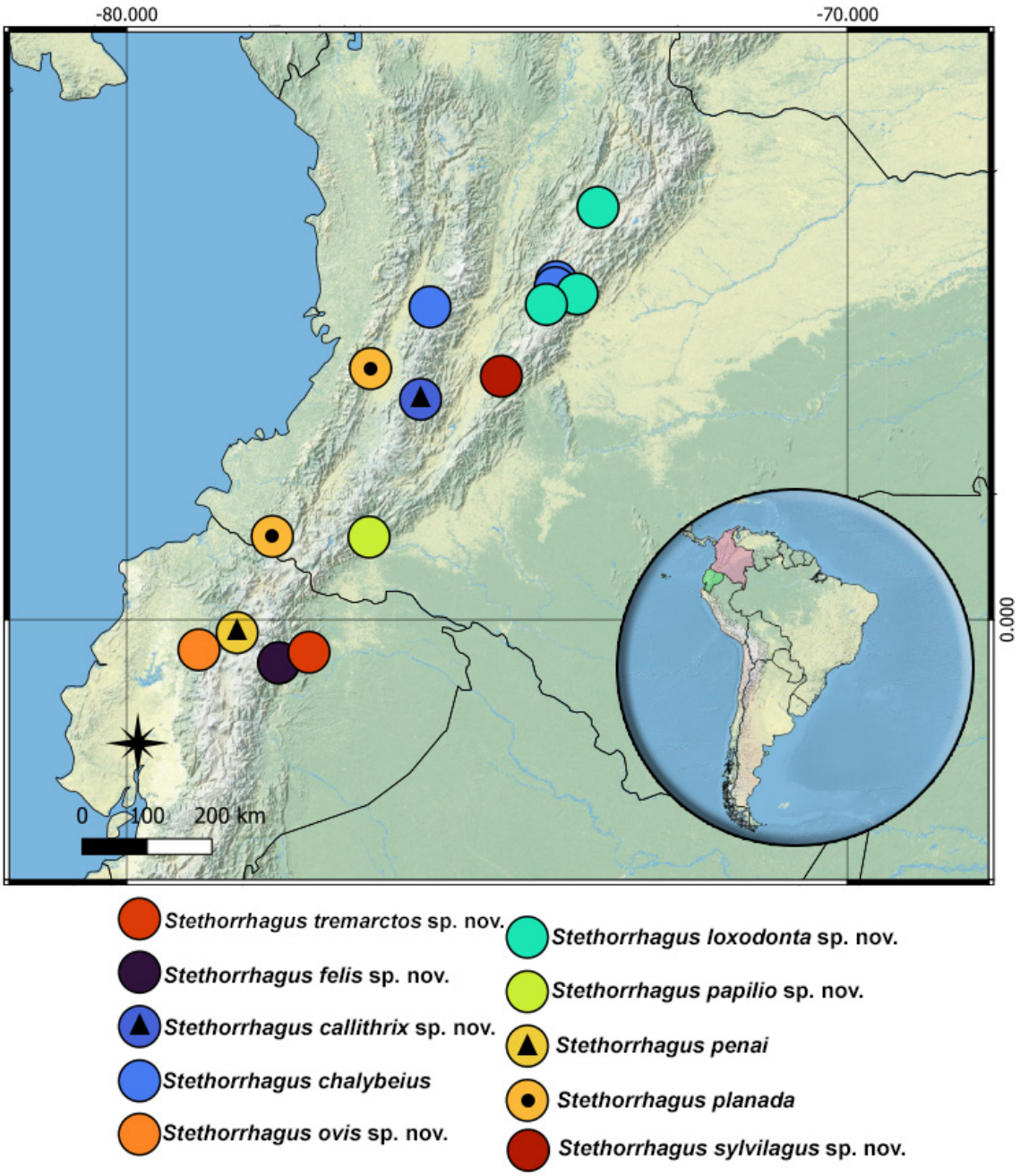

Fig. 51. Distribution records of 10 species of *Stethorrhagus* Simon, 1896 from northwestern South America.

Acknowledgments

We would like to thank the curators for the loan of the material used in this study. This study was supported by Conselho Nacional de Pesquisa e Desenvolvimento Tecnológico – CNPq (CX 140056/2021-1; ABB PQ grant #307165/2022-1 and ADB PQ grant 303903/2019-8). ADB also thanks Fapesp (grant 2022/12588-1). CX would like to thank the International Society of Arachnology for the Oscar and Jan Francke ISA Student Research Fund, which allowed the visit to the Brazilian collections. CX would also like to thank the American Arachnological Society and the Vincent Roth Fund for Systematics Research, which allowed the visit to the Muséum national d'Histoire naturelle (MNHN, Paris) and the Natural History Museum (NHM, London). CX trip to European museums was also partially funded by CNPq, through ABB´s PQ grant. We thank the following curators who kindly welcomed the first author into their collections: Christine Rollard (MNHN), Jan Beccaloni (NHM), Adalberto Santos (UFMG), Viviane Costa (UFMG, curatorial assistant), Adriano Kury (MNRJ) and Carla Barros (MNRJ, curatorial assistant). CX thanks Bruno Rodrigues, Carol Vilanova, Pedro H. Martins, Marcos Vinícius, Humberto Oliveira for the accommodation during her trip to São Paulo and Belo Horizonte and Rubinaldo Ramos for the help in London. We also thank Yvan Montardi for the photos of the MNHN, Ligia Benavides for the photos of the MCZ material, Paulo Pantoja for the photos of AMNH material and Alessandra Mielke for the photos of the MCP material; César Favacho and Petter Svee for the help with the plates, Abel Bustamante for helping with the female genitalia microscope photos of the new species and Fabián García for helping with the maps. We thank Dr Doris Vela and Fernanda Salazar, Museo de Zoologia QCAZ Invertebrados, for clarifying some geographical data. Finally, we thank the reviewers for the comments that helped to improve the manuscript. This paper is part of the doctoral thesis of the first author, advised by ABB.

References

Berland L. 1913. Araignées. *In*: *Mission du Service géographique de l'Armée pour la Mesure d'un Arc du Méridien équatorial en Amérique du Sud (1899–1906)*. Tome 10, fascicule 1. Gauthier-Villars, Paris, pp. 79–119. https://doi.org/10.5962/bhl.title.980

Bonaldo A.B. 2000. Taxonomia da subfamília Corinninae (Araneae, Corinnidae) nas regiões Neotropical e Neárctica. *Iheringia, Série Zoologia* 89: 3–148. https://doi.org/10.1590/S0073-47212000000200001

Bonaldo A.B. & Brescovit A.D. 1994. Revision of the Neotropical spider genus *Stethorrhagus* (Araneae, Corinnidae). *Andrias* 13: 33–64.

Brignoli, P.M. 1985. On the correct dates of publication of the arachnid taxa described in some works by C.W. Hahn and C.L. Koch (Arachnida). *Bulletin of the British Arachnological Society* 6 (9): 414–416.

Caporiacco L. di 1955. Estudios sobre los arácnidos de Venezuela. 2ª parte: Araneae. *Acta Biologica Venezuelica* 1: 265–448.

Chickering A.M. 1937. The Clubionidae of Barro Colorado Island, Panama. *Transactions of the American Microscopical Society* 56 (1): 1–47. https://doi.org/10.2307/3222720

Gertsch W.J. 1942. New American spiders of the family Clubionidae III. *American Museum Novitates* 1195: 1–18. Available from https://www.biodiversitylibrary.org/page/64048259 [accessed 8 Jan. 2025].

Karsch F. 1880. Arachnologische Blätter (Decas I). *Zeitschrift für die gesammten Naturwissenschaften, Dritte Folge* 5: 373–409.

Koch C.L. 1841. *Die Arachniden*. C.H. Zeh′sche Buchhandlung, Nürnberg, Achter Band; Neunter Band. [for the correct year of publication see Brignoli 1985b] https://doi.org/10.5962/bhl.title.43744

Koch L. 1866. *Die Arachniden – Familie der Drassiden*, *Hefte 1–6*. Nürnberg.

Mello-Leitão C.F. de 1948. Contribuição ao conhecimento da fauna araneológica das Guianas. *Anais da Academia Brasileira de Ciências* 20 (2): 151–196.

Petrunkevitch A. 1911. A synonymic index-catalogue of spiders of North, Central and South America with all adjacent islands, Greenland, Bermuda, West Indies, Terra del Fuego, Galapagos, etc. *Bulletin of the American Museum of Natural History* 29: 1–791. https://doi.org/10.5962/bhl.title.23819

QGIS Development Team, 2019. QGIS Geographic Information System. Ver. 3.10. Open Source Geospatial Foundation Project. Available from http://qgis.org [accessed 8 Jan 2025].

Simon E. 1896. Descriptions d'arachnides nouveaux de la famille des Clubionidae. *Annales de la Société entomologique de Belgique* 40 (9): 400–422. https://doi.org/10.5962/bhl.part.2026

Simon E. 1897. *Histoire naturelle des Araignées*. *Deuxième édition, tome second*. Roret, Paris. pp. 1–192. https://doi.org/10.5962/bhl.title.51973

Simon E. 1898. *Histoire naturelle des Araignées. Deuxième édition, tome second*. Roret, Paris. pp. 193–380. [second pdf with detailed publication dates of the single parts] https://doi.org/10.5962/bhl.title.51973

World Spider Catalog 2025. World Spider Catalog. Version 25.5. Natural History Museum Bern, available from http://wsc.nmbe.ch [accessed 8 Jan 2025]. https://doi.org/10.24436/2

Xavier C. & Bonaldo A.B. 2021. Taxonomic revision of the genus *Tupirinna* Bonaldo, 2000 (Araneae: Corinnidae: Corinninae). *Zootaxa* 5004 (2): 201–250. https://doi.org/10.11646/zootaxa.5004.2.1

Printed versions of all papers are deposited in the libraries of four of the institutes that are members of the *EJT* consortium: Muséum national d'Histoire naturelle, Paris, France; Meise Botanic Garden, Belgium; Royal Museum for Central Africa, Tervuren, Belgium; Royal Belgian Institute of Natural Sciences, Brussels, Belgium. The other members of the consortium are: Natural History Museum of Denmark, Copenhagen, Denmark; Naturalis Biodiversity Center, Leiden, the Netherlands; Museo Nacional de Ciencias Naturales-CSIC, Madrid, Spain; Leibniz Institute for the Analysis of Biodiversity Change, Bonn – Hamburg, Germany; National Museum of the Czech Republic, Prague, Czech Republic; The Steinhardt Museum of Natural History, Tel Aviv, Israël.